A NUMERICAL ANALYSIS OF PASSIVE ATTITUDE STABILIZATION USING A TETHERED BALLOON ON A GRAVITY GRADIENT SATELLITE

THESIS

Ernest Matias Maramba, Second Lieutenant, USAF

AFIT/GA/ENY/05-M07

DEPARTMENT OF THE AIR FORCE
AIR UNIVERSITY

AIR FORCE INSTITUTE OF TECHNOLOGY

Wright-Patterson Air Force Base, Ohio

The views expressed in this thesis are those of the author and do not reflect the official policy or position of the United States Air Force, Department of Defense, or the U.S. Government.

AFIT/GA/ENY/05-M07

A NUMERICAL ANALYSIS OF PASSIVE ATTITUDE STABILIZATION USING A TETHERED BALLOON ON A GRAVITY GRADIENT SATELLITE

THESIS

Presented to the Faculty

Department of Aeronautics and Astronautics

Graduate School of Engineering and Management

Air Force Institute of Technology

Air University

Air Education and Training Command

In Partial Fulfillment of the Requirements for the

Degree of Master of Science in Astronautical Engineering

Ernest Matias Maramba, BS

Second Lieutenant, USAF

March 2005

AFIT/GA/ENY/05-M07

A NUMERICAL ANALYSIS OF PASSIVE ATTITUDE STABILIZATION USING A TETHERED BALLOON ON A GRAVITY GRADIENT SATELLITE

Ernest Matias Maramba, B.S.

Second Lieutenant, USAF

Approved:

\signed\	3/10/2005
Dr. William Wiesel Thesis Advisor	Date
\signed\	3/10/2005
LtCol Nathan Titus Committee Member	Date
\signed\	3/10/2005
LtCol Kerry Hicks Committee Member	Date

AFIT/GA/ENY/05-M07

Abstract

This research effort analyzes the fundamental dynamics governing a satellite with a gravity gradient boom and a tethered balloon. Satellites that use gravity gradient booms for passive attitude control are characterized by undamped pitch oscillations and no roll control. The tethered balloon acts as a high drag device that accounts for the most drag on the satellite system. By attaching a drag device, the system resists rolling movements while also damping oscillations. This could potentially be a cost effective method for increasing satellite stabilization. The goal of this research is to model the dynamics and determine the feasibility of a gravity gradient stabilized satellite with an attached balloon. A simulation written in Matlab analyzes the behavior of such a satellite. The research is limited to circular orbits around a spherical Earth and includes only in-plane motion for each mass. Stable ranges for certain tether characteristics are found for three different satellites.

Acknowledgements

First and foremost, thank God for getting me through this program. I praise Him for getting me here and placing the right people in my path, because none of this would be possible without my wife, my family, my friends, and my advisor.

My wife has been a tremendous support to me through it all. She carried me through this program even though she was working on her own Nursing Master's Degree. She also carried, delivered, and has been the best mother for our newborn daughter. I can never repay you for everything you have done for me, but I will always try.

I would also like to thank the rest of my family. Their encouragement got me through this program, and I thank them from the bottom of my heart. I would also like to thank my classmates and friends. You are all true friends, and I appreciate everything you have done for me.

I would also like to thank Dr. William Wiesel for providing me with the idea for this thesis. The idea for this satellite concept, in every way, comes from Dr. Wiesel, and he deserves any and all credit for inventing this attitude control concept. In addition, his guidance throughout my research was critical. He made this an invaluable experience for me and has earned my deepest respect.

Ernest Matias Maramba

Table of Contents

List of Figures

List of Tables

A NUMERICAL ANALYSIS OF PASSIVE ATTITUDE STABILIZATION USING A TETHERED BALLOON ON A GRAVITY GRADIENT SATELLITE

I. Introduction

This research effort analyzes the fundamental dynamics governing a gravity gradient satellite with a tethered balloon in order to determine the feasibility of using such a satellite concept for passive attitude stabilization. Satellites that use gravity gradient booms for passive attitude control are characterized by undamped oscillations and no roll control. The tethered balloon acts as a high drag device that accounts for the most drag on the satellite system, which causes the system to resist rolling movements while also damping pitch angle oscillations. This could potentially be a cost effective method for increasing satellite attitude stabilization. This chapter discusses the motivation behind the analysis of such a system. Then, the objectives of this research are listed, the approach taken to achieve those objectives is given, and the limitations of this research are discussed. The next chapter goes on to provide a more adequate background for this satellite concept. Subsequent chapters go on to derive the equations of motion for the satellite concept, detail the process taken in simulating the satellite concept in orbit, and discuss the results of the simulation program.

1.1 Motivation

"Better, Faster, Cheaper" is a common catch-phrase in the United States Air Force (USAF). In a service centered on maintaining technological superiority over its rivals, this phrase has become the goal for many Air Force engineers. As expressed by the former Secretary of the Air Force Dr. James G. Roche, "There isn't enough money in the budget to replace everything we want nor, in some respects, to replace everything we need. We need to remain committed to investing wisely in our future" (7). The Air Force must be cost efficient in order to sustain the best-equipped military with limited resources.

Furthermore, the actual budget for the Air Force space program is quite small compared to the Department of Defense (DoD) budget and even the Air Force budget. The DoD was given 380 billion dollars in 2004, from which 93.5 billion dollars was allocated to

the Air Force (5:4). In the end, the Air Force allocated about 1.8 billion dollars to space-related operations and 31.2 billion dollars for modernization, a portion of which includes research, development, testing, evaluation, science, technology, and procurement of space systems (5:4). This is a high estimate for space-related programs since the modernization budget actually includes procurement of aircraft and armament. While space technology is a high priority, Air Force space programs must be very efficient with the limited funds that it receives.

Commitment to advanced technology is also a prime characteristic of the U.S. Air Force. As stated by the USAF Future Concepts and Transformation Division:

> "The purpose of Air Force innovation is to rapidly assess and implement new ideas, concepts, and technologies to field the best capabilities to the warfighter while also improving the associated doctrine, organization, training, materiel, leadership and education, personnel, and facilities" (14:21).

The Air Force was founded on the exploitation of new technology and has continued to be the best air force in the world because it researches, develops, and implements the newest technology.

The current trend in satellites is a shift away from large, multi-payload satellites, which carry larger production and launch costs, to micro and nanosatellites that cost much less (8:806). "Recently, spacecraft have become more diverse, with the largest spacecraft now complimented by new systems using a larger number of smaller spacecraft in low-Earth orbit (LEO)" (16:853). Consequently, the smaller size and lower funds drive down the mass and cost budgets of the satellite subsystems. To keep this transition effective, the satellite and satellite subsystems must maintain a high degree of reliability. In addition, increased subsystem reliability decreases the need for back-up systems which in turn decreases the total satellite cost and weight.

Like all other subsystems, the attitude control subsystem must meet the requirements determined by each mission payload with the stricter weight and cost constraints and at the same degree of reliability. In fact, the attitude control subsystem carries additional importance because it has the potential for decreasing satellite operation costs as well as production costs. With greater pointing stability, a satellite can decrease the size of the communications subsystem by decreasing the antenna size while maintaining a low level

of bit error. With a totally passive attitude control system, reliability is increased and operations costs are decreased. A passive system has the added benefits of having no fuel requirements and very little power requirements. The benefits of the attitude control subsystem are felt by all satellite subsystems, decreasing the overall cost and complexity of the satellite.

Additionally, few low budget missions have the financial means to venture beyond low-earth orbit, which includes up to 500 kilometers above the Earth. Gravity gradient and aerodynamic drag torques are the dominating perturbations at these altitudes. Where many satellites must counteract the effects of these perturbations, it would be advantageous for an attitude control subsystem to use these torques to stabilize the satellite and meet the mission pointing requirements. A satellite using passive aerostabilization decreases complexity, weight, and cost by manipulating these perturbative forces rather than working against them.

1.2 Satellite Concept

A satellite concept that could tie together all of these issues would be a low cost, high performance, and high reliability passive attitude control system that would use gravity gradient and drag torques in low-Earth orbit to produce a stable, nadir-looking attitude within a limited time frame. The proposed answer to such an attitude subsystem would look somewhat like Figure 1.1. Essentially starting from a gravity gradient satellite, a main buss mass has an extended gravity gradient boom with a tip-mass at the end. Attached to these two masses is a high drag device, potentially a rigidizable balloon. The balloon is attached by two tethers that are connected to the tip-mass and main buss mass. Figure 1.1 shows the satellite concept in an initial configuration, but it is expected that the two tethers, with high moduli of elasticity and elongation percentages, would extend the balloon mass further behind the gravity gradient satellite. A deeper explanation of this configuration is contained in Section 3.1.

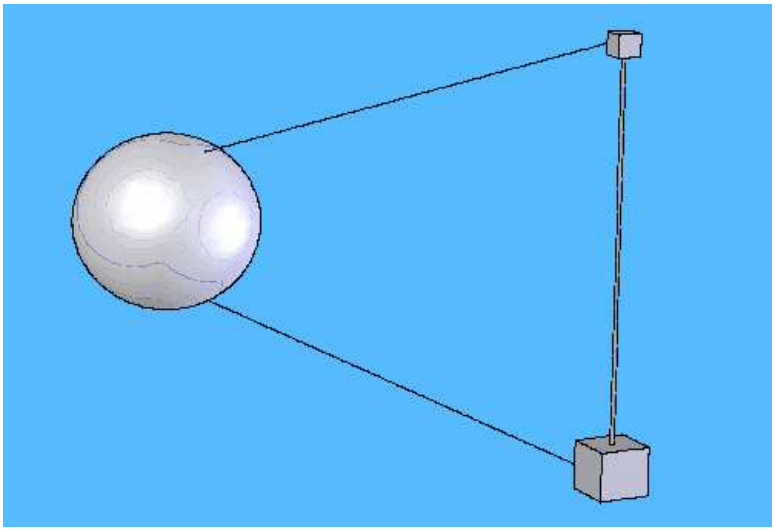

Figure 1.1 Engineering Model of Satellite Concept

1.3 Research Objectives

This research derives and tests a dynamical model for a gravity gradient satellite that uses a tethered balloon for completely passive attitude stabilization. The purposes of this study is to answer the following questions.

- What are the equations of motion for a gravity gradient satellite with a rigid balloon attached by tethers?
- What attitude control system characteristics can be altered to manipulate the effectiveness and efficiency of passive gravity gradient attitude control with aerostabilization?
- What is the impact of certain satellite characteristics, namely modulus of elasticity and damping coefficient, on the steady-state attitude of this satellite concept?
- Where are the regions of stability for these satellite characteristics?

The ideal result of this thesis would be to prove or disprove the feasibility of using a gravity gradient boom and a tethered balloon to stabilize the attitude of a satellite by developing and testing a dynamical model for the satellite system through a computer program. A demonstration of a stable attitude would be shown through the damping of the gravity gradient pitch angle over time. This is the basis for study of this attitude control

concept, and subsequent design studies rely on whether pointing requirements can be met at the base research level.

1.4 Research Approach

In order to accomplish the above established research objectives, this study takes the following steps:

- Review all relevent information surrounding this satellite concept, including attitude control techniques, tethers, aerostabilization, and any other pertinent articles.
- Derive the equations of motion for a gravity gradient satellite with a tethered, rigid balloon.
- Create and validate a computer simulation that models a gravity gradient satellite with aerostabilization.
- Characterize the impact of the moduli of elasticity and damping coefficients of the tethers on the steady-state attitude of a satellite.
- Determine the regions of stability for these satellite characteristics.

1.5 Research Scope and Limitations

The research objectives allow a lot of room for simplifying the system as much as possible in order to focus on the dynamics of this particular concept; however, this baseline study must be thorough enough to determine whether this method of attitude stabilization is even possible. The following assumptions limit the extent of knowledge gaining in this research effort but also concentrate all efforts to produce a deeper understanding at the base level of research.

- Assume two-body equations of motion for the satellite system center-of-mass (COM)
- Assume circular, low-Earth orbit about a spherical Earth
- Assume gravity, drag, tether-spring, and tether-damper are the only forces acting on the tip-mass, main satellite bus, and tethered balloon

- Assume motions of the tip-mass, main satellite bus, and tethered balloon are limited to orbital plane
- Assume rigid masses and point masses for tip-mass, main satellite bus, and tethered balloon
- Assume tethers are not compressed and are massless
- Assume rigid and massless gravity gradient boom
- Assume uniform density for atmosphere at a specific altitude
- Focus on motion of the satellite after deployment of the gravity gradient boom and tethered balloon

These assumptions, while limiting the scope, greatly simplify the dynamics of the satellite system. In most cases, the calculations and equations involved with this study are less complicated and less prone to error. Further discussion of these assumptions and issues is contained in Section 3.1.

II. Literature Review

The Literature Review Chapter discusses pertinent background material that is helpful in understanding this satellite concept. Since the satellite configuration that is being studied involves a gravity gradient boom and tethered balloon used for passive attitude control, this chapter will describe attitude control techniques, gravity gradient booms, tethers in space, and rigidizable balloons. Past research involving passive aerostabilization is also discussed since it is the closest configuration to the presently studied satellite concept. While this is not a comprehensive description of all satellite topics necessary to understand this study, this chapter attempts to explain and discuss all immediately relevant information.

2.1 Attitude Control Techniques

As defined by Space Mission Analysis and Design (SMAD), "the attitude determination and control subsystem measures and controls the spacecraft's angular orientation (pointing direction) or its orientation and linear velocity" (16:302). Pointing control is necessary for several different reasons and at different performance specifications, depending on the mission of the satellite. Reasons for attitude control include orbit insertion, initial attitude stabilization, normal station-keeping, and special or contingency slew maneuvers (16:356). These different operation modes can result in totally different attitude control systems. Additionally under the normal station-keeping mode, satellites are subject to cyclic and secular disturbance torques. Cyclic disturbance torques happen on a periodic basis, while secular torques have linear effects, like the effect of solar pressure. Furthermore, gravity and drag dominate the disturbance torques at LEO while solar pressure and third-body effects have greater influence in high-Earth orbit (HEO). Determining the primary disturbance torques in the mission orbit can help the design engineers focus on certain issues. All of these requirements and issues drive the design of the attitude control system.

In designing the attitude control system, techniques come in the form of passive systems, spin-control systems, and three-axis control systems. A gravity gradient boom is an example of a passive system and is described further in Section 2.2. Passive systems normally have decreased accuracy but are less expensive and complex. "They consume no power, require no hardware for sensing or actuation, and make no demands on software" (6:282). The opposite is true of active systems. Thrusters and magnetic torquers are ex-

amples of active systems. Active systems use either of two concepts, zero momentum or momentum bias. In zero-momentum systems, "reaction wheels respond to disturbances on the vehicle" (16:362). Momentum bias systems use one spinning wheel to give the satellite gyroscopic stiffness and to control the attitude by torquing the wheel. Spin stabilized satellites passively resist disturbance torques by using gyroscopic stability, but extra fuel is needed to reorient the satellite once it begins spinning.

In determining which attitude control technique to use on a satellite, it is important to look at the required performance specifications in terms of accuracy, range, jitter, drift, and settling time (16:357). For example, "In many modern applications, the attitude errors permitted are so small that only a fully automatic (fully 'active') control system can meet mission specifications" (6:281). These requirements may come from different subsystems, for example the payload or the communications subsystem. Accuracy and settling time are the focus of this feasibility study since this satellite concept is for low-budget microsatellites. More stringent requirements would be used for further studies and designs.

2.2 Gravity Gradient Satellites

The prime example for passive attitude control is gravity gradient stabilization. Gravity gradient satellites exploit "some naturally occurring force field [Earth's gravity field] to provide the desired stabilizing torque" (6:282). Figure 2.1 shows an example of a satellite that uses gravity gradient stabilization.

In designing a gravity gradient stabilized satellite, it is important for the moments of inertia to follow certain criteria. First, the inertia ratio parameters k_1 and k_3 must be defined. These ratios essentially make the design a function of two variables, rather than three. In these equations, I_1 is the moment of inertia aligned with the satellite's velocity vector, I_2 is normal to the orbital plane, and I_3 is aligned with the vertical axis.

$$k_1 = \frac{I_2 - I_3}{I_1} \tag{2.1}$$

$$k_3 = \frac{I_2 - I_1}{I_3} \tag{2.2}$$

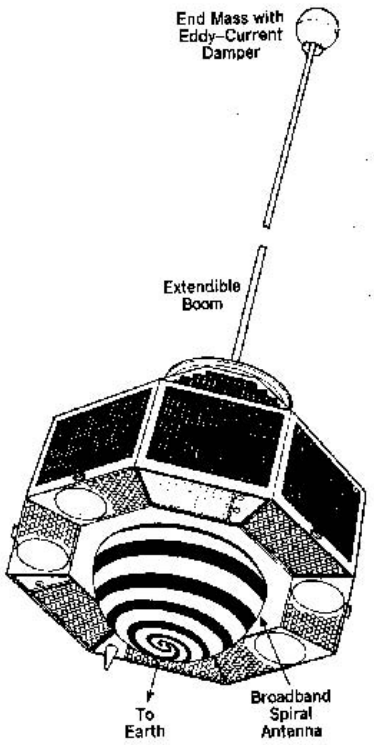

Figure 2.1 GEOS-II Spacecraft (6:328)

The regions of stability can then be seen in Figure 2.2. Hughes outlines the process of determining the stability regions for gravity gradient satellites in chapter nine of his book, Spacecraft Attitude Dynamics (6). From this figure, it can be seen that only certain satellite configurations are acceptable for gravity gradient stabilization. The upper-right region is populated by satellites that have the minor axis in the vertical direction, the intermediate axis pointing in the velocity direction, and the major axis pointing normal to the orbit. The lower region, called the DeBra-Delp region, shows the stability of rigid bodies whose minor axis is normal to the orbit and whose major axis is tangent to the orbit (6:301). The satellite concept under study uses the region of stability described in the upper right of Figure 2.2.

Although these stable regions exist in theory, there are two problems with gravity gradient stabilization. First, gravity gradient torques decrease with increased altitude. This makes it necessary to use inertia augmentation, which means increasing the moments of inertia as much as possible. This can be done by placing long, slender rods along the principal axes. Effectively, moments of inertia are increased, which also increases gravity

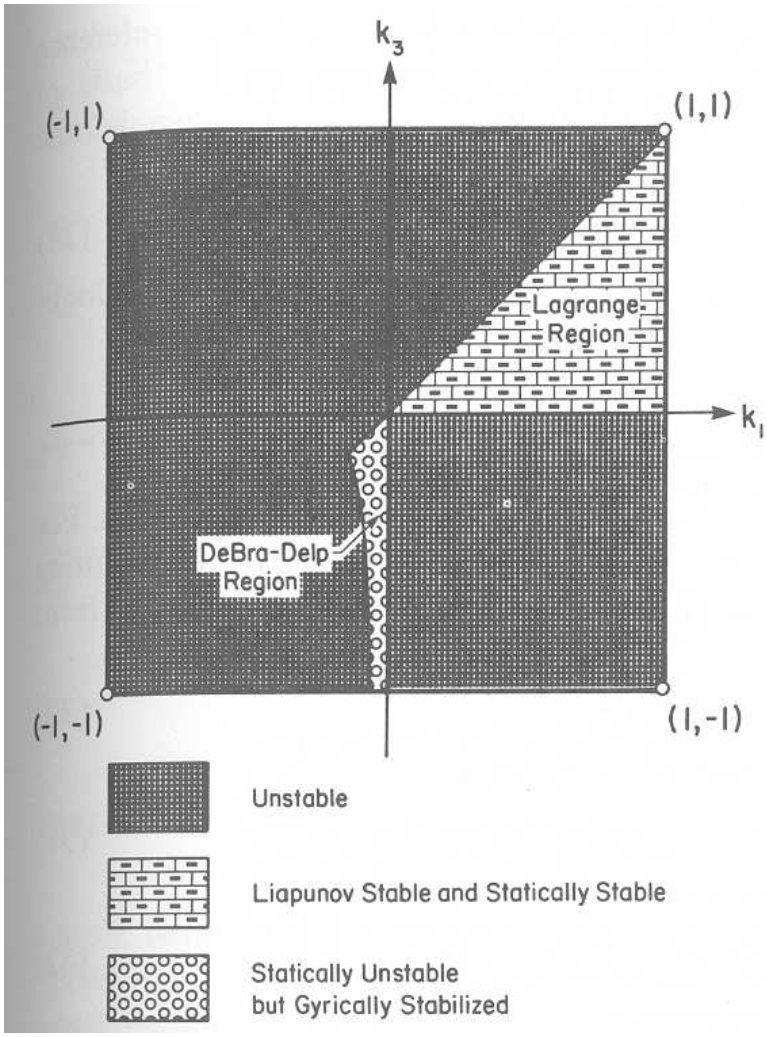

Figure 2.2 Stability Regions for Gravity Gradient Satellites in Circular Orbit (6:297)

gradient restoring torques. This concept is depicted in Figure 2.3. The second issue in dealing with gravity gradient stabilization is effective damping or energy dissipation. In order to dampen out the librations, or oscillations in the pitch direction, the system must dissipate energy. Options for energy dissipation include magnetic-hysteresis rods, spherical tip dampers, and boom articulation. This damping is also a major focus for the satellite concept currently under investigation.

2.3 Tethers in Space

The idea of tethers in space has been around since 1895 (3:7). Since then, the range of applications for space tethers has been ever-growing. The usefulness of tethers span

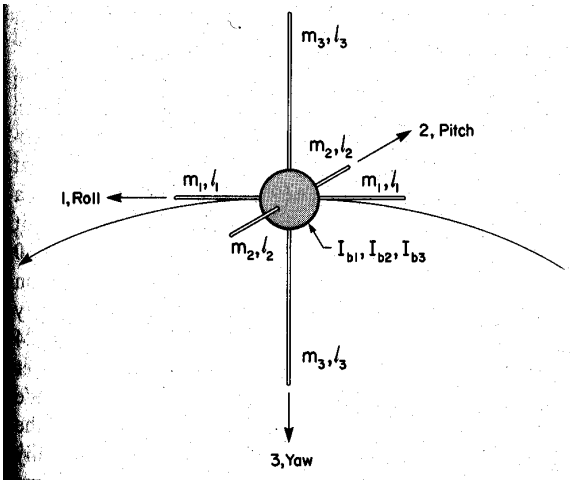

Figure 2.3 Inertia Augmentation (6:315)

all elements of the satellite system architecture. For example, tethered probes can take samples and measurements at different altitudes without having to maneuver the main satellite or spacecraft. This application is shown in Figure 2.4. This of course, eliminates

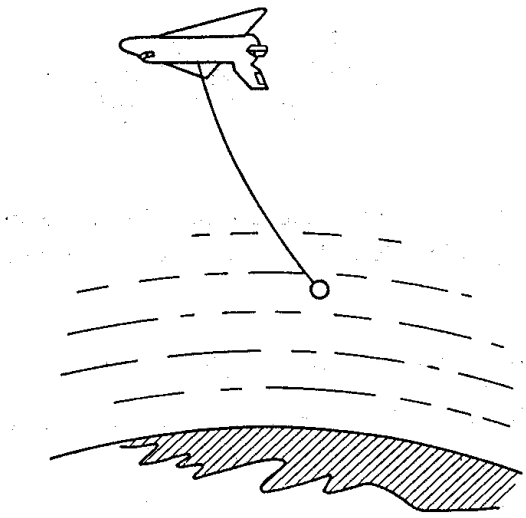

Figure 2.4 Tethered Probe Taking Measurements at Different Altitude than Orbiter (3:26)

the need for extra maneuvering fuel and expends the field of measurement around the main satellite. Tethers also have the potential to collect electric power through a metallic tether when travelling through the Earth's geomagnetic field. The same essential concept makes it possible to produce thrust when electricity is applied to a metallic tether. These two

concepts are depicted in Figure 2.5. Tethers have even more applications involving only

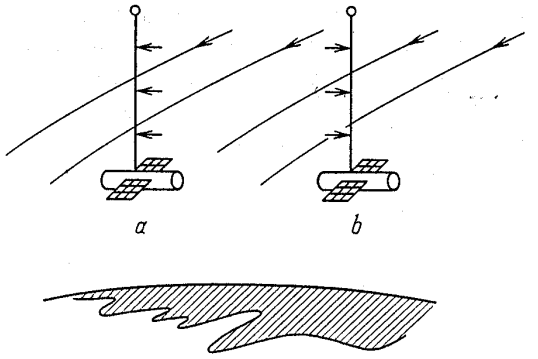

Figure 2.5 Metallic Tethers Travelling through Earth's Geomagnetic Field (a)Producing Thrust (b)Producing Electric Power (3:25)

space transportation. Concepts like the space tether elevator, depicted in Figure 2.6, could be used on the Earth as well as the Moon. Tether elevators attach to either the Earth or

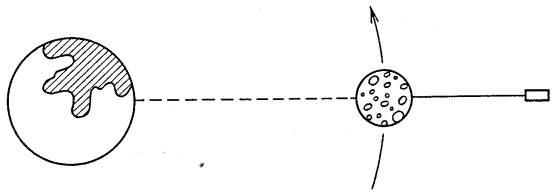

Figure 2.6 Moon Based Space Elevator (3:30)

Moon and extend into normal orbital altitudes. Satellites using this system would travel up the tether elevator and would be implanted into orbit using much less fuel than a typical ground-launched rocket. Space escalators, shown in Figure 2.7, use similar concepts to space elevators but applied to several tether satellites orbiting at different altitudes. Satellites attach at one end of the first tether satellite, travel to the opposite end of the tether, release from that tether satellite, attach to the next tether satellite orbiting further away, and repeat that cycle until the desired orbit is reached. Since the tether systems effectively transfer energy to the payload satellites to boost it to higher altitudes, the orbiting tethers need some kind of station-keeping subsystem to keep each tether in its respective orbit.

There are many hindrances to the implementation of the above-mentioned tether systems. Strength, for one, is a material specification that limits the length of the tethers

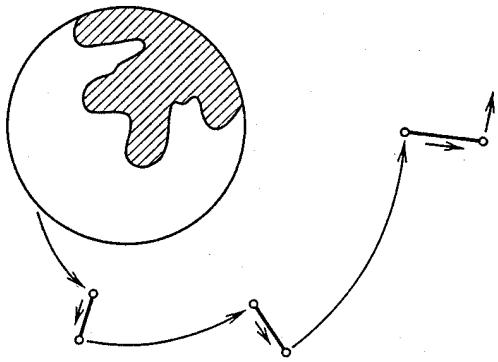

Figure 2.7 Space Escalator (3:29)

required for these applications. Specifically, there are no known materials that can be produced to the lengths necessary for a space elevator (at least 35,800 kilometers to reach geostationary orbit). A tether at this length could not withstand its own weight and definitely not the added weight of a satellite. This mainly impacts tethers extending from Earth since the gravitational force acting on a tether at even the lowest Earth orbits is large enough to "exceed the break lengths on Earth by an order of magnitude" (3:36). Mass is another issue as many applications of space tethers require lengths in units of kilometers. This obstacle is crossed by using several braided fibers rather than one long strand. This method increases strength with lower densities. Debris and micrometeorites pose another threat since a great majority of which have diameters comparable to the diameters of space tethers and travel at an average relative speed of 20 kilometers per second (3:39). While the threat is small for tethers smaller than 100 kilometers, tether tapes have been proposed for decreasing the dangerous impact from small space debris.

2.4 Rigidizable Balloons

Rigidizable, inflatable balloon systems have been studied since the beginning of the National Aeronautics and Space Administration (NASA), but research is beginning to increase due to modern missions which require even larger on-orbit systems, like large aperture optical telescopes, solar arrays, and aerobrakes. Rigidizable balloons are intended to replace typical, rigid mechanical structures. The balloons are flexible when not inflated but become

stiff when inflated to a predesigned size. Such systems are packaged uninflated prior to launch in order to fit what would be systems larger than the launch vehicle envelope. After the satellite is launched, the balloon inflates to a predesigned shape. Rigidizable balloons derive their motivation, in large part, from the same motivation for this research concept - smaller, more light-weight systems. The cost of a satellite increases as its size and weight increases, but inflatable balloons can be fifty percent lighter and twenty-five percent smaller than standard mechanical systems (12:2-3).

The system has high reliability because it does not require complex, mechanical components or joints. Hinges and joints on mechanical systems have the potential to cold weld, making it impossible to extend or deploy a part of the satellite. On the other hand, inflatable balloons continue to increase the pressure and force of deployment in the event the system somehow resists deployment (12:2-3). The only failure point on an inflatable system is the trigger to initiate inflation. Also, inflatable systems can be predesigned to inflate to any shape and can even be packaged to almost any shape. This flexibility can be crucial when trying to fit a satellite system within a launch vehicle's envelope.

Slightly different from rigidizable, inflatable structures are inflatable structures, which require additional gas in order to maintain the structural shape in the event of leaks. Inflatable structures have been the focus of many research efforts even though rigidizable, inflatable structures do not require extra gas and do not cause attitude torques in the case of punctures in the balloon, possibly from micrometeorite impacts. Any leaks in inflatable devices could cause unwanted thrust due to gas being expelled through small holes in the structure. The inflatable structure also adds weight to the total satellite because of the need of additional gas, gas tanks, and regulators.

An example of an inflatable, rigidizable structure is the L'Garde Inflatable Space Truss, shown in Figure 2.8 . The truss is made out of a "composite material that are impregnated with a water soluble resin" (12:2-11). The water in the composite evaporates in the vacuum of space, stiffening the resin material and the structure as a whole. This system had a final weight of 1.917 kilograms and a length of 60.1 inches, although the packing volume was only 1953 cubic inches (12:2-12).

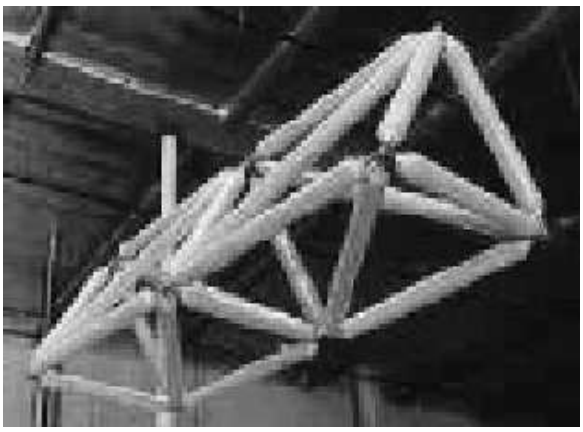

Figure 2.8 L'Garde Inflatable Space Truss (12:2-12)

As inflatable, rigidizable systems are still under development, there are several problems that this technology must overcome. First, it is difficult to test the effects of space on these systems while they are on the ground. For example, the effect of gravity overshadows the force seen in space. Since these forces cannot be properly tested, the guidance and control of the satellite gains additional demands. Gravity also plagues the fabrication of the material and the structure on the ground. The effects of gravity can make it difficult to achieve uniformity in the material. This can cause a distortion in the shape when deployed in space. These problems will hopefully be overcome by creating modeling and simulation software that can more accurately test these structures and materials in a simulated space environment without actually being in space.

2.5 Past Research

NASA was the first to develop and demonstrate a totally passive, aerodynamically stabilized satellite for LEO in the years 1993 to 1997. The NASA Goddard Space Flight Center developed the Passive Aerodynamically Stabilized Magnetically Damped Satellite (PAMS), shown in Figure 2.9, as the first flight experiment to demonstrate the concept of passive aerostabilization. This technology demonstration was required so that this concept could be used on another satellite, the Gravity and Magnetic Earth Surveyor (GAMES), which would be flown in order to evaluate the gravity field of the Earth to a high precision. Passive aerostabilization was seen as a "low-cost, low-weight, long-lifetime option" for the satellite (9:228).

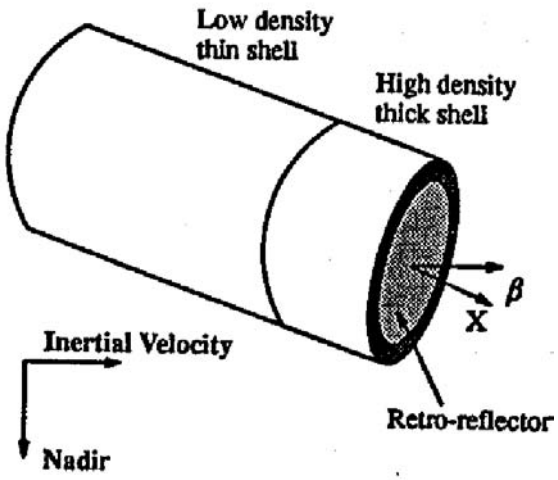

Figure 2.9 PAMS Schematic (9:228)

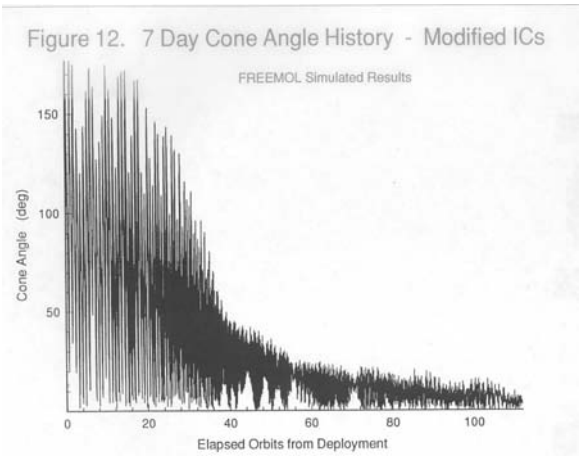

Figure 2.10 PAMS Results (15)

PAMS used a configuration similar to a shuttlecock where the center of mass was placed forward, in the ram direction, of the center of pressure, while magnetic hysteresis rods were used for rate damping. Aerodynamic stabilization was chosen as the primary stabilization force because as Psiaki explains, "At altitudes below 400 km, aerodynamic drag torque tends to overwhelm the gravity gradient torque for practical lightweight deployable boom designs" (13:2). NASA's method for attitude stabilization avoided the gravity gradient disturbance torque by designing the satellite to have equal moments of inertia. NASA produced the computer program Free Molecular Aerodynamic Satellite Attitude Dynamic Simulation (FREEMOL) to predict and numerically confirm the feasibility of aerostabi-

lization. This simulation, shown in Figure 2.10, predicted worst-case angular rates of 0.1 degress per second in yaw and pitch and 0.05 degrees per second in roll.

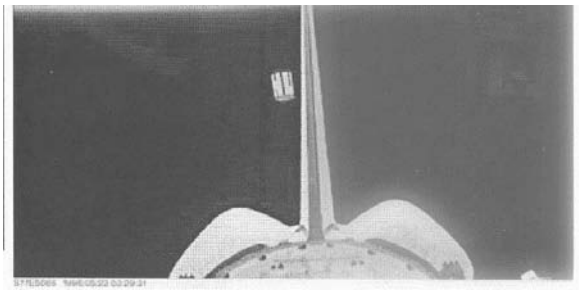

Figure 2.11 NASA Flight of PAMS (15)

PAMS was flown on the Space Shuttle Mission STS-77 on May 1996. The PAMS flight measurements met complications that prevented validation and calibration of the FREEMOL software, but the cone angle estimates made by space shuttle astronauts during rendezvous verified that the satellite's attitude stabilized. During flight, the instrument intended to measure the satellite's attitude failed. Although this portion of the PAMS flight was a failure, the overall project was still deemed a success. While PAMS is a similar passively stabilized system developed and tested by NASA, the satellite concept currently under study has never been tried.

III. Dynamics

This section will outline and describe the fundamental mathematics that are used to model the dynamics of this satellite concept. The chapter first describes the satellite concept and the assumptions made. Next, the chapter defines the coordinate frames used in this study. Finally, the two body equation of motion is derived as well as the equations of motion for this satellite concept.

3.1 Basic Configuration and Assumptions

The distance from the gravity gradient tip-mass to the center of mass is defined as 'b' whereas the distance to the main satellite bus from the tip-mass is defined as 'a'. The length of each tether when taut is defined as 'l_1' for tether one and 'l_2' for tether two. The moduli of elasticity for each tether are 'E_1' and 'E_2' and the damping coefficients are 'c_1' and 'c_2', respectively. Also, the tip-mass is defined as mass one or m_1, the main bus mass is m_2, and the balloon mass is m_3. Tether one connects the tip-mass to the balloon mass, and tether two connects the main bus mass to the balloon mass. These characteristics are depicted in Figure 3.1.

For this study, the tension in the tether is mathematically modelled as a simple spring with a modulus of elasticity. Normally, moduli of elasticity are in units of force per cross-sectional area of the spring. In this case, the moduli of elasticity have units of Newtons per millimeter squared, but the cross-sectional area is assumed to be one millimeter squared. In order to make use of this assumption, the moduli of elasticity are in units of Newtons in the equations of motion and in the simulation program. However, this characteristic is listed in force per unit area in the rest of this paper. The damping coefficient serves as a model for energy dissipation in the spring. Energy dissipation is the factor that will cause the librations, or oscillations due to gravity gradient torque, to dampen. The damping coefficients are in units of Newton seconds per meter. This is regardless of the cross-sectional area, and these are the units used for this characteristic in the dynamical model.

The center of mass of the satellite system is approximated as residing on the gravity gradient boom at all times. The gravity gradient boom and tethers are assumed to have zero mass. The tethered balloon is assumed to have a mass much smaller than the tip-mass.

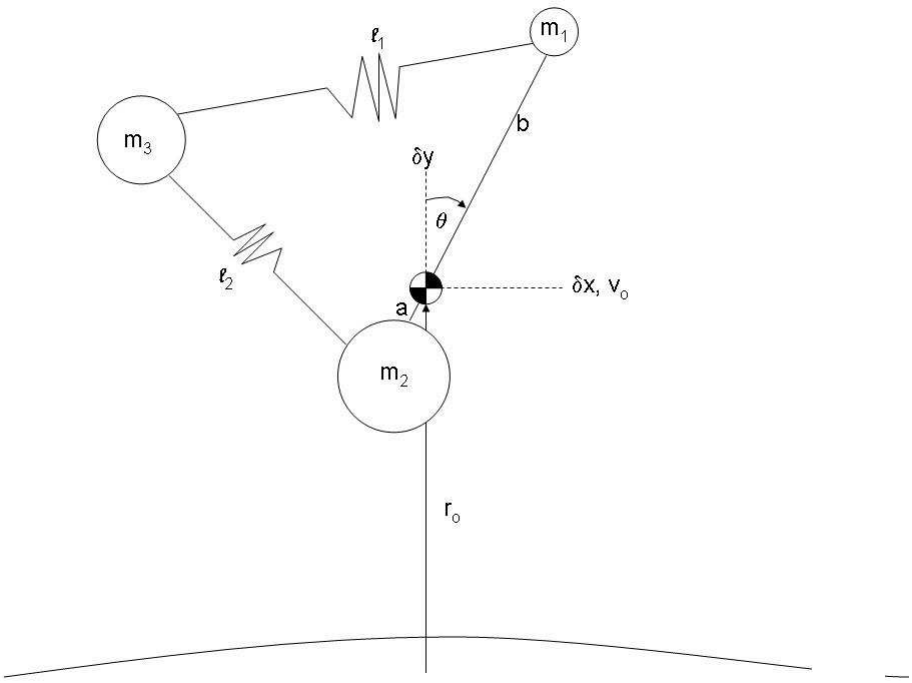

Figure 3.1 Depiction of Satellite Concept

By definition, the satellite's main bus has much more mass than the tip-mass. Also, the satellite is modelled as if the gravity gradient boom were already deployed. In addition, the tethered balloon is assumed to have been deployed and inflated. The dynamics in this model begin as if the satellite system depicted in Figure 3.1 is deployed as shown. As the steady state stabilization is the focus of this baseline study, it is not necessary to consider the system's response in the transient mode. In fact, the mechanism for deploying both the gravity gradient boom and tethered balloon is not within the scope of this study. These assumptions are in addition to those listed in Section 1.5.

3.2 Coordinate Frames

To keep the model's dynamics as simple as possible, this study uses a local coordinate frame to the satellite as shown in Figure 3.1 of Section 3.1. This non-inertial coordinate frame's first two axes are in the orbital plane with the origin at the center of mass. The first axis, δx, points in the direction of the satellite's velocity vector, the second axis, δy, points

in the radial direction away from Earth, and the third axis, δz, points out of the orbital plane, completing the right-handed coordinate frame.

The radius, r_c, of the satellite's orbit is measured from the center of the Earth to the center of mass of the satellite system. For this study, the altitude is assumed to be 200 kilometers above the Earth's surface ($R_{Earth} = 6375km$). This project also assumes a circular orbit about a spherical Earth.

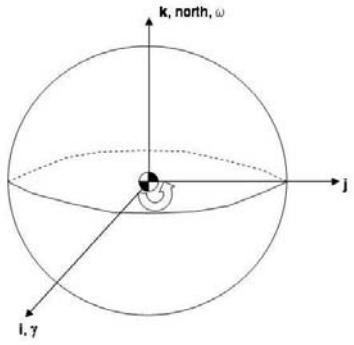

Figure 3.2 Geocentric Equatorial Coordinate Frame

The Geocentric Equatorial (GCE) coordinate frame, which is inertially fixed in space and shown in Figure 3.2, is used in this study in defining the two-body equations of motion in Section 3.3. The first axis points toward the vernal equinox, the second axis is normal to the first and in the equatorial plane, and the third axis is normal to the first two axes.

3.3 Two-Body Equation of Motion

The two-body equation of motion mathematically describes the motion of a satellite. The two bodies in this system are the Earth, with mass m_E, and a satellite, with mass m_s, both assumed to be point masses as shown in Figure 3.3. With respect to the inertial frame, the positions of each mass are $\vec{R}_E$ and $\vec{R}_s$ while the accelerations are $\ddot{\vec{R}}_E$ and $\ddot{\vec{R}}_s$. The position of the satellite with respect to the Earth is defined as $\vec{r_o}$, where:

$$\vec{r_o} = \vec{R}_s - \vec{R}_E \tag{3.1}$$

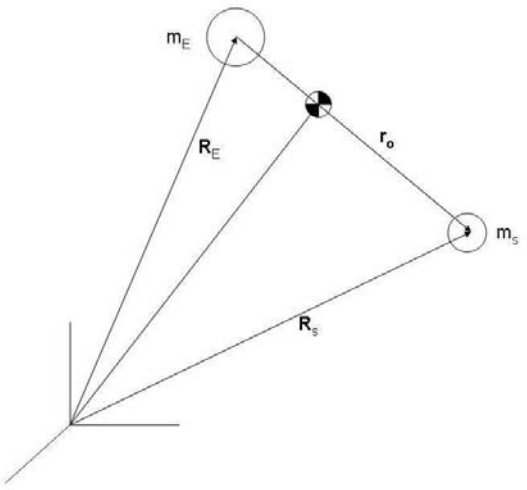

Figure 3.3 Inertial Frame for Two-Body Equations of Motion

The acceleration of the satellite with respect to the Earth is determined by taking the second derivative of the position vector, $\vec{r_o}$.

$$\ddot{\vec{r_o}} = \ddot{\vec{R}}_s - \ddot{\vec{R}}_E \tag{3.2}$$

Using Newton's second law, $\vec{F} = m\,\vec{a}$, the only force acting on each mass is the gravitational force due to the other mass and is defined by the following equations.

$$\vec{F_s} = -\frac{G\,m_s\,m_E}{\left|\vec{R}_s - \vec{R}_E\right|^3}\left(\vec{R}_s - \vec{R}_E\right) \tag{3.3}$$

$$\vec{F_E} = -\frac{G\,m_s\,m_E}{\left|\vec{R}_E - \vec{R}_s\right|^3}\left(\vec{R}_E - \vec{R}_s\right) \tag{3.4}$$

In Equations 3.3 and 3.4, G is defined as the gravitation constant. After substituting the above equations into Newton's second law and replacing $\vec{a}$ with $\ddot{\vec{R}}_E$ and $\ddot{\vec{R}}_s$, Equations 3.5 and 3.6 are found.

$$m_s\,\ddot{\vec{R}}_s = -\frac{G\,m_s\,m_E}{\left|\vec{R}_s - \vec{R}_E\right|^3}\left(\vec{R}_s - \vec{R}_E\right) \tag{3.5}$$

$$m_E\,\ddot{\vec{R}}_E = -\frac{G\,m_s\,m_E}{\left|\vec{R}_E - \vec{R}_s\right|^3}\left(\vec{R}_E - \vec{R}_s\right) \tag{3.6}$$

Substituting these into Equation 3.2, the equation of motion is found to be:

$$\ddot{\vec{r_o}} = -\frac{G\ (m_s + m_E)}{\left|\vec{R}_s - \vec{R}_E\right|^3}\left(\vec{R}_s - \vec{R}_E\right) \tag{3.7}$$

To further simplify this equation of motion, the standard gravitational parameter is defined in Equation 3.8.

$$\mu = G\ (m_s + m_E) \tag{3.8}$$

This quantity is known more accurately than the separate constituent values. For man-made satellites, μ is approximated as $\mu = G\,m_E$ since m_s is much smaller than m_E. After substituting μ and Equation 3.1 into Equation 3.7, the final two-body equation of motion is:

$$\ddot{\vec{r_o}} = -\frac{\mu}{|\vec{r_o}|^3}\,\vec{r_o} \tag{3.9}$$

The Geocentric Equatorial (GCE) coordinate frame, described in Section 3.2, and the two-body equation of motion are used to propagate the position and velocity vectors of the satellite's center of mass forward in time. The derivation of the two-body equation of motion is fundamentally extracted from and further explained in Section 2.2 of Spacecraft Dynamics by Dr. William Wiesel (17).

3.4 Satellite Concept Equations of Motion

The two-dimensional configuration for the studied satellite concept is the most straightforward case on which to determine the feasibility of this system. This case is based on a circular orbit defined by two-body motion and includes the force of drag. The local coordinate frame used in this case is described in Section 3.2. The process used to determine the satellite concept's equations of motion is known as Lagrange's Equations of Motion. This process was selected for its simplicity and ability to factor in additional non-conservative forces without altering the basic equations of motion, which only include conservative forces.

The equations of motion for this satellite concept use the generalized coordinates δx, δy, and θ. These are shown in Figure 3.1 of Section 3.1. There are only three coordinates because there are three masses with a total of only three degrees of freedom. The number of

degrees of freedom is found by subtracting the number of constraints from three times the number of masses. From the assumptions, none of the masses move out of the orbital plane, which equates to one constraint for each mass or three total constraints. The tip-mass and main bus mass can move in the δx and δy directions, but both are fixed in distance from the center of mass which accounts for two more constraints for the total system. Also, the tip-mass and the main satellite bus are fixed rigidly to each other, accounting for the sixth constraint. Therefore, three masses start with nine total degrees of freedom from which six constraints are subtracted.

The balloon is essentially free to move in the δx and δy directions within the bounds of the two tethers so δx and δy are a good choice for the first two generalized coordinates. The tip-mass and main satellite bus are fixed to each other and pivot about the center of mass. This is the same as a pendulum so an angle, θ, is a typical choice for the generalized coordinate. The coordinate δy is measured from the center of mass of the satellite system radially away from the center of the Earth. The coordinate δx is measured in the ram direction emanating from the center of mass of the satellite system. The pitch angle, θ, is measured from the δy axis to the gravity gradient boom, b. This angle is defined to be positive as rotated clockwise about the negative δz axis.

To begin the process in determining the equations of motion for this system, the position of each mass is determined in terms of the local reference, or body, frame. Since all masses are in the orbital plane, the position and velocity components along the third axis are zero. The three masses (tip-mass, main satellite bus, and balloon) have respective position vectors:

$$\vec{\delta r}_1 = \begin{pmatrix} \delta x_1 \\ \delta y_1 \end{pmatrix} = \begin{pmatrix} b\,\sin(\theta) \\ r_o + b\,\cos(\theta) \end{pmatrix} \tag{3.10}$$

$$\vec{\delta r}_2 = \begin{pmatrix} \delta x_2 \\ \delta y_2 \end{pmatrix} = \begin{pmatrix} -a\,\sin(\theta) \\ r_o - a\,\cos(\theta) \end{pmatrix} \tag{3.11}$$

$$\vec{\delta r}_3 = \begin{pmatrix} \delta x_3 \\ \delta y_3 \end{pmatrix} = \begin{pmatrix} \delta x \\ r_o + \delta y \end{pmatrix} \tag{3.12}$$

The velocity vectors in terms of the body frame are determined by taking the first derivative of the position vectors with respect to the inertial GCE frame according to Equation 3.13.

$$\dot{\vec{r}}_B^{\,I} = \dot{\vec{r}}_B^{\,B} + (\omega \times \vec{r}_B) \tag{3.13}$$

Using Equation 3.13 with ω equal to the angular velocity of the satellite system about the Earth,

$$\omega = \sqrt{\frac{\mu}{r_0^3}} \tag{3.14}$$

the velocities of each mass are calculated to be:

$$\dot{\vec{\delta r}}_1 = \begin{pmatrix} b\,\dot{\theta}\,\cos(\theta) - \omega\,\left(r_0 + b\,\cos(\theta)\right) \\ -b\,\dot{\theta}\,\sin(\theta) + \omega\,b\,\sin(\theta) \end{pmatrix} \tag{3.15}$$

$$\dot{\vec{\delta r}}_2 = \begin{pmatrix} -a\,\dot{\theta}\,\cos(\theta) - \omega\,\left(r_0 - a\,\cos(\theta)\right) \\ a\,\dot{\theta}\,\sin(\theta) - \omega\,a\,\sin(\theta) \end{pmatrix} \tag{3.16}$$

$$\dot{\vec{\delta r}}_3 = \begin{pmatrix} \dot{\delta x} - \omega\,\left(r_0 + \delta y\right) \\ \dot{\delta y} + \omega\,\delta x \end{pmatrix} \tag{3.17}$$

Next, the kinetic energy of the system is found by summing the kinetic energies of each mass.

$$T = \frac{1}{2}\,m_1\,\left(\dot{\vec{\delta r}}_1 \cdot \dot{\vec{\delta r}}_1^{\,t}\right) + \frac{1}{2}\,m_2\,\left(\dot{\vec{\delta r}}_2 \cdot \dot{\vec{\delta r}}_2^{\,t}\right) + \frac{1}{2}\,m_3\,\left(\dot{\vec{\delta r}}_3 \cdot \dot{\vec{\delta r}}_3^{\,t}\right) \tag{3.18}$$

The potential energy of the system is found in similar fashion by summing the gravitational potentials acting on each mass.

$$V = -\frac{\mu\,m_1}{\left|\vec{\delta r}_1\right|} - \frac{\mu\,m_2}{\left|\vec{\delta r}_2\right|} - \frac{\mu\,m_3}{\left|\vec{\delta r}_3\right|} \tag{3.19}$$

The denominators of the potential energies in Equation 3.19 are approximated using the binomial theorem expanded to order three.

$$(\alpha + \beta)^n = \alpha^n + n\,\alpha^{n-1}\,\beta + \frac{1}{2!}\,n\,\left(n-1\right)\,\alpha^{n-2}\,\beta^2 + ... \tag{3.20}$$

By making the following substitutions:

$$\alpha = {r_o}^2 \tag{3.21}$$

$$\beta = \left(2\, r_o\, y + y^2 + x^2\right) \tag{3.22}$$

where x and y are place holders for the corresponding components of the positions of each mass, δr_i, this approximation is carried out with the following results:

$$\begin{aligned}\left|\vec{\delta r}_1\right|^{-1} = {r_o}^{-1} - \frac{1}{2\,{r_o}^3}\left(2\, r_o\, b\,\cos(\theta) + b^2\,\cos(\theta)^2 + b^2\,\sin(\theta)^2\right) \\ + \frac{3}{8\,{r_o}^5}\left(2\, r_o\, b\,\cos(\theta) + b^2\,\cos(\theta)^2 + b^2\,\sin(\theta)^2\right)^2 + \vartheta\,(3)\end{aligned} \tag{3.23}$$

$$\begin{aligned}\left|\vec{\delta r}_2\right|^{-1} = {r_o}^{-1} - \frac{1}{2\,{r_o}^3}\left(-2\, r_o\, a\,\cos(\theta) + a^2\,\cos(\theta)^2 + a^2\,\sin(\theta)^2\right) + ... \\ + \frac{3}{8\,{r_o}^5}\left(-2\, r_o\, a\,\cos(\theta) + a^2\,\cos(\theta)^2 + a^2\,\sin(\theta)^2\right)^2 + \vartheta\,(3)\end{aligned} \tag{3.24}$$

$$\left|\vec{\delta r}_3\right|^{-1} = {r_o}^{-1} - \frac{1}{2\,{r_o}^3}\left(2\, r_o\,\delta y + \delta y^2 + \delta x^2\right) + \frac{3}{8\,{r_o}^5}\left(2\, r_o\,\delta y + \delta y^2 + \delta x^2\right)^2 + \vartheta\,(3) \tag{3.25}$$

The results of Equations 3.18 and 3.19 are used to define the Lagrangian.

$$L = T - V \tag{3.26}$$

The Lagrangian equations of motion are found for n-generalized coordinates by Equation 3.27.

$$\frac{d}{dt}\left(\frac{\partial\, L}{\partial\,\dot{q}_k}\right) - \left(\frac{\partial\, L}{\partial\, q_k}\right) = Q_k, k = 1, 2, ...n \tag{3.27}$$

For the generalized coordinates, δx, δy, and θ, the Lagrangian equations of motion are as follows:

$$m_3\,\ddot{\delta x} - 2\, m_3\,\omega\,\dot{\delta y} - \frac{3\, m_3\,\omega^2\,\delta y\,\delta x}{r_o} = Q_{\delta x} \tag{3.28}$$

$$m_3\,\ddot{\delta y} + 2\,m_3\,\omega\,\dot{\delta x} - 3\,m_3\,\omega^2\,\delta y - \frac{9\,m_3\,\omega^2\,\delta y^2}{2\,r_o} - \frac{3\,m_3\,\omega^2\,\delta x^2}{2\,r_o} = Q_{\delta y} \tag{3.29}$$

$$\begin{aligned} m_1 &\left(b^2\,\ddot{\theta} + 3\,\omega^2\,b^2\,\cos(\theta)\,\sin(\theta) + \frac{3\,\omega^2\,b^3}{2\,r_0}\,\sin(\theta)\right) \\ &+ m_2\,\left(a^2\,\ddot{\theta} + 3\,\omega^2\,a^2\,\cos(\theta)\,\sin(\theta) - \tfrac{3\,\omega^2\,a^3}{2\,r_0}\,\sin(\theta)\right) = Q_\theta \end{aligned} \tag{3.30}$$

The generalized forces, Q_k, are found according to Equation 3.31 in order to complete the equations of motion.

$$Q_k = \sum_{i=1}^{N} \vec{F}_i \cdot \frac{\partial\,\vec{r}_i}{\partial\,q_k} = \sum_{i=1}^{N} \vec{F}_i \cdot \frac{\partial\,\dot{\vec{r}}_i}{\partial\,\dot{q}_k} \tag{3.31}$$

The first force used in calculating the generalized forces is the force of drag acting on each mass, i.

$$\vec{F}_{drag_i} = -\frac{1}{2}\,C_{D_i}\,A_i\,\rho\,\left|\vec{V}_{rel_i}\right|^2\,\hat{V}_{rel_i} \tag{3.32}$$

A coefficient of drag, C_D, of 2 is generally the value used in analyzing objects in space. Also, the density, ρ, is approximated using an atmospheric model written by David Vallado at the Air Force Academy, which is provided in Appendix F. The relative velocity, $\vec{V_{rel}}$, is found by rotating the local velocity vector to the inertial reference frame and subtracting the velocity of the Earth's atmosphere.

$$\vec{V}_{rel_i} = Rot\,(\omega\,t)\,\dot{\vec{\delta r}}_i - \left(\omega_{Earth}\,\hat{z} \times Rot\,(\omega\,t)\,\vec{\delta r}_i\right) \tag{3.33}$$

The rotation matrix between the inertial and body frame is:

$$Rot\,(\phi) = \begin{pmatrix} -\sin(\phi) & \cos(\phi) & 0 \\ \cos(\phi) & \sin(\phi) & 0 \\ 0 & 0 & -1 \end{pmatrix} \tag{3.34}$$

The drag force is rotated back into the local body frame by multiplying it by the same rotation matrix shown in Equation 3.34.

The next forces considered in this case are the tension forces of the tether, modelled as spring forces, acting on each mass. These forces are modelled as a simple spring when

the tether is taut and are defined as:

$$\vec{F}_{spring_1} = \begin{cases} \vec{\tau}_1 \, E_1 \, (\gamma_1 - 1) \, , \gamma_1 > 1 \\ 0, \gamma_1 \leq 1 \end{cases} \tag{3.35}$$

$$\vec{F}_{spring_2} = \begin{cases} \vec{\tau}_2 \, E_2 \, (\gamma_2 - 1) \, , \gamma_2 > 1 \\ 0, \gamma_2 \leq 1 \end{cases} \tag{3.36}$$

The unit vectors, $\vec{\tau}$, along which the forces act are:

$$\vec{\tau}_1 = \frac{1}{\lambda_1} \begin{pmatrix} b \, \sin(\theta) - \delta x \\ b \, \cos(\theta) - \delta y \end{pmatrix} \tag{3.37}$$

$$\vec{\tau}_2 = \frac{1}{\lambda_2} \begin{pmatrix} -a \, \sin(\theta) - \delta x \\ -a \, \cos(\theta) - \delta y \end{pmatrix} \tag{3.38}$$

As explained in Section 3.1, the moduli of elasticity have units of Newtons per millimeter squared, but the cross-sectional area is assumed to be one millimeter squared. Based on this assumption, the moduli of elasticity are in units of Newtons in the equations of motion and in the computer simulation explained in Chapter IV. The quantities, γ, are defined by the ratio of the tether length at a certain time to the initial tether length:

$$\gamma_1 = \frac{\lambda_1}{\lambda_{10}} \tag{3.39}$$

$$\gamma_2 = \frac{\lambda_2}{\lambda_{20}} \tag{3.40}$$

The tether lengths, λ, at a certain time are defined by:

$$\lambda_1 = \sqrt{(b \, \sin(\theta) - \delta x)^2 + (b \, \cos(\theta) - \delta y)^2} \tag{3.41}$$

$$\lambda_2 = \sqrt{(-a \, \sin(\theta) - \delta x)^2 + (-a \, \cos(\theta) - \delta y)^2} \tag{3.42}$$

These forces are developed from equations of motion derived in Dynamics of Space Tethers by Beletsky and Levin for the motion of masses at the ends of a tether (3:42-48). These equations are altered in order to be used as generalized forces using the chosen generalized

coordinates. The motion of the end bodies is simplified by assuming a massless tether. This focuses the equations of motion for the system solely on the end masses. Equations 3.35 and 3.36 are conditionals which make an allowance for a slack tether since compression is not a factor when looking at the tether as a whole.

Similarly, a dissipative force must be added to account for energy losses due to each tether. This energy dissipation allows the system to stabilize over time. This damping is modelled as:

$$\vec{F}_{damper_1} = \begin{cases} c_1 \left(\dot{\vec{r}}_3 - \dot{\vec{r}}_1\right), \gamma_1 > 1 \\ 0, \gamma_1 \leq 1 \end{cases} \tag{3.43}$$

$$\vec{F}_{damper_2} = \begin{cases} c_2 \left(\dot{\vec{r}}_3 - \dot{\vec{r}}_2\right), \gamma_2 > 1 \\ 0, \gamma_2 \leq 1 \end{cases} \tag{3.44}$$

with damping coefficients for tether one and tether two, c_1 and c_2, respectively.

Considering the forces of drag and tether tensions described in Equations 3.32 through 3.44 and substituting into Equation 3.31, the generalized forces are:

$$\begin{aligned} Q_{\delta x} = \vec{F}_{spring_1} \cdot \frac{\partial\, \dot{\vec{\delta r}}_3}{\partial\, \dot{\delta x}} + \vec{F}_{spring_2} \cdot \frac{\partial\, \dot{\vec{\delta r}}_3}{\partial\, \dot{\delta x}} + \vec{F}_{damper_1} \cdot \frac{\partial\, \dot{\vec{\delta r}}_3}{\partial\, \dot{\delta x}} \\ + \ \vec{F}_{damper_2} \cdot \frac{\partial\, \dot{\vec{\delta r}}_3}{\partial\, \dot{\delta x}} + \vec{F}_{drag_3} \cdot \frac{\partial\, \dot{\vec{\delta r}}_3}{\partial\, \dot{\delta x}} \end{aligned} \tag{3.45}$$

$$\begin{aligned} Q_{\delta y} = \vec{F}_{spring_1} \cdot \frac{\partial\, \dot{\vec{\delta r}}_3}{\partial\, \dot{\delta y}} + \vec{F}_{spring_2} \cdot \frac{\partial\, \dot{\vec{\delta r}}_3}{\partial\, \dot{\delta y}} + \vec{F}_{damper_1} \cdot \frac{\partial\, \dot{\vec{\delta r}}_3}{\partial\, \dot{\delta y}} \\ + \ \vec{F}_{damper_2} \cdot \frac{\partial\, \dot{\vec{\delta r}}_3}{\partial\, \dot{\delta y}} + \vec{F}_{drag_3} \cdot \frac{\partial\, \dot{\vec{\delta r}}_3}{\partial\, \dot{\delta y}} \end{aligned} \tag{3.46}$$

$$\begin{aligned} Q_{\theta} = -\vec{F}_{spring_1} \cdot \frac{\partial\, \dot{\vec{\delta r}}_1}{\partial\, \dot{\theta}} - \vec{F}_{spring_2} \cdot \frac{\partial\, \dot{\vec{\delta r}}_2}{\partial\, \dot{\theta}} + \vec{F}_{damper_1} \cdot \frac{\partial\, \dot{\vec{\delta r}}_1}{\partial\, \dot{\theta}} \\ + \ \vec{F}_{damper_2} \cdot \frac{\partial\, \dot{\vec{\delta r}}_2}{\partial\, \dot{\theta}} + \vec{F}_{drag_1} \cdot \frac{\partial\, \dot{\vec{\delta r}}_1}{\partial\, \dot{\theta}} + \vec{F}_{drag_2} \cdot \frac{\partial\, \dot{\vec{\delta r}}_2}{\partial\, \dot{\theta}} \end{aligned} \tag{3.47}$$

The above generalized forces are then substituted into Equations 3.28 through 3.28 to get the final equations of motion for the two-dimensional case of the satellite concept depicted

in Figure 3.1.

$$m_3\,\ddot{\delta x} - 2\,m_3\,\omega\,\dot{\delta y} - \frac{3\,m_3\,\omega^2\,\delta y\,\delta x}{r_o} = -\frac{1}{2}\,C_{D_3}\,A_3\,\rho\,\left|\vec{V}_{rel3}\right|^2\,Rot\;(\omega\,t)\;\hat{V}_{rel3_{\delta x}} \tag{3.48}$$
$$+\;\begin{cases}((b\,\sin(\theta)) - \delta x)\,E_1\;(\gamma_1 - 1)\;\lambda_1^{-1}, \gamma_1 > 1\\ 0, \gamma_1 \le 1\end{cases}$$
$$+\;\begin{cases}((-a\,\sin(\theta)) - \delta x)\,E_2\;(\gamma_2 - 1)\;\lambda_2^{-1}, \gamma_2 > 1\\ 0, \gamma_2 \le 1\end{cases}$$
$$+\;\begin{cases}c_1\;\left(\dot{\delta x} - \omega\,\delta y - b\,\dot{\theta}\;\cos(\theta) + \omega\,b\;\cos(\theta)\right), \gamma_1 > 1\\ 0, \gamma_1 \le 1\end{cases}$$
$$+\;\begin{cases}c_2\;\left(\dot{\delta x} - \omega\,\delta y + a\,\dot{\theta}\;\cos(\theta) - \omega\,a\;\cos(\theta)\right), \gamma_2 > 1\\ 0, \gamma_2 \le 1\end{cases}$$

$$m_3\,\ddot{\delta y} + 2\,m_3\,\omega\,\dot{\delta x} - 3\,m_3\,\omega^2\,\delta y - \frac{9\,m_3\,\omega^2\,\delta y^2}{2\,r_o} - \frac{3\,m_3\,\omega^2\,\delta x^2}{2\,r_o} = \tag{3.49}$$
$$-\;\frac{1}{2}\,C_{D_3}\,A_3\,\rho\,\left|\vec{V}_{rel3}\right|^2\,Rot\;(\omega\,t)\;\hat{V}_{rel3_{\delta y}}$$
$$+\;\begin{cases}((b\,\cos(\theta)) - \delta y)\,E_1\;(\gamma_1 - 1)\;\lambda_1^{-1}, \gamma_1 > 1\\ 0, \gamma_1 \le 1\end{cases}$$
$$+\;\begin{cases}((-a\,\cos(\theta)) - \delta y)\,E_2\;(\gamma_2 - 1)\;\lambda_2^{-1}, \gamma_2 > 1\\ 0, \gamma_2 \le 1\end{cases}$$
$$+\;\begin{cases}c_1\;\left(\dot{\delta y} + \omega\,\delta x + b\,\dot{\theta}\;\sin(\theta) - \omega\,b\;\sin(\theta)\right), \gamma_1 > 1\\ 0, \gamma_1 \le 1\end{cases}$$
$$+\;\begin{cases}c_2\;\left(\dot{\delta y} + \omega\,\delta x - a\,\dot{\theta}\;\sin(\theta) + \omega\,a\;\sin(\theta)\right), \gamma_2 > 1\\ 0, \gamma_2 \le 1\end{cases}$$

$$m_1\,\left(b^2\,\ddot{\theta} + 3\,\omega^2\,b^2\;\cos(\theta)\;\sin(\theta) + \frac{3\,\omega^2\,b^3}{2\,r_0}\;\sin(\theta)\right) \tag{3.50}$$
$$+\;m_2\,\left(a^2\,\ddot{\theta} + 3\,\omega^2\,a^2\;\cos(\theta)\;\sin(\theta) - \frac{3\,\omega^2\,a^3}{2\,r_0}\;\sin(\theta)\right)\;=$$
$$-\;\frac{1}{2}\,C_{D_1}\,A_1\,\rho\,\left|\vec{V}_{rel1}\right|^2\,Rot\;(\omega\,t)\;\left(\hat{V}_{rel1_{\delta x}}\,b\,\cos(\theta) - \hat{V}_{rel1_{\delta y}}\,b\,\sin(\theta)\right)$$

$$
\begin{aligned}
&- \frac{1}{2} C_{D_2} A_2 \rho \left|\vec{V}_{rel2}\right|^2 Rot\ (\omega t) \left(\hat{V}_{rel2_{\delta x}} - a\ \cos(\theta) + \hat{V}_{rel2_{\delta y}}\ a\ \sin(\theta)\right) \\
&- \begin{cases} [(b\ \sin(\theta) - \delta x)\ b\ \cos(\theta) - (b\ \cos(\theta) - \delta y)\ b\ \sin(\theta)]\ E_1\ (\gamma_1 - 1)\ \lambda_1^{-1}, \gamma_1 > 1 \\ 0, \gamma_1 \leq 1 \end{cases} \\
&- \begin{cases} [(-a\ \sin(\theta) - \delta x)\ - a\ \cos(\theta) + (-a\ \cos(\theta) - \delta y)\ a\ \sin(\theta)]\ E_2\ (\gamma_2 - 1)\ \lambda_2^{-1}, \gamma_2 > 1 \\ 0, \gamma_2 \leq 1 \end{cases} \\
&+ \begin{cases} c_1 \left(b\ \cos(\theta) \left(\dot{\delta x} - \omega\, \delta y - b\, \dot{\theta}\ \cos(\theta) + \omega\, b\ \cos(\theta)\right)\right), \gamma_1 > 1 \\ 0, \gamma_1 \leq 1 \end{cases} \\
&+ \begin{cases} c_1 \left(-b\ \sin(\theta) \left(\dot{\delta y} + \omega\, \delta x + b\, \dot{\theta}\ \sin(\theta) - \omega\, b\ \sin(\theta)\right)\right), \gamma_1 > 1 \\ 0, \gamma_1 \leq 1 \end{cases} \\
&+ \begin{cases} c_2 \left(-a\ \cos(\theta) \left(\dot{\delta x} - \omega\, \delta y - b\, \dot{\theta}\ \cos(\theta) + \omega\, b\ \cos(\theta)\right)\right), \gamma_2 > 1 \\ 0, \gamma_2 \leq 1 \end{cases} \\
&+ \begin{cases} c_2 \left(a\ \sin(\theta) \left(\dot{\delta y} + \omega\, \delta x + b\, \dot{\theta}\ \sin(\theta) - \omega\, b\ \sin(\theta)\right)\right), \gamma_2 > 1 \\ 0, \gamma_2 \leq 1 \end{cases}
\end{aligned}
$$

These equations of motion are used in a fourth-order Runge-Kutta numerical integrator which propagates the system parameters, δx, δy, and θ forward in time. These equations of motion are solved for the accelerations before being used in the numerical integrator, which is described further in Section 4.3.

IV. Methodology

The program used to simulate the attitude of this satellite concept is described in this section. While defining the equations of motion is paramount to creating a simulation, writing this program has been the pith of this study. Contained in this chapter is a description of the simulation program in terms of the satellite values tested. A general program algorithm is provided that describes the simulation at the conceptual level. The chapter also describes the approach taken to run the simulations whose results are found in Chapter V and discusses the method of program validation. The actual code of the program is provided in Appendices A through H. The program code has been separated into each subprogram and is generally listed in the order in which it is called. Contained within each program code in the appendices is an algorithm as well as a list of variables, constants, and coupled programs.

4.1 Satellite Characteristics

The characteristics of the satellites used in this simulation represent modest estimations of microsatellites with a gravity gradient boom. Since no satellite similar to that depicted in Figure 3.1 exists, each variable either was defined by comparison to similar satellite components or by determining a range of values through iterative simulation. The satellite specifications used in this study are listed in Table 4.1.

The listed units are the same units used within the simulation program with the exception of the moduli of elasticity. As stated in the assumptions, the listed moduli of elasticity are first multiplied by the assumed cross-sectional area of the tethers, which is one millimeter squared, before being used in the simulation. Also, the listed moduli of elasticity and damping coefficients are nominal values for each satellite. These were found by iteration of the simulation, which is described further in Chapter V. For these characteristics, many values are possible within a range dependent on stability and performance specifications. This is also discussed in Chapter V.

The first satellite, Satellite I or SatI, to be modelled represents a very general case. The values for this satellite are a compromise between reality and simplicity. For example, these general values make the calculations for the position of the center of mass (COM) and

Table 4.1 Satellite Specifications

Variable	Symbol	Satellite I	Satellite II	DumbSat	Units
Tip-Mass	mone	10	3	50	kg
Main Bus Mass	mtwo	100	70	50	kg
Balloon Mass	mthree	1	0.5	1	kg
Tip-Mass Frontal Area	areaone	0.1	0.0231	0.2	m^2
Main Bus Frontal Area	areatwo	0.5	0.2275	0.2	m^2
Balloon Frontal Area	areathree	5	2	2	m^2
Boom Length	a + b	6	5	5	m
Tip to COM Distance	b	5.5	4.7945	2.5	m
Bus to COM Distance	a	0.5	0.2055	2.5	m
T1 Taut Length	lonenote	6	5	5	m
T2 Taut Length	ltwonot	6	5	5	m
T1 Modulus of Elasticity	Eone	0.002065	0.0003	0.00317	N/mm^2
T2 Modulus of Elasticity	Etwo	0.0202	0.006	0.00317	N/mm^2
T1 Damping Coefficient	cone	0.0007	0.0007	0.0016	Ns/m
T2 Damping Coefficient	ctwo	0.0007	0.0007	0.0016	Ns/m

inertia matrix easier. Although the values are realistic, they do not represent a microsatellite as well as the second satellite. The main criteria for the first satellite is that it be a stable gravity gradient satellite. The criteria for stability is to have the principle moments of inertia be such that the major axis (C) points normal to the orbit, the intermediate axis (B) points in the velocity direction, and the minor axis (A) points in the radial direction. This stability criteria is explained further in Section 2.2 and Section 4.4. The equations and values for the moments of inertia are outlined in Section 4.4.

Satellite II, or SatII, uses more realistic values to increase the validity of the results. For example, the mass of the main satellite bus was taken from a range of values given by Surrey Satellite Technology Ltd. Their information was used because their flight-proven systems are designed with the microsatellite concept in mind (4). In addition, the specifications for the gravity gradient boom were defined based on information provided on an actual boom created by Northrop-Grumman specifically for microsatellites (11).

The last satellite tested, DumbSat, is essentially a dumbbell configuration. This satellite tests a completely different configuration from Satellite I, adding a breadth to the simulation results. Also, the tether characteristics for a stable configuration are more intuitive. Since both ends of DumbSat are equal in mass, length, and frontal area, the attached equal length tethers should have equal characteristics.

4.2 Simulation Approach

In the simulations run, each satellite described in Table 4.1 is simulated with the initial generalized coordinates in Table 4.2. The velocity terms for each generalized coordinate are

Table 4.2 Initial Generalized Coordinates

Generalized Coordinate	Variable	SatI	SatII	DumbSat	Units
Balloon Position in x-direction	δx	-3.25	-2.6028	-3.75	meters
Balloon Position in y-direction	δy	4.7631	4.1522	2.1651	meters
Pitch of Gravity Gradient Satellite	θ	$\pi/6$	$\pi/6$	$\pi/6$	radians

assumed to be zero in all cases. Each simulated satellite also begins at the same position as described in Table 4.3 for the satellite center of mass. These initial coordinates simulate

Table 4.3 Initial Inertial Coordinates

Inertial Coordinate	Value	Units
R_x	6578.1	kilometers
R_y	0	kilometers
R_z	0	kilometers
V_x	0	kilometers/sec
V_y	7.7843	kilometers/sec
V_z	0	kilometers/sec

a circular, equatorial satellite. Although an equatorial orbit is not an assumption, a non-equatorial orbit would provide the same results since a spherical Earth is assumed. In addition, the number of steps and step size varied depending on what was the aim of the simulation. For example, to get a general picture of a certain case, fewer steps allows the simulation to run faster. On the other hand, more steps are required when measurements are taken directly from the graph. The number of steps is also constrained by the numerical integrator, discussed further in Section 4.3. A small number of steps decreases accuracy because there are not enough data points to produce an accurate graph, but a large number of steps results in a longer run time for the simulation. The number of steps and interval for each presented simulation result is detailed in the corresponding section of the report or graph.

4.3 Program Algorithm

The algorithm of this program stems from a basic orbit prediction program self-written for an undergraduate degree. The original program uses a method called Cowell to predict and track the position of a satellite using the two-body equations of motion and certain orbital perturbations, like drag and the effects of the Earth's oblateness. That algorithm has been adapted to use the equations of motion described in Section 3.4 and produce results that are used to determine this satellite concept's feasibility.

The numerical integrator is to simulate the motion of the satellite was coded in Matlab. The equations of motion derived in Section 3.4 are rearranged slightly to solve for acceleration and placed into a fourth order Runge-Kutta numerical integrator. The Runge-Kutta numerical integrator is based on Equation 4.1 (2:414).

$$\mathbf{X}_{n+1} = \mathbf{X}_n + \frac{1}{6}\left(k_1 + 2\,k_2 + 2\,k_3 + k_4\right) \tag{4.1}$$

In this equation, the k's are defined as:

$$k_1 = h\,f\left(t_n, \mathbf{X}_n\right) \tag{4.2}$$

$$k_2 = h\,f\left(t_n + \frac{h}{2}, \mathbf{X}_n + \frac{k_1}{2}\right) \tag{4.3}$$

$$k_3 = h\,f\left(t_n + \frac{h}{2}, \mathbf{X}_n + \frac{k_2}{2}\right)$$

$$k_4 = h\,f\left(t_n + h, \mathbf{X}_n + k_3\right)$$

where h is the step size and the function $f\left(t, \mathbf{X}\right)$ is equal to the derivative of the state vector or $\dot{X}$. This integrator is normally used for a state vector, $\mathbf{X}$, with six variables - three position vectors and three rate vectors. According to Bate, Mueller, and White, the Runge-Kutta algorithm is stable and has a small truncation error (2:415).

To use this integrator, the simulation program begins by declaring all constants and satellite variables as listed in Table 4.1. Second, the number of steps and the step size are defined based on the period of the orbit and the number of orbits intended for inclusion. Then, the program iterates through the number of steps in increments of the defined step

size, calling subprograms that determine the future position of the center of mass as well as the three masses of the satellite system. These subprograms calculate the state vector and its derivative, which depends on the position of the balloon. If the balloon's position causes either tether to be taut, then that tether's spring and damping forces are included in the equations of motion. The state vector and its derivative are then used in Equation 4.1 to calculate the future state vector. At each time step, the state vector is recorded so that at the end of the program a plot can be made of the progress of δx, δy, and θ.

4.4 Program Validation

In order to determine whether the Matlab simulation program functions properly, a case has been run which has known results. The case of a satellite with a gravity gradient boom without the effects of drag has a known response to initial conditions so it was used to test the computer simulation of this satellite concept. For this case, the forces due to the tether have been neglected regardless of the position of the balloon mass. The resulting oscillations in pitch angle, θ, have a predictable frequency that is dependent on the principal moments of inertia. Using the specifications for each satellite listed in Table 4.1 and assuming a box-shaped main satellite bus and tip-mass, the principal moments of inertia were calculated using the following equation:

$$I_{xx} = I_{yy} = I_{zz} = \frac{1}{12}\, m\, (2 \cdot Area) \tag{4.4}$$

where Area is the frontal area (1:702). The resulting principal moments of inertia for the gravity gradient portions of each satellite are listed in Table 4.4. These values are based on θ equal to zero. The frequency of oscillations in the pitch direction, n_p, has a predictable

Table 4.4 Principal Moments of Inertia

Principal Axis	Satellite I	Satellite II	DumbSat	Units
Minor Axis (B)	336	74.583	628	kg/m^2
Intermediate Axis (A)	8.5	2.666	3.333	kg/m^2
Major Axis (C)	336	74.583	628	kg/m^2

value as defined by Equation 4.5 and has units of radians per second (17:153).

$$n_p = \left[\frac{3\,\mu\,(B-A)}{r_{com}^3\,C}\right]^{1/2} \tag{4.5}$$

The resulting predicted oscillation frequencies for the pitch angle are listed in Table 4.5.

Table 4.5 Frequencies of Pitch Angle Oscillation

Result	Satellite I	Satellite II	DumbSat	Units
Predicted	0.002024	0.002013	0.002044	rad/sec
Simulated	0.00190978	0.00190851	0.00190974	rad/sec
Percent Error	5.68	5.17	6.60	Percent

The simulated values were calculated by examining the output graph of pitch angle, θ, versus time. The output for Satellite I is provided in Figure 4.1, and the simulated oscillation frequency is listed in Table 4.5. The interval in this test is two periods with 400 steps. Sequential maximums are recorded to determine the period in terms of number of

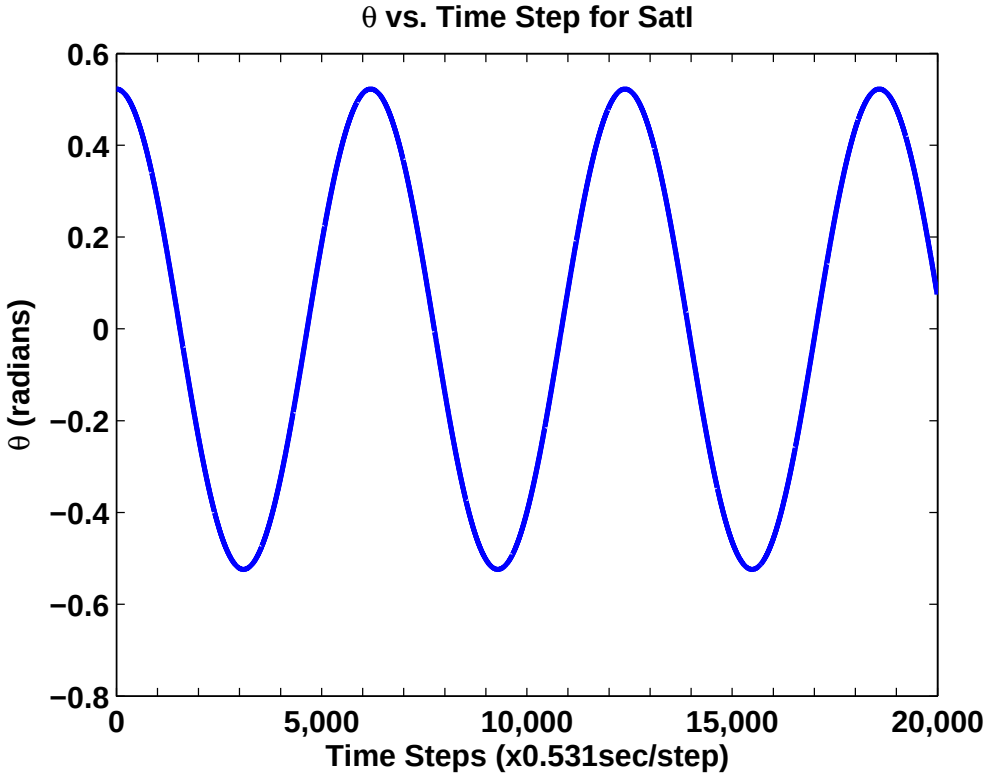

Figure 4.1 Simulated Results for Oscillation Frequency Validation for SatI

steps, X. The oscillation frequency is then found by Equation 4.6.

$$n_p\,(simulated) = \frac{2\,\pi}{stepsize \cdot X} \tag{4.6}$$

The step size has units of seconds per step, and the resulting frequency from Equation 4.6 is in units of radians per second.

This test case was also run for Satellite II. The results are also in Tables 4.4 and 4.5, while the output for Satellite II is provided in Figure 4.2. This test case was also run for

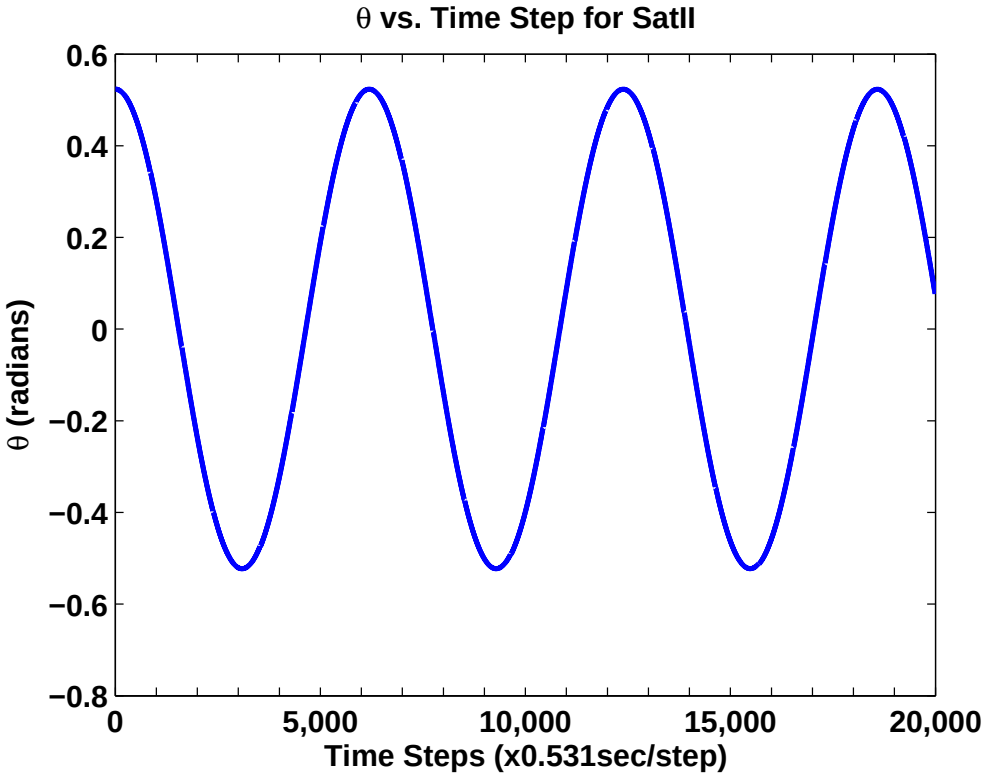

Figure 4.2 Simulated Results for Oscillation Frequency Validation for SatII

DumbSat. The results are also in Tables 4.4 and 4.5. The output is provided in Figure 4.3.

It is important to note that all of these graphs show pitch angle oscillations varying between $\pi/6$ and negative $\pi/6$, and these oscillations do not dampen. Hughes, mentioned previously in Section 2.2, points out that certain satellite configurations produce oscillations with marginal stability. One of these configurations is when k_3 is approximately zero and

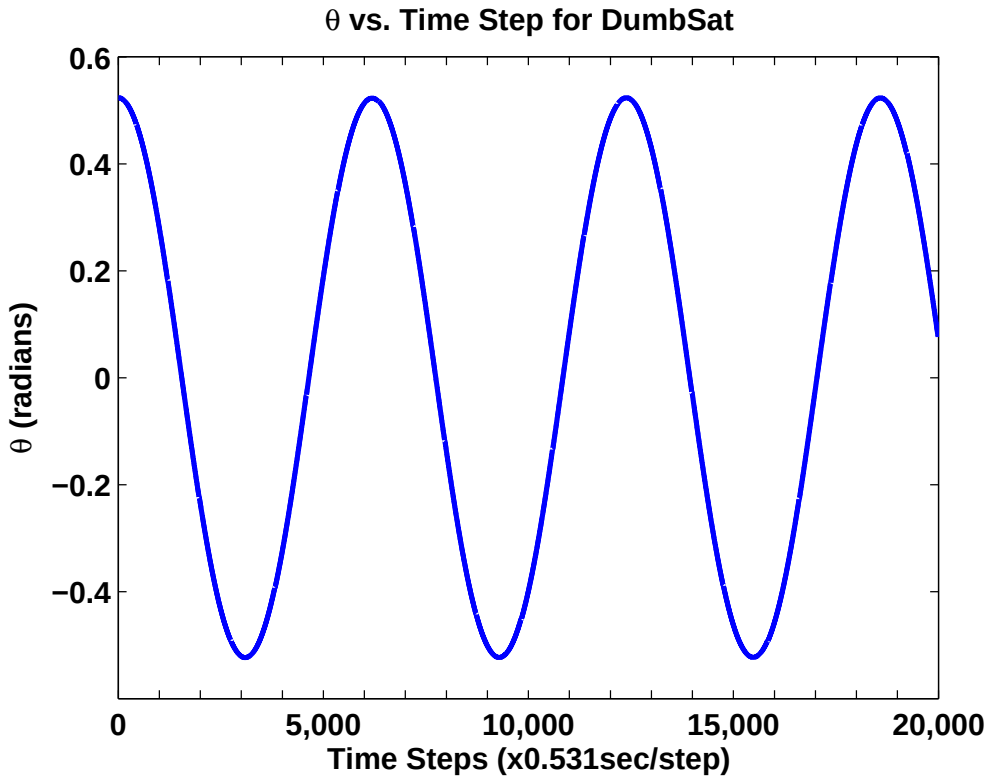

Figure 4.3 Simulated Results for Oscillation Frequency Validation for DumbSat

when k_1 is positive (6:302). This is equivalent to a slender rod with the long axis pointed in the radial direction. As seen in Figure 3.1, these satellites closely resemble slender rods with the long axis pointed in the radial direction. Furthermore, marginal stability is characterized by an inability to dampen oscillations in a specified direction. As shown in the results of this test case, none of the satellites have pitch angle graphs that decrease in amplitude, demonstrating marginal stability.

These three tests demonstrate the accuracy of the system in that they have very low percent error. Using the three satellites also shows consistency and a breadth in usability for the simulation. The error in the simulated results stems from the assumptions made, mainly that there is no motion outside of the orbital plane. Because of this assumption, the dynamics and simulation do not account for any rolling or yawing motions. Also, these satellites are quite similar and therefore have similar oscillation frequencies.

V. Results

After the program was written and validated, the focus was placed on the main research objective, determining whether passive attitude stabilization can be achieved by manipulating aerodynamic and gravity gradient torques. Attention was first placed on determining the effect of altering the modulus of elasticity for the two tethers in the satellite system. Once a stable oscillation, or acceptable steady state pitch angle, was observed, the damping coefficients were then altered to determine their impact on the system. It was also important to ascertain a legitimate damping of the pitch angle over a limited time, which is the same as an acceptable settling time. These factors were then broken down into forces applied on each mass for each generalized coordinate. Once the influence of these forces was understood, the regions of stability for the moduli of elasticity and damping coefficients were determined for the three satellites. This analysis was first performed on Satellite I so the first set of results discussed are all for this satellite. The results of Satellite II and DumbSat are provided following the analysis of Satellite I.

5.1 Modulus of Elasticity

The modulus of elasticity was the first variable to be inspected. This is the first simulation to include the effects of the attached balloon mass and air drag acting on all three masses. The damping coefficient was held constant at zero to isolate the effects of the moduli of elasticity on the system. This simulation was iterated until an acceptable value for the moduli of elasticity was found which produced a stable system. For these iterative simulations, the inspected time interval was five periods with 1500 steps and a step size of 17.7 seconds. After iterating through this case, an acceptable pitch angle output was established for E_1 equal to 0.002065 N/mm^2 and E_2 equal to 0.0202 N/mm^2, shown in the output graph of pitch angle,θ, in Figure 5.1.

The nominal moduli of elasticity found are very small values when compared to typical materials used for space tethers. As shown in Table 5.1, typical moduli of elasticity have values several orders of magnitude greater than the values found for the nominal case. This is due in part on the application of typical space tethers. In general, space tethers are not intended to be used as springs but are used more to hold components together at a certain distance. In this satellite concept, the moduli of elasticity are intended to act as springs

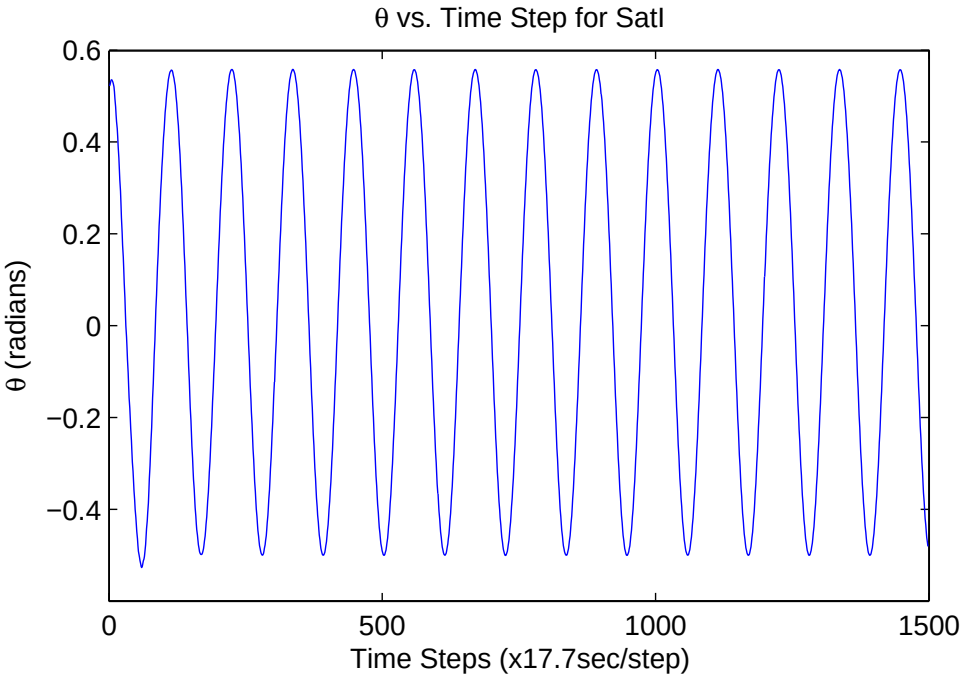

Figure 5.1 Nominal Moduli of Elasticity for SatI

Table 5.1 Moduli of Elasticity for Space Tethers (3:35)

Material	Modulus of Elasticity (kN/mm^2)	Percent Elongation
Kevlar-49	130	2.5
Alloyed Aluminum	70	10
Stainless Steel	200	1.4

so that a damping coefficient can be added in a realistic manner. Table 5.2 lists moduli of elasticity closer to those found in the simulation. Although there is no known flight

Table 5.2 Moduli of Elasticity for Possible Tethers (10)

Material	Modulus of Elasticity (N/mm^2)	Percent Elongation
Silastic (R) 24005 Silicon Rubber	0.0588	950
Silastic (R) 24064 Silicon Rubber	0.1449	790
Silastic (R) 29051 Silicon Rubber	0.2373	436

experience of these materials, they are able to operate in temperatures well below freezing (10).

The average of the pitch angles for the entire interval is 0.0412 radians or 2.36 degrees and is within a very small margin of error from the ideal zero degree angle. This average pitch angle correlates to a gravity gradient satellite with the main satellite in a nadir pointing

configuration. This system is acceptable since it is marginally stable as the oscillations do not extend beyond the initial amplitude. Also in Figure 5.1, the pitch angle is oscillating between positive $\pi/6$, which is the initial pitch angle value, and negative $\pi/6$. This correlates to the gravity gradient portion of the satellite oscillating like an undamped pendulum. This is expected for a marginally stable gravity gradient satellite.

Figure 5.2 shows the motion of the balloon mass for the coordinate δx. The values of

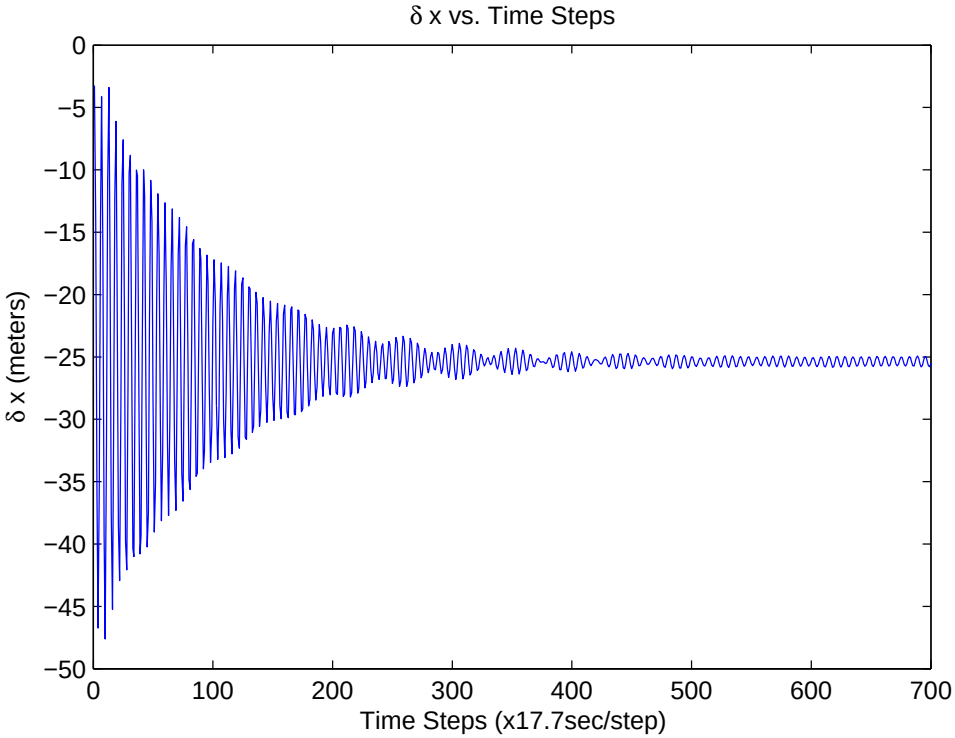

Figure 5.2 Nominal Moduli of Elasticity for SatI

δx continue to oscillate in this case because the pitch angle of the gravity gradient portion of the satellite oscillates in an undamped manner. Figure 5.2 shows that, while the taut length of the tether is set to six meters, the steady state length is about 25.25 meters. This is as if the spring has reached its maximum length or is completely stretched. Table 5.1 also includes percent elongation for typical tether materials while Table 5.2 includes values for possible materials. The main difference in values is again attributed to the difference in applications. The tethers in this satellite concept are intended to act as springs, and springs typically extend much further than the initial taut length.

Figure 5.3 shows the motion of the balloon for δy over the simulated interval. The

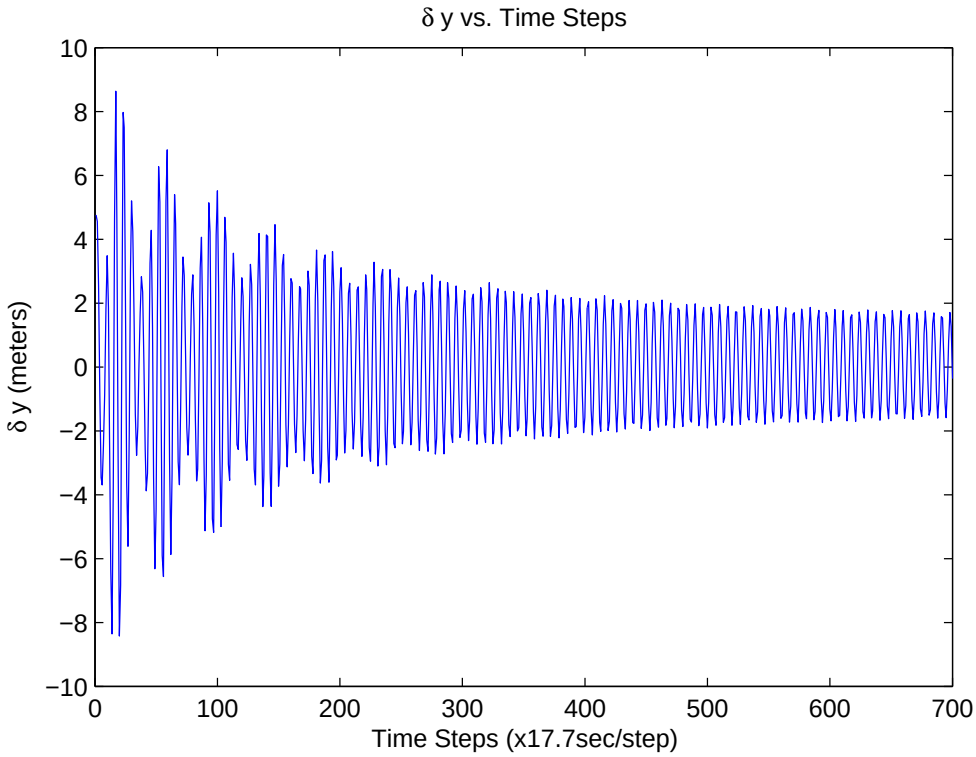

Figure 5.3 Nominal Moduli of Elasticity for SatI

balloon mass is oscillating in the vertical direction between approximately positive and negative two meters. This is also due to the oscillation in the pitch angle.

An analysis was also conducted for unacceptable values for moduli of elasticity. When the modulus of elasticity was well out of range, it was easy to see that the pitch angle spun off into infinity. An example is shown in Figure 5.4 where E_1 is equal to 0.0030975 N/mm^2 and E_2 is equal to 0.0202 N/mm^2. The pitch angle values are limited to between negative two pi and positive two pi in the figure so when the satellite tumbles past two pi radians or 360 degrees, the graph shows pitch angles going from two pi directly back to zero. Since Figure 5.4 shows the pitch angle continually doing this, the simulated satellite is actually unstable and is tumbling end-over-end. This shows the volatility of the system since the modulus of elasticity for tether one is only fifty percent more than its nominal value of 0.002065 N/mm^2.

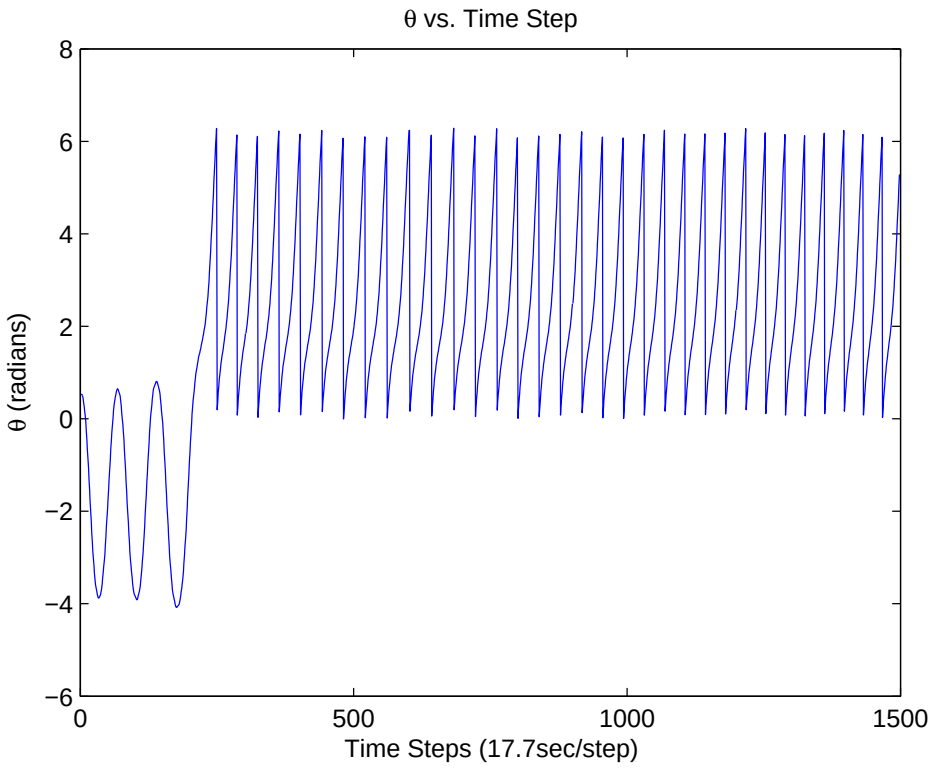

Figure 5.4 Modulus of Elasticity Out of Range by 50 Percent for SatI

Furthermore, it was necessary to observe the average of the pitch angles to ensure that it was stabilizing to zero degree. This corresponds to the nadir pointing orientation. An example of pitch angles oscillating about a non-zero value is shown in Figure 5.5 where E_1 is equal to 0.0022715 N/mm^2 and E_2 is equal to 0.0202 N/mm^2. The average in this case is -1.5504 radians, which corresponds to oscillations about ninety degrees off the vertical axis. If damping were added to this case, the satellite would be oriented with the main satellite mass pointed in the ram direction and the tip mass trailing directly behind in the horizontal direction. This may be desired in certain missions, but that is not the intended steady state orientation of this simulation.

The impact of increasing and decreasing either moduli of elasticity is also important to know when attempting to alter the system to meet certain criteria. As shown in Figure 5.5, increasing the first tether's modulus of elasticity decreases the average pitch angle; therefore, a decrease in the first tether's modulus of elasticity increases the average pitch angle. The opposite is true for the second tether's modulus of elasticity. A change in the

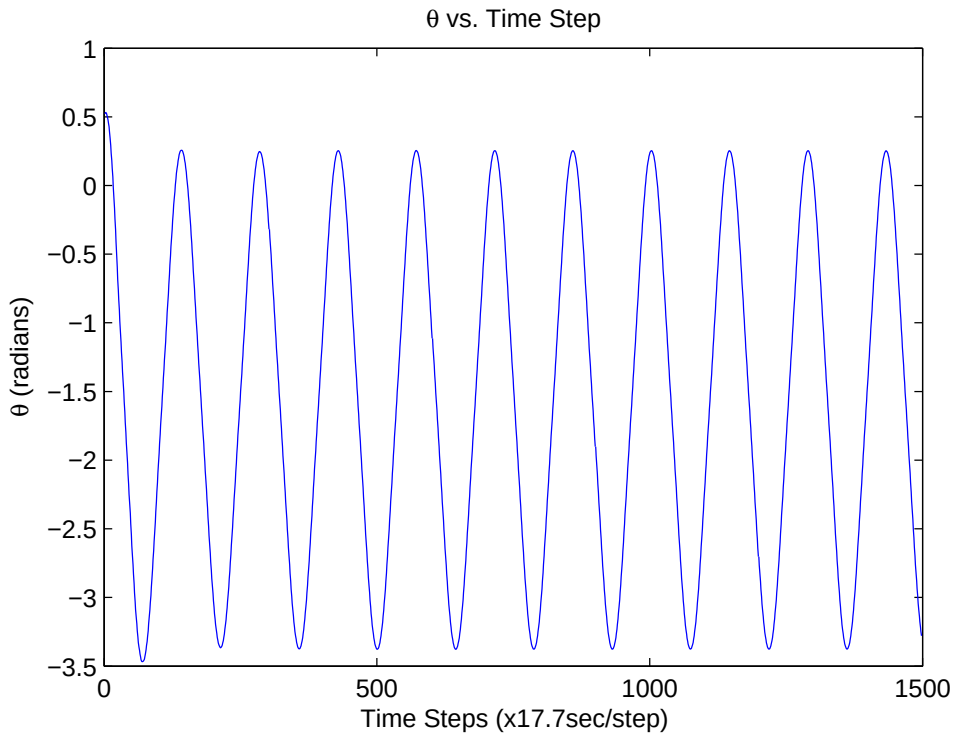

Figure 5.5 Modulus of Elasticity Out of Range by 10 Percent for SatI

second modulus of elasticity has a directly proportional impact on the average pitch angle. For example, increasing the second modulus of elasticity increases the average pitch angle.

5.2 Damping Coefficient

The next variables introduced into the system are the damping coefficients for both tethers, which simulate energy dissipation in the tethers due to real-world imperfections. This first-level inspection of damping coefficient is important to establish that this satellite characteristic is the major factor in damping down the oscillating pitch angle. The criteria for this variable is that the average pitch angle stays close to zero degree. Second, the settling time for the satellite system must be within three days, which equates to about fifty orbits for a 200 kilometer altitude, circular orbit. The last criteria is that the forces exerted on each mass and the value for the damping coefficient cannot be too excessive. In terms of the former, large forces exerted on the masses could cause the tethers, tether connections, or on-board instruments to fail. In terms of the latter, the damping coefficient should not

be too large as this variable is only meant to model imperfections in the tether material. In reality, energy would be lost through the tether in the form of radiation to space so an overly large damping coefficient would be unrealistic.

During these simulations, the inspected time interval was fifty periods with 10,000 steps and a step size of 26.55 seconds. This case was run with the nominal moduli of elasticity shown in Table 4.1 and depicted in Figures 5.1 through 5.3. Nominal values for damping coefficients were found around 0.0007 Ns/m for both tethers for Satellite I. The results, shown in Figure 5.6, had an average of 0.02 radians and settled to 0.0219 radians after a little over two days.

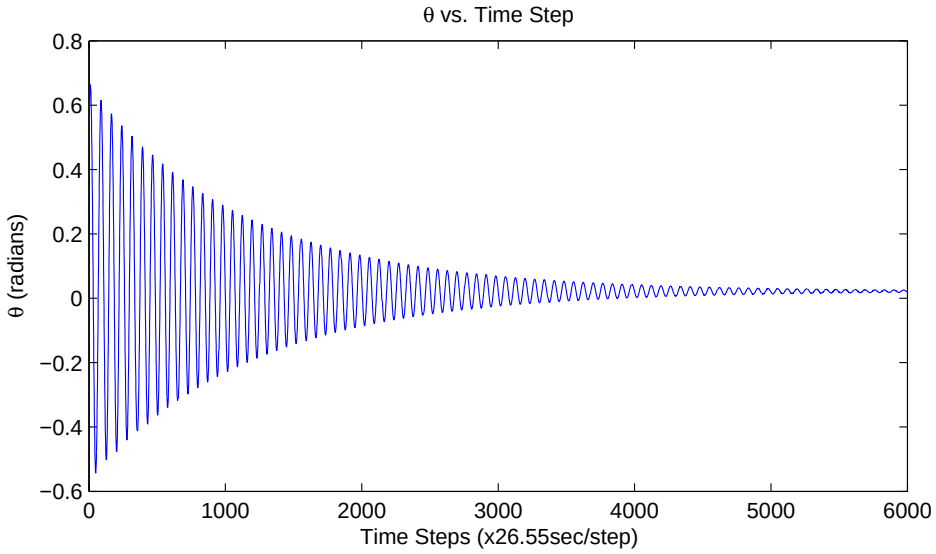

Figure 5.6 Stable Damping Coefficients for SatI

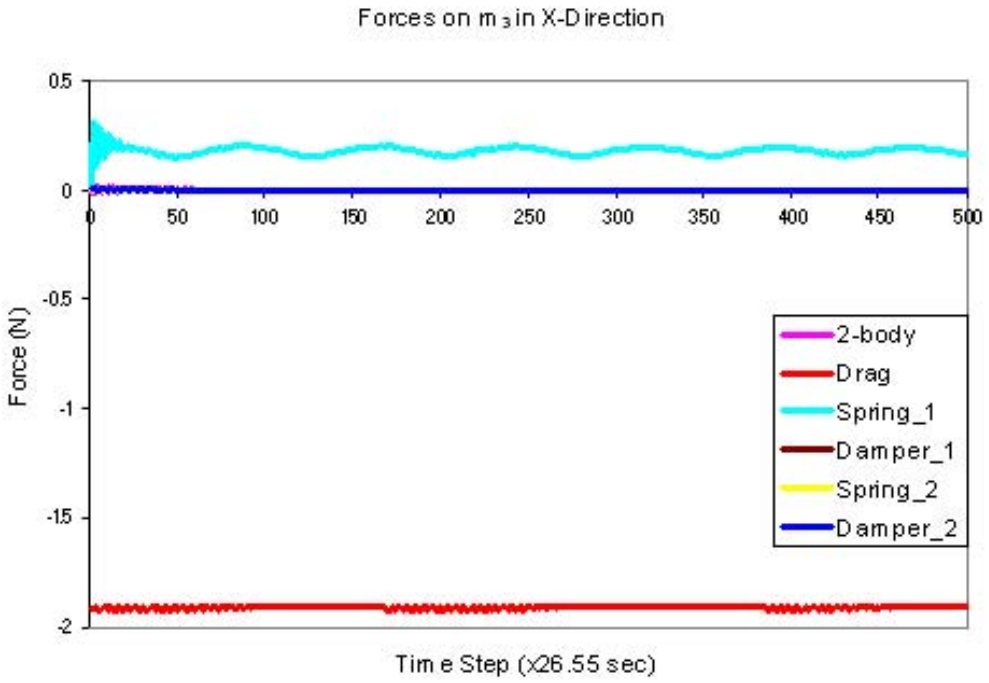

Figure 5.7 Forces Acting on Balloon Mass in X-Direction for SatI

The forces acting on each generalized coordinate are shown in Figures 5.7 through 5.12. The first graph shows the impacts of each force on δx. The maximum force felt by the balloon in the x-direction is about two Newtons. The major forces acting on the balloon

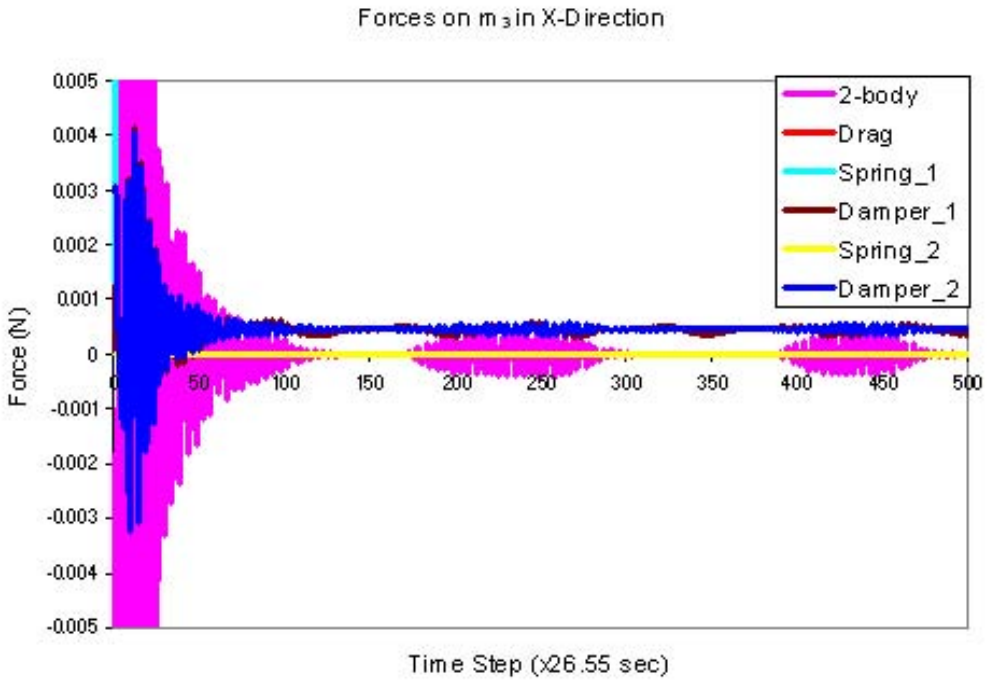

Figure 5.8 Zoomed In View of Forces Acting on Balloon Mass in X-Direction for SatI

mass in the x-direction are drag and the spring force of tether one. The drag force pulls the balloon mass in the negative velocity direction while the spring force from tether one pulls it in the positive velocity direction. The forces due to the second spring, both tether damping effects, and two-body effects are very small so that region is expanded in Figure 5.8.

Figure 5.9 shows the impact of each force on the balloon mass in the δy coordinate. The maximum force felt by the balloon in the y-direction is about 1.2 Newtons. The major forces acting on the balloon mass in the y-direction are the damping forces of each tether. This shows that the damping forces of each tether are the dominating mechanism in settling the balloon mass to a certain value in the radial or vertical direction. Each force except the first and second dampers are very small so the region close to zero Newtons is expanded in Figure 5.10. These show that the damping force and spring force for each tether act in opposition, as is the case for spring-damper systems.

Figure 5.11 shows the impacts of each force on θ. The maximum force felt by the gravity gradient portion of the satellite system is 102 Newtons. The dominating forces for

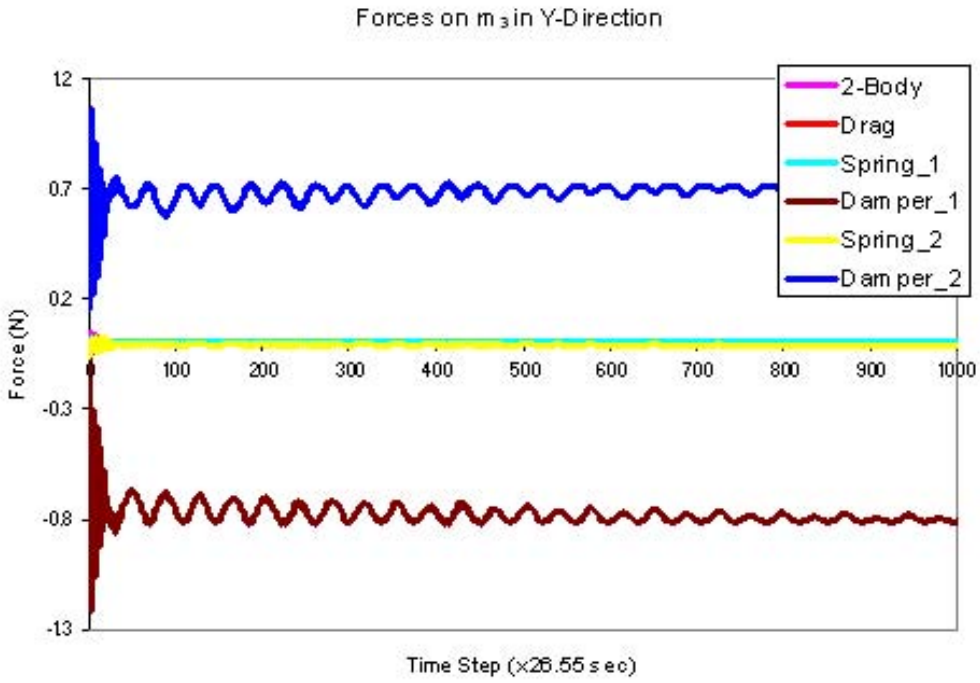

Figure 5.9 Forces Acting on Balloon Mass in Y-Direction for SatI

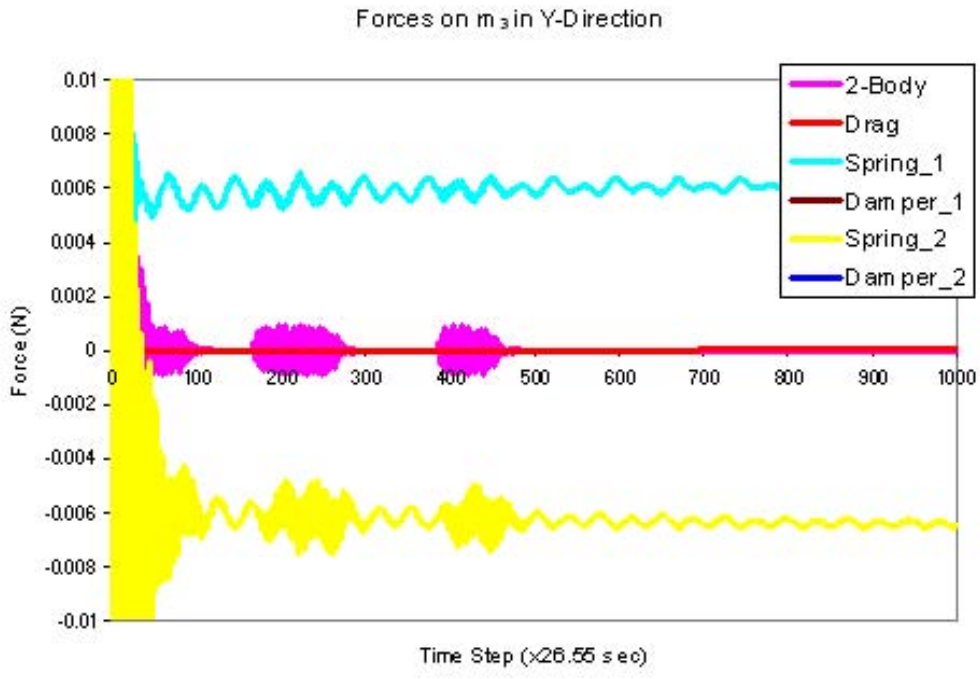

Figure 5.10 Zoomed In View of Forces Acting on Balloon Mass in Y-Direction for SatI

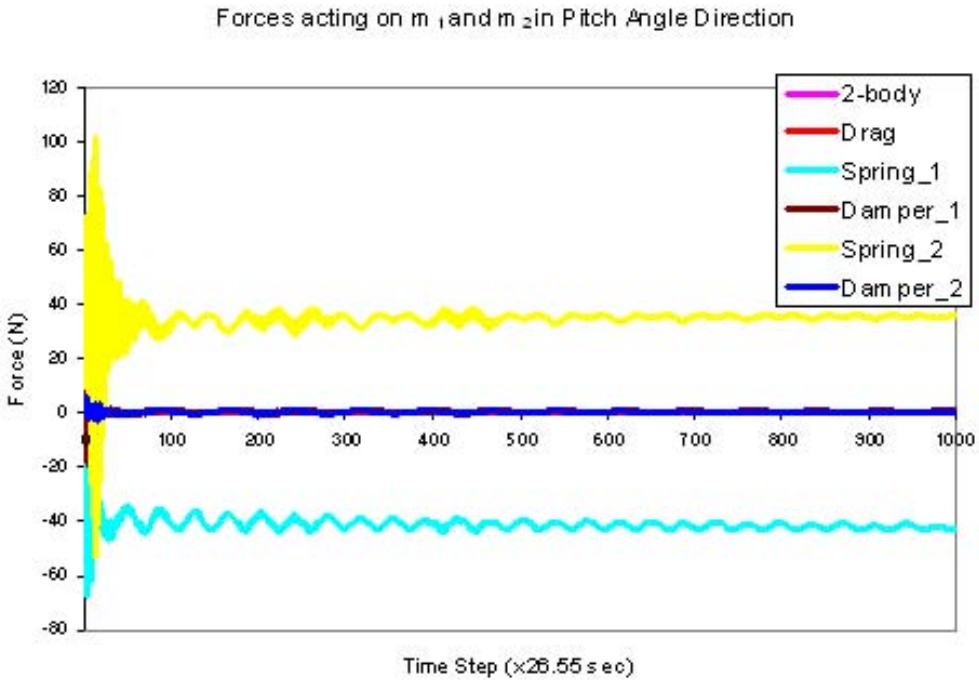

Figure 5.11 Forces Acting on Tip-Mass and Main Bus Mass along θ for SatI

this coordinate are the spring forces of both tethers. Each force except the first and second springs are very small so that region is expanded in Figure 5.12.

In analyzing the effect of damping coefficient on pitch angle stability, it can be seen that there are upper and lower ranges. The lower range fails to meet the settling time requirement of three days. This lower limit is dependent on other satellite characteristics, like moduli of elasticity, the masses of each system part, and the gravity gradient boom length. In the case of Satellite I and using the nominal moduli of elasticity in Table 4.1, the lower limits for the damping coefficients are illustrated in Figure 5.13.

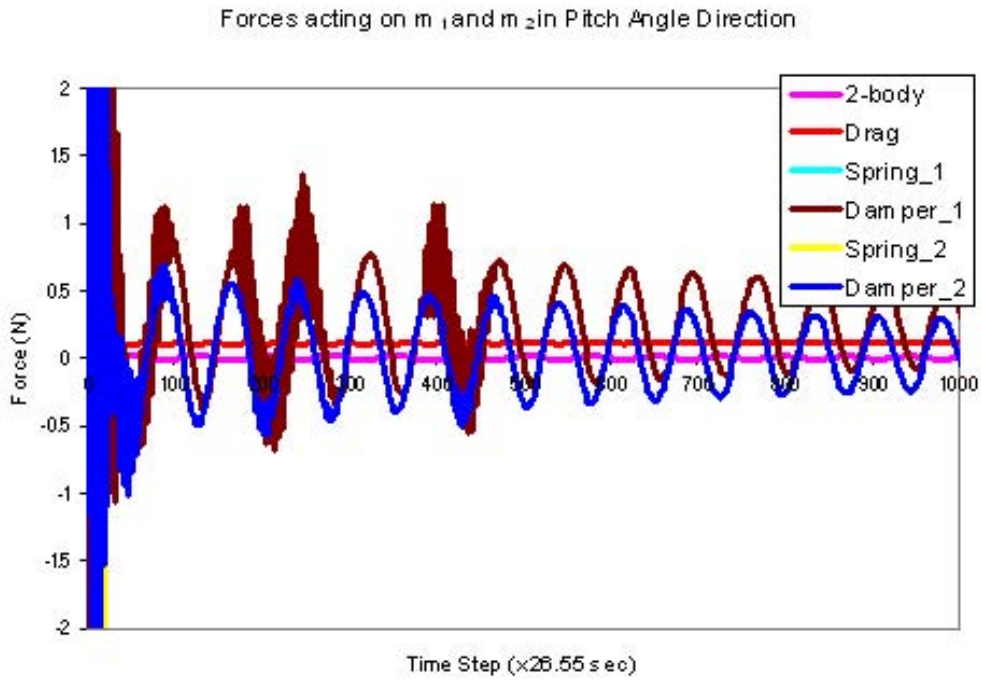

Figure 5.12 Zoomed In View of Forces Acting on Tip-Mass and Main Bus Mass along θ for SatI

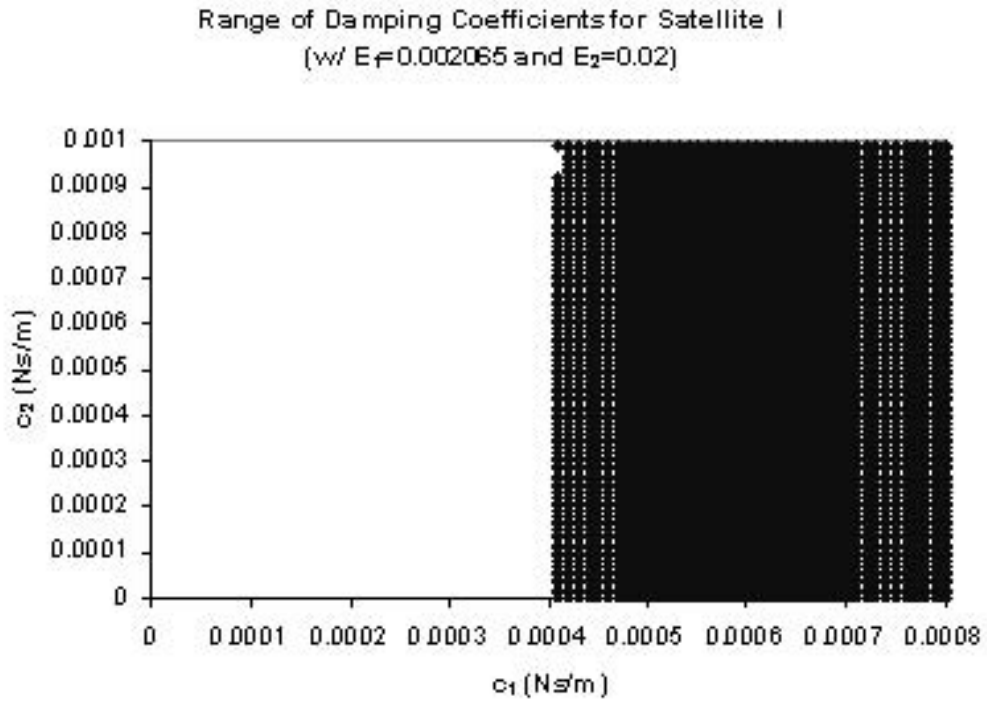

Figure 5.13 Stability Region for Damping Coefficients for SatI

On the other hand, the upper range produces pitch angles which are above the desired average. When the nominal damping coefficients are multiplied by ten, the result is as shown in Figure 5.14. The steady state pitch angle for this case is 3.18 or about π

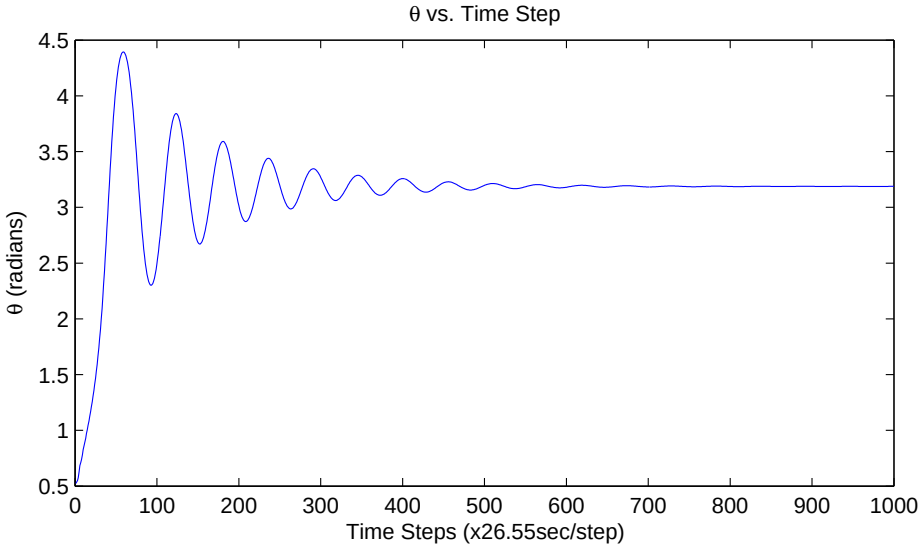

Figure 5.14 Damping Coefficients Out of the Desired Range for SatI

radians. This is the same as the satellite being oriented upside-down at steady state, which is possible in normal gravity gradient satellites as well. One problem with normal gravity gradient satellites is that the upside-down orientation is actually an equilibrium point and has been the result for some gravity gradient satellites. If the damping coefficient is not modelled correctly, an upside-down orientation is a possibility. Just as normal gravity gradient satellites require a mechanism to avoid the upside-down orientation, gravity gradient satellites with a tethered balloon may require such a mechanism if the tether characteristics are not modelled and designed correctly.

In addition, the forces applied to each mass were also increased. The maximum force felt by the balloon in the x-direction is about 1.9 Newtons, as shown in Figure 5.15. The dominating forces on the balloon in this direction is the spring force of the first tether and the drag force, which remains the same from the nominal damping coefficients results. Each force except the first spring force and drag are very small so that region is expanded in Figure 5.16.

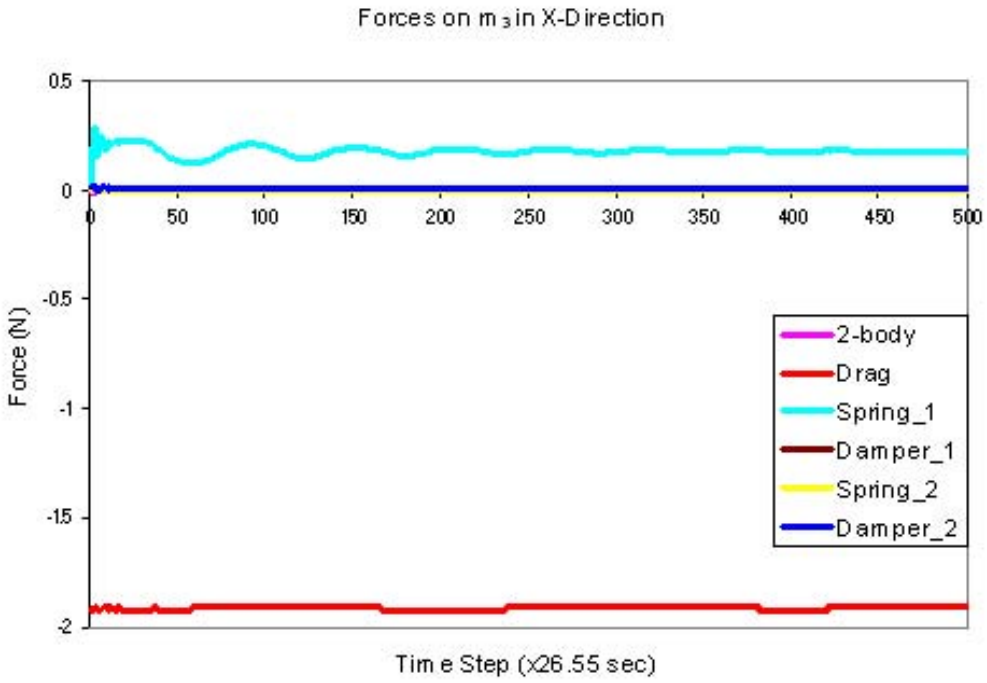

Figure 5.15 Forces Acting on Balloon Mass in X-Direction For Damping Coefficient Out of Range for SatI

Figure 5.17 shows the impacts of each force on δy. The maximum force felt by the balloon in the y-direction is 1.1 Newtons. The major contributing forces in this direction are the damping forces from each tether, as is the case from the nominal damping coefficients results. Each force except the first and second dampers are very small so that region is expanded in Figure 5.18.

Figure 5.19 shows the impacts of each force on the pitch angle. The maximum force felt by the gravity gradient portion of the satellite system is 157 Newtons. Just like the results for the nominal damping coefficients, the spring forces from both tethers are the dominating forces. Each force, except the first and second springs, are very small so that region is expanded in Figure 5.20. As shown, the satellite masses experience a maximum force greater by a factor of fifty percent when the damping coefficients were increased by an order of magnitude.

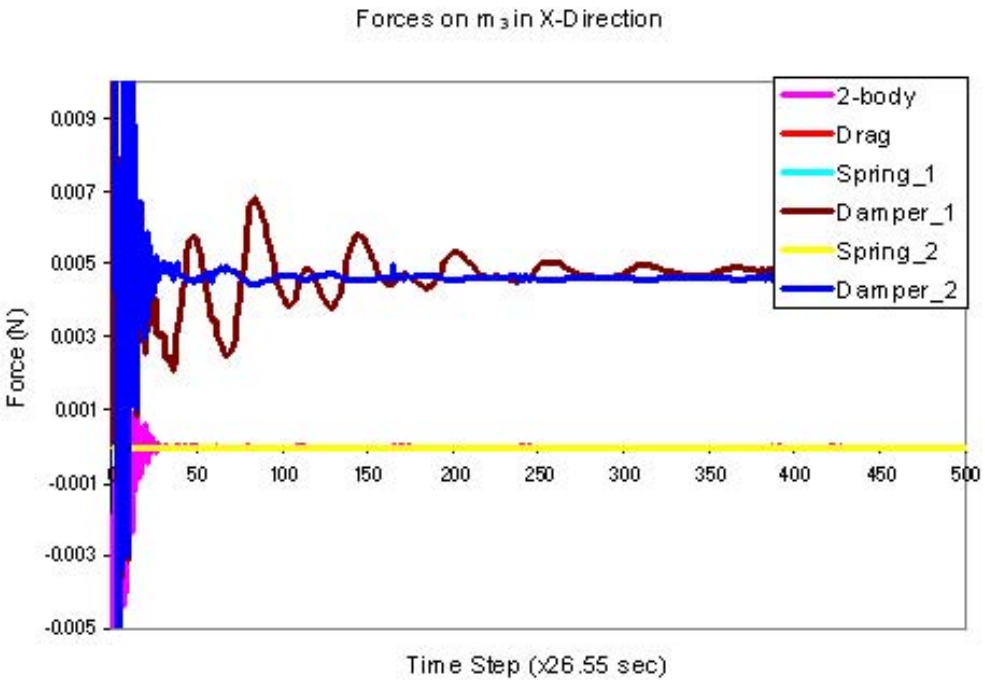

Figure 5.16 Zoomed in View of Forces Acting on Balloon Mass in X-Direction For Damping Coefficient Out of Range for SatI

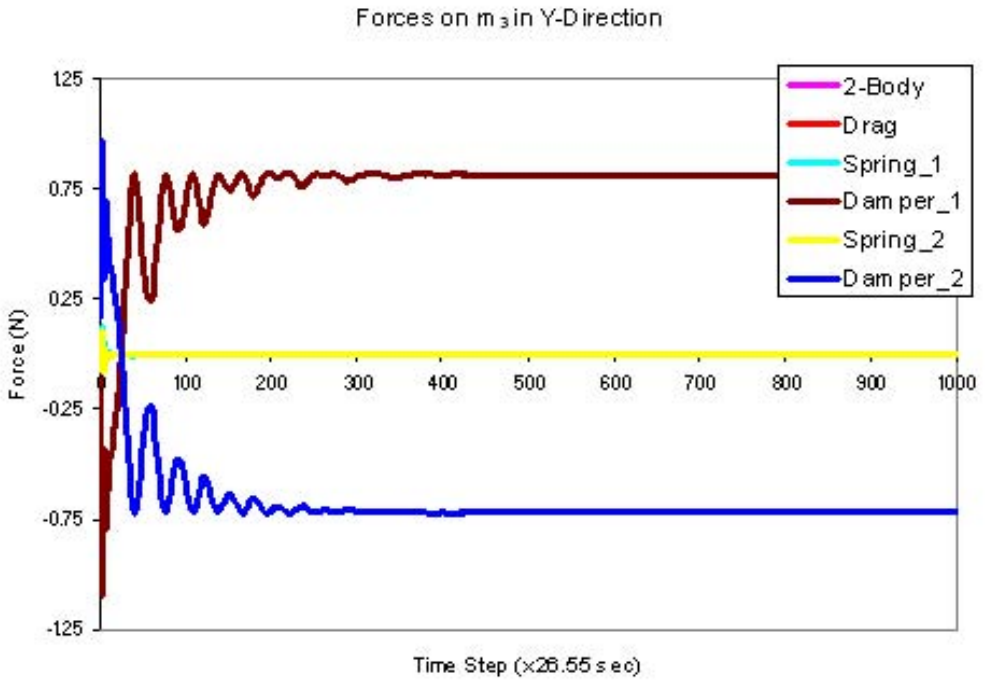

Figure 5.17 Forces Acting on Balloon Mass in Y-Direction For Damping Coefficient Out of Range for SatI

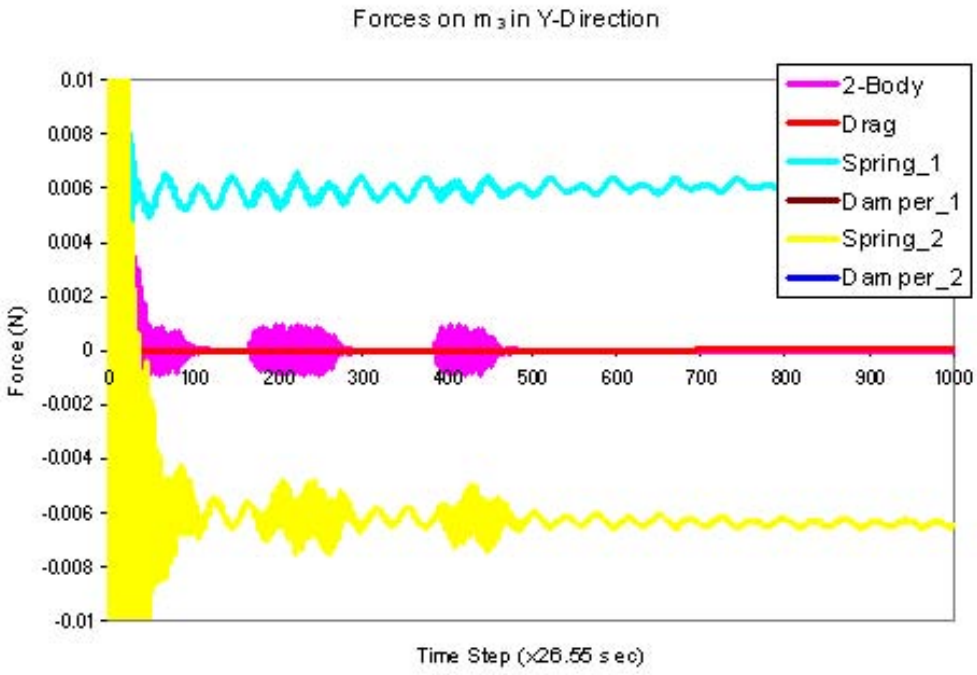

Figure 5.18 Zoomed in View of Forces Acting on Balloon Mass in Y-Direction For Damping Coefficient Out of Range for SatI

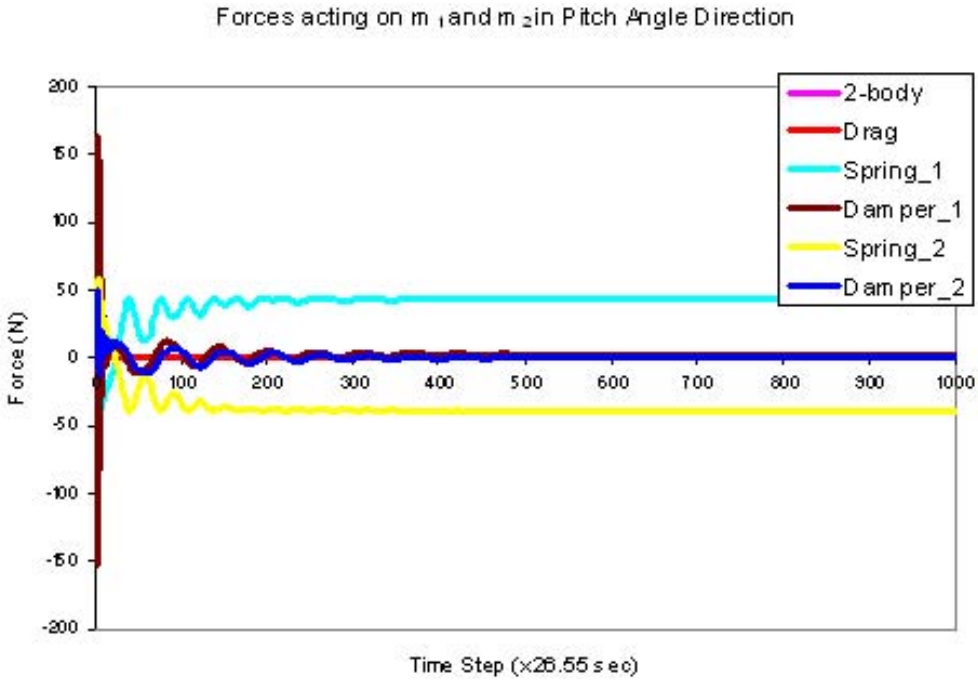

Figure 5.19 Forces Acting on Tip-Mass and Main Bus Mass For Damping Coefficient Out of Range for SatI

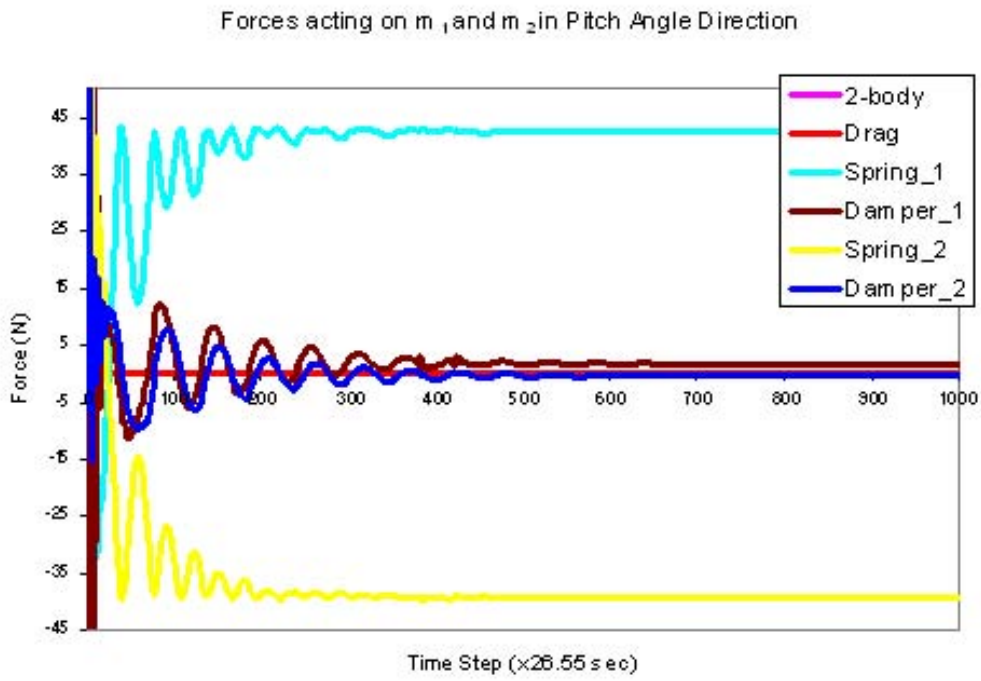

Figure 5.20 Zoomed in View of Forces Acting on Tip-Mass and Main Bus Mass For Damping Coefficient Out of Range for SatI

5.3 Stability Region

Although values for the moduli of elasticity and damping coefficients are provided in Table 4.1, these are not the only values which work. The values used in the initial program validation were chosen because they lie in the middle of the stability region. In fact, a range of values had to be established through iterative simulation. By running the simulation for many different tether characteristics, a region of stability was determined. The criteria for this stability region is based on the steady state pitch angle and the settling time.

The criteria established for the modulus of elasticity uses a steady state pitch angle of zero radian plus or minus one-twentieth radian. In this configuration, the main satellite bus maintains a nadir pointing attitude. The region of stability for the modulus of elasticity was first determined while holding constant the dampening coefficient at 0.0007 Ns/m for Satellite I. After varying the modulus of elasticity for tether one between zero and 0.006 N/mm^2 and the modulus of elasticity for tether two between zero and 0.06 N/mm^2, the stable range was found as depicted in Figure 5.21. This shows that stable values of moduli

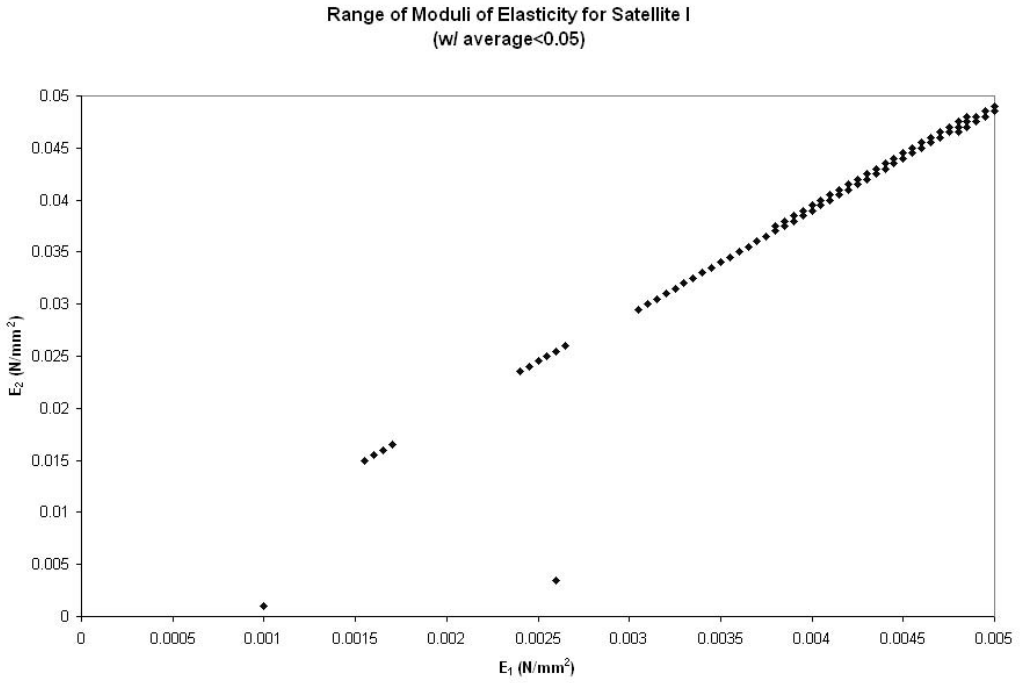

Figure 5.21 Stability Region for Moduli of Elasticity for SatI

of elasticity exist in a region around the relationship of E_2 equal to about ten times E_1.

This relationship may be explained by the fact that the distance "b" is a little over ten times the value of "a". Also, the main satellite bus mass is about ten times the tip-mass. This relationship, however, needs more support before a correlation can be confirmed. However, there are a few data points shown on Figure 5.21 that are not actually stable values for moduli of elasticity. These are quite apparent because they are isolated data points that do not follow the same relationship between the two moduli of elasticity.

5.4 Additional Satellite Results

This section provides the results of Satellite II and DumbSat. The specifications for these satellites are provided in Table 4.1. These results serve to further validate the program by demonstrating its flexibility. The following results give this research a breadth of inputs upon which to make a more educated conclusion. Although Satellites I and II are very similar, DumbSat demonstrates the effectiveness of this satellite concept and simulation for a completely different satellite.

5.4.1 Satellite II Results. The results for Satellite II are summarized in this section. Although similar analysis has been performed on this satellite's simulation results, that discussion is not necessary as it only serves to back up the conclusions drawn from Satellite I. For Satellite II, the region of stability for the moduli of elasticity is shown in Figure 5.22. The relationship in this case is that E_2 is equal to about 20 times E_1. Also, the distance "b" is about 24 times the value of "a", and the main satellite bus mass is about 23 times the tip-mass. Again, there is not enough data to show a definite correlation.

For Satellite II, the lower limit for stability of the damping coefficient is shown in Figure 5.23. For the nominal values of moduli of elasticity and damping coefficients from Table 4.1, the resultant graph of pitch angle is shown in Figure 5.24. For this graph and the others in this section, the simulation uses 1500 steps and an interval of five periods. Figure 5.25 is the graph of the δx results, and Figure 5.26 is the graph of the δy results. The steady state value of δx is about 28 meters in the wake of the satellite while oscillations in the δy direction are less than a meter in both the positive and negative directions.

As shown in these graphs, the results for Satellite I and Satellite II are very similar. The satellite system is stable, and the pitch angle dampens to approximately zero radian.

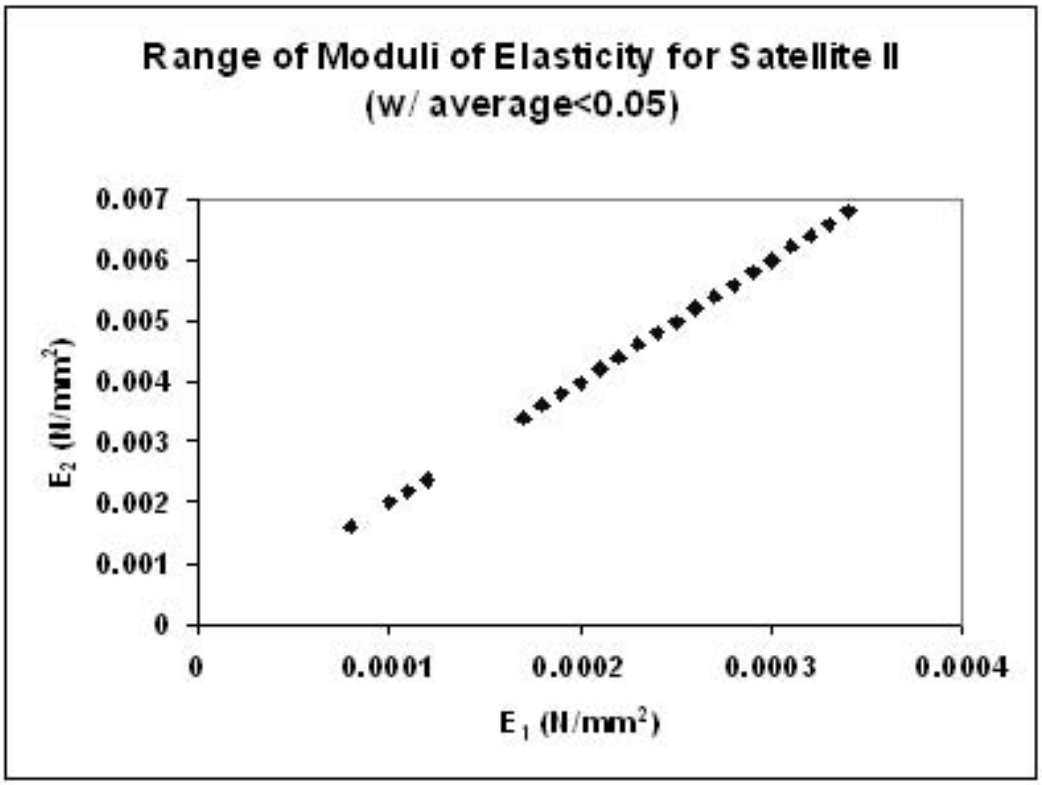

Figure 5.22 Stability Region for Moduli of Elasticity for SatII

This additional case supports the conclusions drawn from Satellite I. These results demonstrate and support the conclusion that this satellite concept is capable of stabilizing the attitude to a relatively constant, nadir orientation within a limited time of three days.

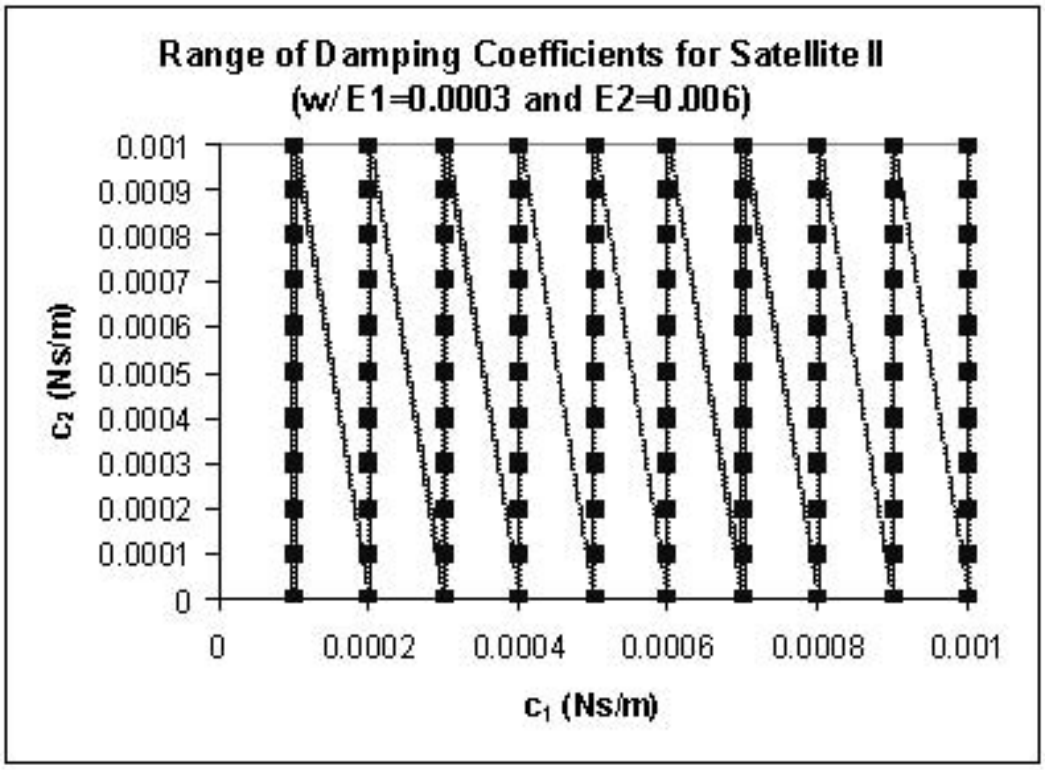

Figure 5.23 Stability Region for Damping Coefficients for SatII

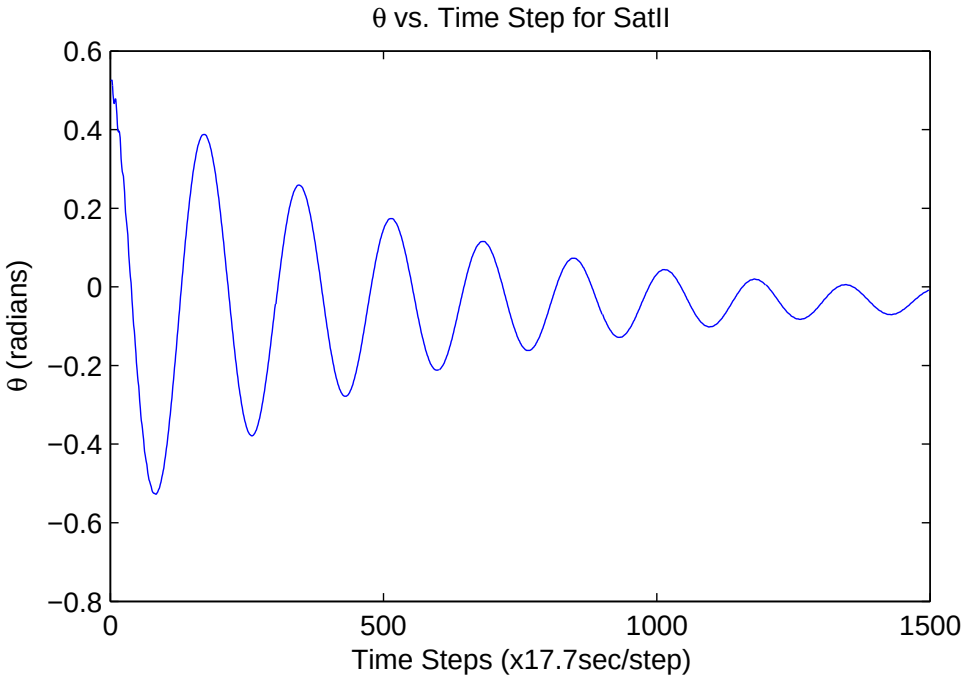

Figure 5.24 Nominal Tether Characteristics for SatII

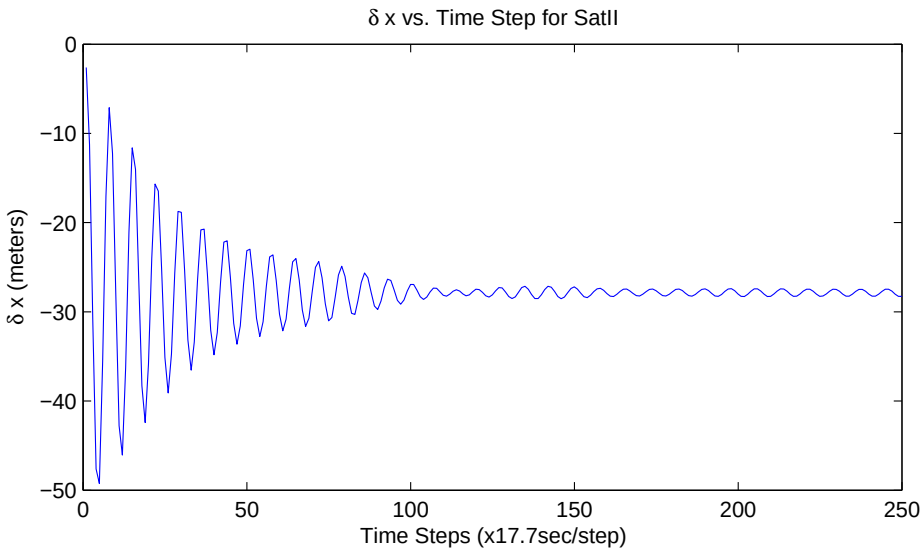

Figure 5.25 Nominal Tether Characteristics for SatII

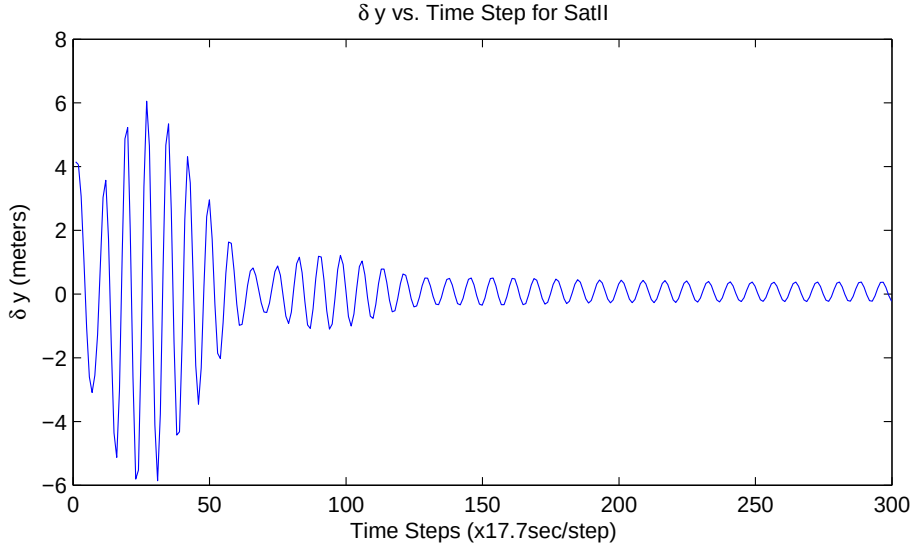

Figure 5.26 Nominal Tether Characteristics for SatII

5.4.2 DumbSat Results. The results for DumbSat are summarized in this section. Although similar analysis was performed on this satellite's simulation results, that discussion is not necessary as it only served to back up the conclusions drawn from Satellite I and Satellite II. For DumbSat, the region of stability for the moduli of elasticity is shown in Figure 5.27. This region of stability shows a one-to-one ratio for the moduli of elasticity.

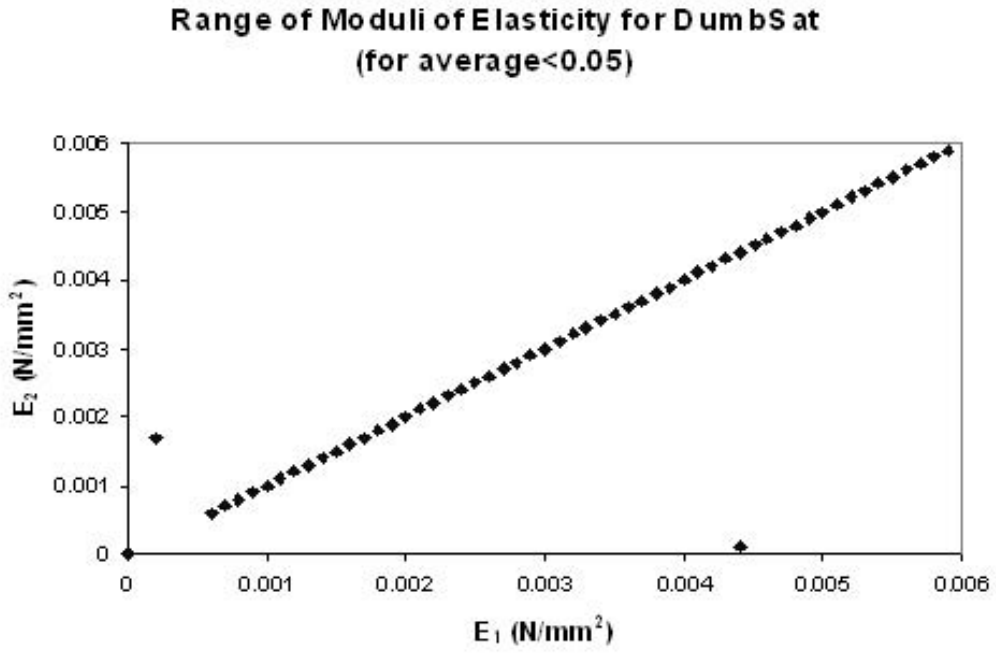

Figure 5.27 Stability Region for Moduli of Elasticity for DumbSat

This makes sense since the satellite is a dumbbell configuration with equal end masses and equal distances to each end mass from the center of mass. There are a few data points shown on Figure 5.27 that are not actually stable values for moduli of elasticity because they do not follow the same relationship between the two moduli of elasticity.

The region of stability for the damping coefficients is shown in Figure 5.28. For the nominal values of moduli of elasticity and damping coefficients from Table 4.1, the resulting graph of pitch angle is shown in Figure 5.29 For this output and the following graphs in this section, the simulation uses 1500 steps and an interval of five periods. Figure 5.31 shows the graph of δx results, and Figure 5.31 is the graph of δy results. The steady state value of δx is about 28 meters in the wake of the satellite. Oscillations in the δy direction are less

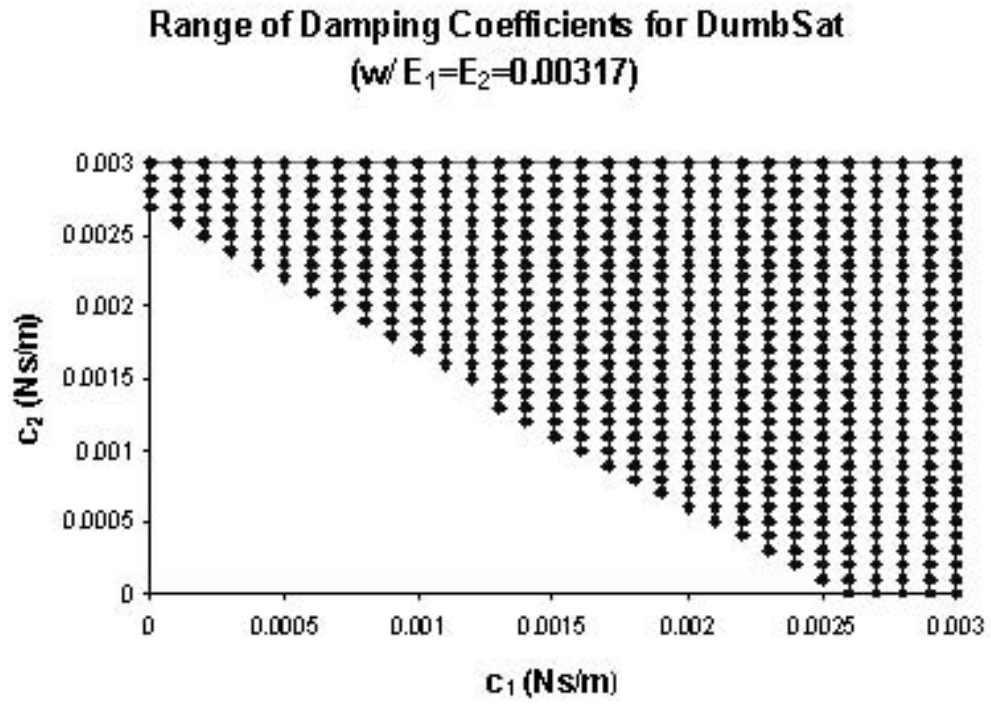

Figure 5.28 Stability Region for Damping Coefficients for DumbSat

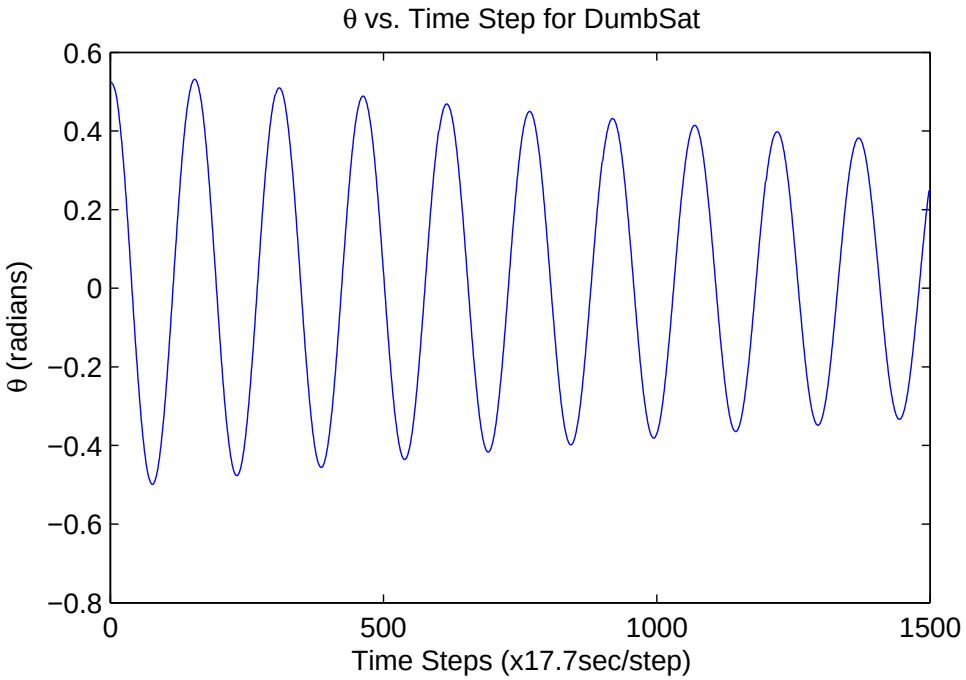

Figure 5.29 Nominal Tether Characteristics for DumbSat

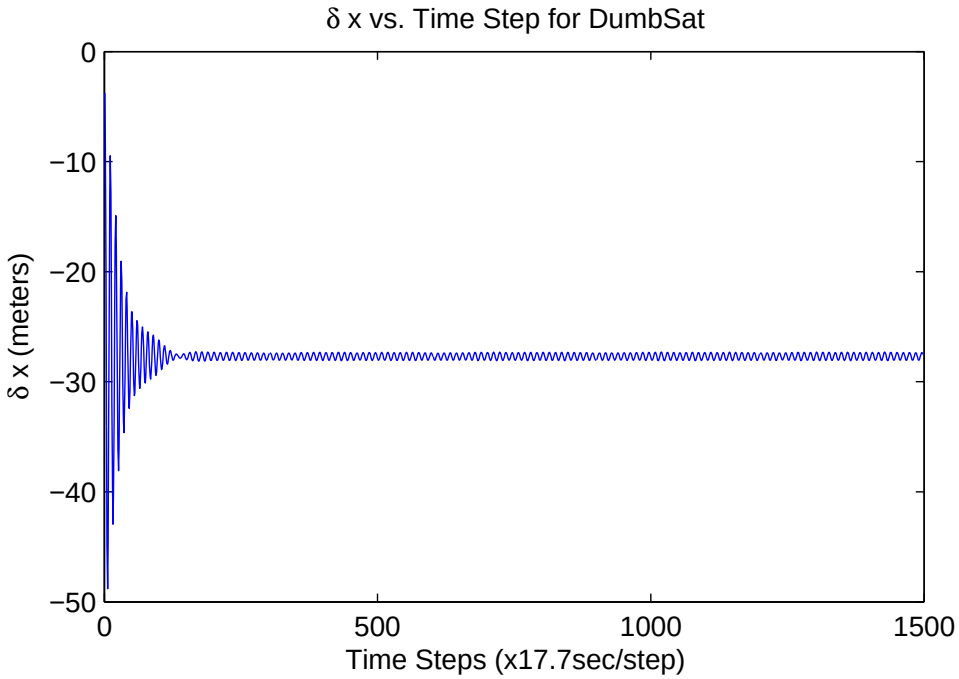

Figure 5.30 Nominal Tether Characteristics for DumbSat

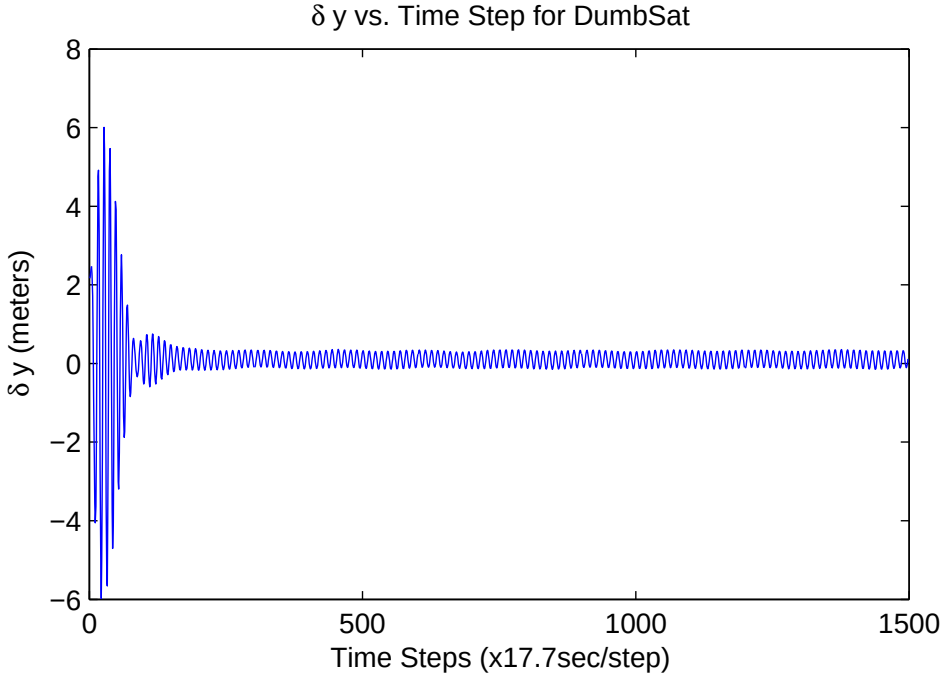

Figure 5.31 Nominal Tether Characteristics for DumbSat

than a meter in both the positive and negative directions.

This final case supports the conclusions drawn from Satellites I and II. These results demonstrate and support the conclusion that this satellite concept is capable of stabilizing the attitude to a relatively constant, nadir orientation within a limited time of three days. This case also shows that the satellite concept can be used for different gravity gradient configurations, largely different from Satellites I and II. Although stability is achieved, this configuration has a much larger settling time than those of Satellites I and II and so would not normally be chosen over Satellites I or II.

VI. Conclusions

The main objective of this research was to determine the feasibility of using a gravity gradient boom and a tethered balloon for passive attitude stabilization. This was to be accomplished by developing and testing a dynamical model for the satellite system through a computer program that shows the progress of the pitch angle over time. A literature review was conducted to understand the components involved in this satellite concept. The literature review also discussed past research that used similar concepts for passive attitude stabilization. Equations of motion were calculated for the three mass system that models the satellite concept under study. The program was validated by calculating the frequency of oscillations and comparing them to predicted values calculated from the moments of inertia. The simulation program was run for three different satellites. A range of stability for the moduli of elasticity and damping coefficients was found for each satellite.

The simulations run show that a gravity gradient satellite with a tethered balloon can achieve attitude stabilization over time. While these are limited cases, this basic simulation demonstrates the feasibility of using this satellite concept for aerostabilization. The gravity gradient portion of the attitude control system provides basic stabilization, oscillating about its equilibrium point. The tethered balloon dampens the motion by dissipating energy through the tethers.

The system was limited to a circular orbit about a spherical Earth and subjected to only drag and gravity perturbations. The simulation also assumed that motion was restricted to the orbital plane. The simulation also focused on modelling only microsatellites. Further study should include non-circular orbits and include more orbital perturbations, like an oblate Earth. This would make it necessary to include motion outside of the orbital plane and determine the satellite concept's effectiveness in damping motion in the roll and yaw directions. Other orbital factors could be analyzed to determine its impact on attitude stability for the satellite concept. For example, the maximum altitude with effective amounts of aerodynamic drag should be determined.

Once the simulation is updated to include out-of-plane motion, the model should be run to determine the stable range for other satellite characteristics. The size of the tethered balloon should also be varied to determine the minimum size that would create enough of a

drag force. The relationship between mission lifetime and attitude settling time should be analyzed to determine an optimum trade-off. The length of the tethers and gravity gradient boom could also be analyzed to determine minimum values under different conditions. The initial conditions should also be varied to determine if the satellite concept can dampen out unwanted motion despite its initial orientation. Since there are so many variables to include, a graphical user interface should be created that can make it easier to vary certain quantities and provide graphical and numerical results for analysis.

Further research should also include analysis and inspection of possible materials for the tethers and balloon. A mechanism for deployment of the gravity gradient boom and tethered balloon would have to be designed. If all further research supports the feasibility and effectiveness of this satellite concept for attitude control, a test flight would eventually have to be conducted to verify the accuracy of the simulation.

```
function Thesis;
%%%%%%%%%%%%%%%%%%%%%%%%%%%%%%%%%%%%%%%%%%%%%%%%%%%%%%%%%%%%%%%%%%%%%%%%%%%%
%%
%%                              PROCEDURE Thesis
%%
%% This procedure uses a numerical integrator for orbital prediction of
%% a three body system.
%%
%% Author     : 2Lt Ernest Maramba  AFIT/ENY  937-369-6956 27 Oct 2004
%%
%% Algorithm: 1. Initialize constants and variables
%%            2. Declare initial conditions and satellite characteristics
%%            3. Call RK4 and RK4forRandV which predicts generalized
%%            coordinates, R for COM, and V for COM at next time step
%%            4. Increment time step and loop to step 3 for time interval
%%            5. Calculate generalized coordinates, R for COM, and V for
%%            COM for any time left over
%%            6. Plot generalized coordinates
%%
%% Locals        :
%%  Derivtype   - Defines which equations of motion to use
%%  time        - Time that is propagated forward in Julian time
%%  nsteps      - Number of steps to propagate over
%%  leftover    - Any amount of time not integrated over by initial loop
%%  lamone      - Length of tether one at (time)
%%  lamtwo      - Length of tether two at (time)
%%  X           - State vector for R and V
%%  Y           - State vector for generalized coordinates
%%  steps       - Defines number of steps to iterate over
%%  period      - Period of the orbit
```

```
%%  interval    - Total time to iterate over
%%  stepsize    - Stepsize for iterations
%%
%%  Constants     :
%%    Rad           - Conversion for degrees to radians
%%    Deg           - Conversion for radians to degrees
%%    TwoPI         - Pi times two
%%    MU            - Constant
%%    a             - Distance from main satellite bus to COM (m)
%%    b             - Distance from tip-mass to COM (m)
%%    lonenot       - Taut length of top tether (m)
%%    ltwonot       - Taut length of bottom tether (m)
%%    ri            - Radius of circular orbit of system (km)
%%    vi            - Velocity of circular orbit of system (km/sec)
%%    mone          - Mass of tip-mass (kg)
%%    mtwo          - Mass of main satellite (kg)
%%    mthree        - Mass of main balloon (kg)
%%    JDstart       - Starting Julian date
%%    JDstop        - End Julian date
%%
%%  Coupling      :
%%    Data          - Provides global constants
%%    JulianDay     - Converts year, month, etc. into a Julian Date
%%    RK4forRandV   - Propagates R and V forward in time
%%    RK4           - Propagates delx, dely, and theta forward in time
%%
%%%%%%%%%%%%%%%%%%%%%%%%%%%%%%%%%%%%%%%%%%%%%%%%%%%%%%%%%%%%%%%%%%%%%%%%%%%%%%%
%% Which Satellite?
question=1;
%% Open file with globals and declare them
Data(question) global Rad Deg MU TwoPI a b lonenot ltwonot ri vi
```

```
JDstart JDstop mone mtwo mthree

%% Initialize Derivtype - 2 means the com is only subject to 2-body
%% motion
Derivtype='ynnnnnnnn2';

%% Initialize state vector Y (del x, del y, theta)
%%    - Y is in terms of the local frame
theta=pi/6; delx=b*sin(theta)-lonenot*cos(theta-(pi/6));
dely=b*cos(theta)+lonenot*sin(theta-(pi/6)); delxdot=0; delydot=0;
thetadot=0;
Y = [delx; dely; theta; delxdot; delydot; thetadot];

%% Initialize state vector X (satellite COM)
%%    - X is in terms of the inertial GCE frame
%%    - Initialize input COE's and convert units %%
tempa=ri; tempe=0.00; tempi=0; tempomega=0; tempargp=0; tempnu=0;
tempu=0; templ=0; tempcappi=0;

%% Convert units %%
tempi=tempi*Rad; tempomega=tempomega*Rad; tempargp=tempargp*Rad;
tempnu=tempnu*Rad; tempu=tempu*Rad; templ=templ*Rad;
tempcappi=tempcappi*Rad;

%% Calculate semi-latus rectum %%
tempp=tempa*(1-tempe^2);

%% Calculate R and V %%
[R,V] =
RandV(tempp,tempe,tempi,tempomega,tempargp,tempnu,tempu,templ,tempcappi);
X = [R(1:3);V(1:3)];
```

```
%% Define time increment variable and number of steps
steps=400; period=TwoPI*sqrt(ri^3/MU); interval=2*period;
JDstop=JDstart+interval/86400; stepsize=interval/steps;
time=JDstart; nsteps=(JDstop-JDstart)/(stepsize/86400);

%% Initialize E1, E2, c1, and c2
factor=1;
if question==1
%% Specs for Sat I
Eone=0.002065;          %% Modulus of Elasticity for tether one (N/mm^2)
Etwo=0.0202;            %% Modulus of Elasticity for tether two (N/mm^2)
cone=0.0007*factor;     %% Damping coefficient for tether one (N*s/m)
ctwo=0.0007*factor;     %% Damping coefficient for tether two (N*s/m)
elseif question==2
%% Specs for Sat II
Eone=0.0003;            %% Modulus of Elasticity for tether one (N/mm^2)
Etwo=0.006;             %% Modulus of Elasticity for tether two (N/mm^2)
cone=0.0007;            %% Damping coefficient for tether one (N*s/m)
ctwo=0.0007;            %% Damping coefficient for tether two (N*s/m)
elseif question==3
%% Specs for DumbSat
Eone=0.00317;           %% Modulus of Elasticity for tether one (N/mm^2)
Etwo=0.00317;           %% Modulus of Elasticity for tether two (N/mm^2)
cone=0.0016;            %% Damping coefficient for tether one (N*s/m)
ctwo=0.0016;            %% Damping coefficient for tether two (N*s/m)
end

%% Propagate X and Y forward
for i=1:nsteps
    %% Save Y data to be plotted in the body frame
```

```
    xdata(i)=Y(1);
    ydata(i)=Y(2);
    thetadata(i)=Y(3);

    %% Calculate Y at (time) by calling RK4
    [Y, Rot] = RK4 (time, stepsize, Derivtype, Y, X, Eone, Etwo,
    cone, ctwo);

    %% Calculate X at (time) by calling RK4forRandV
    X = RK4forRandV ( time, stepsize, Derivtype, X, Y, Rot );

    %% Increment time
    time=time+(stepsize/86400);
end aver = sum(thetadata(1:fix(nsteps)))/fix(nsteps);
maxt=max(thetadata(fix(nsteps)-100:fix(nsteps)));
mint=min(thetadata(fix(nsteps)-100:fix(nsteps)));

%% Propagate after any time left over %%
leftover=(JDstop-time)*86400;
[Y, Rot] = RK4 (time, leftover, Derivtype, Y, X, Eone, Etwo,
cone, ctwo);
X = RK4forRandV ( time, leftover, Derivtype, X, Y, Rot);

%%  Plot generalized coordinates in local coordinate frame
subplot(2,2,1:2)
plot(thetadata)
xlabel('Time Steps')
ylabel('\theta (radians)')
if question==1
    title('\theta vs. Time Steps for Sat I')
elseif question==2
```

```
    title('\theta vs. Time Steps for Sat II')
elseif question==3
    title('\theta vs. Time Steps for DumbSat')
end
subplot(2,2,3)
plot(xdata)
xlabel('Time Steps')
ylabel('\delta x (meters)')
if question==1
    title('\delta x vs. Time Steps for Sat I')
elseif question==2
    title('\delta x vs. Time Steps for Sat II')
elseif question==3
    title('\delta x vs. Time Steps for DumbSat')
end
subplot(2,2,4)
plot(ydata)
xlabel('Time Steps')
ylabel('\delta y (meters)')
if question==1
    title('\delta y vs. Time Steps for Sat I')
elseif question==2
    title('\delta y vs. Time Steps for Sat II')
elseif question==3
    title('\delta y vs. Time Steps for DumbSat')
end
```

```
function [Y2, Rot] = RK4 (time, stepsize, Derivtype, Y, X, Eone,
Etwo, cone, ctwo);

%%%%%%%%%%%%%%%%%%%%%%%%%%%%%%%%%%%%%%%%%%%%%%%%%%%%%%%%%%%%%%%%%%%%%%%%%%%
%%
%% function RK4
%%
%% This is a fourth order Runge-Kutta integrator for a 6 dimension
%% First Order differential equation. It is for a satellite
%% equation of motion. The user must provide an external function
%% containing the system Equations of Motion.
%% The integration is done for one time step only.
%%
%% This program was altered in order to be used for this thesis.
%% Algorithm : Evaluate each term depending on the derivtype
%% Find the final answer
%%
%% Author : Capt Dave Vallado USAFA/DFAS 719-472-4109 5 Jun 1991
%% In Ada : Dr Ron Lisowski USAFA/DFAS 719-472-4110 12 Jan 1996
%% In MatLab : Dr Ron Lisowski USAFA/DFAS 719-333-4109 16 Jan 2002
%% Altered by : 2Lt Ernest Maramba AFIT/ENY 937-369-6956 8 Nov 2004
%%
%% Inputs :
%% time - Initial Time Julian Date days since 4713 B.C.
%% stepsize - Step size sec
%% DerivType - String containing YN for tension forces "YYNYNYNY2"
%% Y - State vector of delx, dely, theta at initial time m, m/sec
%% X - State vector of R and V at initial time km, km/sec
%%
%% Outputs :
```

```
%% Y - State vector of delx, dely, theta at new time m, m/sec
%%
%% Locals :
%% YDot - Derivative of State Vector
%% K1,K2,K3 - Storage for values of state vector at different times
%% (The standard Runge-Kutta K constants)
%% TEMP - Storage for state vector
%% TempDate - Temporary date storage half way between dt days since
%% 4713 B.C.
%%
%% Constants :
%% TwoPI - 2 times pi
%% w - Angular rate of the satellite's com
%% JDstart - The initial time for integration
%%
%% Coupling :
%% TetherDeriv function for Derivatives of E.O.M.
%%
%% References :
%% Mathews, "Numerical Methods" pg. 423-427
%% BMW pg. 414-415
%%
%%%%%%%%%%%%%%%%%%%%%%%%%%%%%%%%%%%%%%%%%%%%%%%%%%%%%%%%%%%%%%%%%%%%%%%%%%%

%% Declare constants
global TwoPI MU JDstart a b lonenot ltwonot mone mtwo mthree

%%calculate angular rate of orbit (rad/sec)
w=sqrt(MU/mag(X(1:3))^3);

%% Calculate rotation angle and perform revolution check
```

```
rotang=w*(time-JDstart)*86400; rotang = revcheck(rotang, TwoPI);

%% Calculate rotation matrix
Rot=[-sin(rotang) cos(rotang) 0;cos(rotang) sin(rotang) 0;0 0 -1];

%% Redefine the tether lengths according to Y at (time)
lamone = sqrt((b*sin(Y(3)) - Y(1))^2 + (b*cos(Y(3)) - Y(2))^2);
lamtwo = sqrt((a*sin(Y(3)) + Y(1))^2 + (a*cos(Y(3)) + Y(2))^2);

%% Determine whether to add the tension forces of each tether
%% - The tether length must be greater than its initial length to
%% include tension forces on each mass to which it is connected.
if lamone/lonenot > 1.000
Derivtype(3)='y';
else
Derivtype(3)='n';
end if lamtwo/ltwonot > 1.000
Derivtype(4)='y';
else
Derivtype(4)='n';
end

%% Local VARIABLES
%%%%%%%%%%%%%%%% Evaluate 1st Taylor Series Term %%%%%%%%%%%%%%%%
[YDot,ax2body,ay2body,at2body,axdrag,aydrag,atdrag,Tether1springx,
Tether1damperx,Tether1springy,Tether1dampery,Tether1springtheta,
Tether1dampertheta,Tether2springx,Tether2damperx,Tether2springy,
Tether2dampery,Tether2springtheta,Tether2dampertheta] =
TetherDeriv(Derivtype, Y, lamone, lamtwo, X, Rot, Eone, Etwo,
cone, ctwo);
```

```
%%%%%%%%%%%%%%% Update Julian Date for a half Dt %%%%%%%%%%%%%%-
TempDate = time + stepsize * 0.5 / 86400.0;

%%%%%%%%%%%%%%% Evaluate 2nd Taylor Series Term %%%%%%%%%%%%%%%
K1Y = stepsize * YDot;
K1(2) = stepsize * ax2body;
K1(3) = stepsize * ay2body;
K1(4) = stepsize * at2body;
K1(5) = stepsize * axdrag;
K1(6) = stepsize * aydrag;
K1(7) = stepsize * atdrag;
K1(8) = stepsize * Tether1springx;
K1(9) = stepsize * Tether1damperx;
K1(10) = stepsize * Tether1springy;
K1(11) = stepsize * Tether1dampery;
K1(12) = stepsize * Tether1springtheta;
K1(13) = stepsize * Tether1dampertheta;
K1(14) = stepsize * Tether2springx;
K1(15) = stepsize * Tether2damperx;
K1(16) = stepsize * Tether2springy;
K1(17) = stepsize * Tether2dampery;
K1(18) = stepsize * Tether2springtheta;
K1(19) = stepsize * Tether2dampertheta;
Temp = Y + 0.5 * K1Y;
%% Redefine the tether lengths according to Y at (time)
lamone = sqrt((b*sin(Temp(3)) - Temp(1))^2 + (b*cos(Temp(3))...
- Temp(2))^2); lamtwo = sqrt((a*sin(Temp(3)) + Temp(1))^2 +...
(a*cos(Temp(3)) + Temp(2))^2);
[YDot,ax2body,ay2body,at2body,axdrag,aydrag,atdrag,Tether1springx,
Tether1damperx,Tether1springy,Tether1dampery,Tether1springtheta,
Tether1dampertheta,Tether2springx,Tether2damperx,Tether2springy,
```

```
Tether2dampery,Tether2springtheta,Tether2dampertheta] =
TetherDeriv(Derivtype, Temp, lamone, lamtwo, X, Rot, Eone, Etwo,
cone, ctwo);

%%%%%%%%%%%%%% Evaluate 3rd Taylor Series Term %%%%%%%%%%%%%%
K2Y = stepsize * YDot;
K2(2) = stepsize * ax2body;
K2(3) = stepsize * ay2body;
K2(4) = stepsize * at2body;
K2(5) = stepsize * axdrag;
K2(6) = stepsize * aydrag;
K2(7) = stepsize * atdrag;
K2(8) = stepsize * Tether1springx;
K2(9) = stepsize * Tether1damperx;
K2(10) = stepsize * Tether1springy;
K2(11) = stepsize * Tether1dampery;
K2(12) = stepsize * Tether1springtheta;
K2(13) = stepsize * Tether1dampertheta;
K2(14) = stepsize * Tether2springx;
K2(15) = stepsize * Tether2damperx;
K2(16) = stepsize * Tether2springy;
K2(17) = stepsize * Tether2dampery;
K2(18) = stepsize * Tether2springtheta;
K2(19) = stepsize * Tether2dampertheta;
Temp = Y + 0.5 * K2Y;
%% Redefine the tether lengths according to Y at (time)
lamone = sqrt((b*sin(Temp(3)) - Temp(1))^2 + (b*cos(Temp(3))...
 - Temp(2))^2); lamtwo = sqrt((a*sin(Temp(3)) + Temp(1))^2 +...
(a*cos(Temp(3)) + Temp(2))^2);
[YDot,ax2body,ay2body,at2body,axdrag,aydrag,atdrag,Tether1springx,
Tether1damperx,Tether1springy,Tether1dampery,Tether1springtheta,
```

```
Tether1dampertheta,Tether2springx,Tether2damperx,Tether2springy,
Tether2dampery,Tether2springtheta,Tether2dampertheta] =
TetherDeriv(Derivtype, Temp, lamone, lamtwo, X, Rot, Eone, Etwo,
cone, ctwo);

%%%%%%%%%%%%%% Evaluate 4th Taylor Series Term %%%%%%%%%%%%%%
K3Y = stepsize * YDot;
K3(2) = stepsize * ax2body;
K3(3) = stepsize * ay2body;
K3(4) = stepsize * at2body;
K3(5) = stepsize * axdrag;
K3(6) = stepsize * aydrag;
K3(7) = stepsize * atdrag;
K3(8) = stepsize * Tether1springx;
K3(9) = stepsize * Tether1damperx;
K3(10) = stepsize * Tether1springy;
K3(11) = stepsize * Tether1dampery;
K3(12) = stepsize * Tether1springtheta;
K3(13) = stepsize * Tether1dampertheta;
K3(14) = stepsize * Tether2springx;
K3(15) = stepsize * Tether2damperx;
K3(16) = stepsize * Tether2springy;
K3(17) = stepsize * Tether2dampery;
K3(18) = stepsize * Tether2springtheta;
K3(19) = stepsize * Tether2dampertheta;
Temp = Y + K3Y;

%%%%%%%%%%%%%% Update Julian Date for a full Dt %%%%%%%%%%%%%-
TempDate = time + stepsize / 86400.0;
%% Redefine the tether lengths according to Y at (time)
lamone = sqrt((b*sin(Temp(3)) - Temp(1))^2 + (b*cos(Temp(3))...
```

```
 - Temp(2))^2); lamtwo = sqrt((a*sin(Temp(3)) + Temp(1))^2 +...
(a*cos(Temp(3)) + Temp(2))^2);
[YDot,ax2body,ay2body,at2body,axdrag,aydrag,atdrag,Tether1springx,
Tether1damperx,Tether1springy,Tether1dampery,Tether1springtheta,
Tether1dampertheta,Tether2springx,Tether2damperx,Tether2springy,
Tether2dampery,Tether2springtheta,Tether2dampertheta] =
TetherDeriv(Derivtype, Temp, lamone, lamtwo, X, Rot, Eone, Etwo,
cone, ctwo);

%%%%%%%%%- Update the State vector, perform integration %%%%%%-
K4Y = stepsize * YDot;
K4(2) = stepsize * ax2body;
K4(3) = stepsize * ay2body;
K4(4) = stepsize * at2body;
K4(5) = stepsize * axdrag;
K4(6) = stepsize * aydrag;
K4(7) = stepsize * atdrag;
K4(8) = stepsize * Tether1springx;
K4(9) = stepsize * Tether1springy;
K4(10) = stepsize * Tether1springtheta;
K4(11) = stepsize * Tether1damperx;
K4(12) = stepsize * Tether1dampery;
K4(13) = stepsize * Tether1dampertheta;
K4(14) = stepsize * Tether2springx;
K4(15) = stepsize * Tether2springy;
K4(16) = stepsize * Tether2springtheta;
K4(17) = stepsize * Tether2damperx;
K4(18) = stepsize * Tether2dampery;
K4(19) = stepsize * Tether2dampertheta;

Y = Y + ( K1Y + 2.0 * ( K2Y + K3Y ) + K4Y)/ 6.0 ;
```

```
for i=2:19
acceleration(i)=( K1(i) + 2.0 * ( K2(i) + K3(i) ) + K4(i)) / 6.0;
end

%% Perform revolution check on theta
% Y(3) = revcheck (Y(3), TwoPI);
%% For some reason, revcheck doesn't work.
%% - something to do with theta being close to zero
Y(3) = Y(3) - TwoPI * fix(Y(3) / TwoPI);

%% Define output Y vector
Y2 = Y;
```

```
function
[YDot,ax2body,ay2body,at2body,axdrag,aydrag,atdrag,Tether1springx,
Tether1damperx,Tether1springy,Tether1dampery,Tether1springtheta,
Tether1dampertheta,Tether2springx,Tether2damperx,Tether2springy,
Tether2dampery,Tether2springtheta,Tether2dampertheta]
= TetherDeriv(Derivtype, Y, lamone, lamtwo, X, Rot, Eone, Etwo,
cone, ctwo);
%%%%%%%%%%%%%%%%%%%%%%%%%%%%%%%%%%%%%%%%%%%%%%%%%%%%%%%%%%%%%%%%%%%%%%%%%%%
%%
%% PROCEDURE TetherDeriv
%%
%% This procedure calculates Ydot.
%%
%% Algorithm: 1. Call global variables
%% 2. Call Deriv to calculate generalized
%% coordinates without generalized forces
%% 3. Calculate tether tension forces and dissipative
%% forces
%% 4. Sum accelerations to get final generalized coordinates
%%
%% Author : 2Lt Ernest Maramba AFIT/ENY 937-369-6956 27 Oct 2004
%%
%% Inputs :
%% Derivtype - Defines which equation of motion to use
%% Y - State vector of delx, dely, theta at initial time m, m/sec
%% lamone - Length of tether one at (time)
%% lamtwo - Length of tether two at (time)
%% X - State vector of R and V km, km/sec
%% Rot - Rotation matrix
%%
```

```
%% Outputs :
%% YDot - Derivative of Y state vector
%%
%% Locals :
%% R - Position vector km
%% V - Velocity vector km/s
%% ax - Acceleration in x direction from perturbations
%% ay - Acceleration in x direction from perturbations
%% az - Acceleration in x direction from perturbations
%% r - Magnitude of R
%% temp(2) - Variables that increase coding efficiency
%% RSun - Vector to sun from the satellite
%% RtAsc - Place holder for calling Sun
%% Decl - Place holder for calling Sun
%% dotsunr - Dot product of the RSun and R
%% rho - Density of the atmosphere
%% VRel - Relative velocity vector of satellite
%%
%% Globals :
%% MU - Mu of the Earth
%% OmegaEarth - Earth's rotational rate
%% a - Length of boom from COM to main satellite bus (m)
%% b - Length of boom from COM to tip-mass (m)
%% mone - Mass of tip-mass (kg)
%% mtwo - Mass of main satellite bus (kg)
%% mthree - Mass of balloon (kg)
%% lonenot - Taut length of top tether (m)
%% ltwonot - Taut length of bottom tether (m)
%% E - Modulus of Elasticity of both tethers (N)
%%
%% Coupling :
```

```
%% Data - Provides constants
%% Deriv - Calculates Ydot without tension forces
%%
%%%%%%%%%%%%%%%%%%%%%%%%%%%%%%%%%%%%%%%%%%%%%%%%%%%%%%%%%%%%%%%%%%%%%%%%%%%%
%% Declare global variables %%
global MU OmegaEarth a b mone mtwo mthree lonenot ltwonot


%% calculate radius to com
r=mag(X(1:3));
%%calculate angular rate of orbit (rad/sec)
w=sqrt(MU/mag(X(1:3))^3);

%% initialize accelerations %%
ax=0; ay=0; atheta=0;

    Tether1springx = 0;
    Tether1damperx = 0;
    Tether1springy = 0;
    Tether1dampery = 0;
    Tether1springtheta = 0;
    Tether1dampertheta = 0;
    Tether2springx = 0;
    Tether2damperx = 0;
    Tether2springy = 0;
    Tether2dampery = 0;
    Tether2springtheta = 0;
    Tether2dampertheta = 0;


%% Call the function Deriv to calculate EOM with tethers slack %%
```

```
[YDot,ax2body,ay2body,at2body,axdrag,aydrag,atdrag] = Deriv (Y, X,
Rot);


%% Calculate acceleration with taut l-one %%

if Derivtype(3)=='y',
    Tether1springx = Eone*(1/lonenot - 1/lamone)*(b*sin(Y(3))-Y(1));
    Tether1damperx = -cone*(Y(4)-w*Y(2)-b*Y(6)*cos(Y(3))+w*b*cos(Y(3)));
    Tether1springy = Eone*(1/lonenot - 1/lamone)*(b*cos(Y(3))-Y(2));
    Tether1dampery = -cone*(Y(5)+w*Y(1)+b*Y(6)*sin(Y(3))-w*b*sin(Y(3)));
    Tether1springtheta = - Eone*(1/lonenot - 1/lamone)*((b*sin(Y(3)))...
    -Y(1))*b*cos(Y(3)) - (b*cos(Y(3))-Y(2))*b*sin(Y(3)));
    Tether1dampertheta = cone*(b*cos(Y(3))*(Y(4)-w*Y(2)-b*Y(6)...
    *cos(Y(3))+w*b*cos(Y(3))) - b*sin(Y(3))*(Y(5)+w*Y(1)+b*Y(6)...
    *sin(Y(3))-w*b*sin(Y(3))));
    ax=ax + Tether1springx + Tether1damperx;
    ay=ay + Tether1springy + Tether1dampery;
    atheta=atheta + Tether1springtheta + Tether1dampertheta;
end

%% Calculate acceleration with taut l-two %%
if Derivtype(4)=='y',
    Tether2springx = Etwo*(1/ltwonot - 1/lamtwo)*(-a*sin(Y(3))-Y(1));
    Tether2damperx = -ctwo*(Y(4)-w*Y(2)+a*Y(6)*cos(Y(3))-w*a*cos(Y(3)));
    Tether2springy = Etwo*(1/ltwonot - 1/lamtwo)*(-a*cos(Y(3))-Y(2));
    Tether2dampery = -ctwo*(Y(5)+w*Y(1)-a*Y(6)*sin(Y(3))+w*a*sin(Y(3)));
    Tether2springtheta = - Etwo*(1/ltwonot - 1/lamtwo)*((-a*sin(Y(3)))...
    -Y(1))*-a*cos(Y(3)) + (-a*cos(Y(3))-Y(2))*a*sin(Y(3)));
    Tether2dampertheta = ctwo*(-a*cos(Y(3))*(Y(4)-w*Y(2)+a*Y(6)...
    *cos(Y(3))-w*a*cos(Y(3))) - b*sin(Y(3))*(Y(5)+w*Y(1)-a*Y(6)...
```

```
    *sin(Y(3))+w*a*sin(Y(3))));
    ax=ax + Tether2springx + Tether2damperx;
    ay=ay + Tether2springy + Tether2dampery;
    atheta=atheta + Tether2springtheta + Tether2dampertheta;
end

% Define Acceleration Terms of YDot %%
YDot(4:6) = [YDot(4) + ax/mthree; ...
             YDot(5) + ay/mthree; ...
             YDot(6) + atheta/(mone*b^2 + mtwo*a^2)];
```

```
function [YDot,ax2body,ay2body,at2body,axdrag,aydrag,atdrag] =
Deriv (Y, X, Rot)

%%%%%%%%%%%%%%%%%%%%%%%%%%%%%%%%%%%%%%%%%%%%%%%%%%%%%%%%%%%%%%%%%%%%%%%%%%%%
%%
%% function DERIV
%%
%% This function calculates the derivative of the state vector for
%% use with the Runge-Kutta algorithm.
%%
%% Author : 2Lt Ernest Maramba AFIT/ENY 937-369-6956 27 Oct 2004
%%
%% Algorithm: 1. Call global variables
%% 2. Call Drag program to calculate the forces of drag and
%% direction of drag
%% 3. Calculate accelerations due to drag and gravity
%% 4. Sum accelerations to get YDot
%%
%% Inputs :
%% X - State Vector for R and V km, km/sec
%% Y - State Vector for generalized coordinates
%% Rot - Rotation matrix
%%
%% Outputs :
%% YDot - Derivative of State Vector
%%
%% Locals :
%% Rrel - Position vector of mass three
%% r - Distance from center of Earth to satellite center of mass
%% w - Orbital spin rate
```

```
%% Vrel - Relative velocity
%% rho - Density
%% Fdrag - Drag force on balloon
%%
%%
%% Constants :
%% MU - Global constant
%% OmegaEarth - Spin rate of Earth
%% a - Length from center of mass to main satellite (mass two)
%% b - Length from center of mass to tip mass (mass one)
%% mone - Tip mass
%% mtwo - Main satellite mass
%% bcthree - Ballistic coefficient of tethered balloon
%% w - Angular rate of the satellite's com
%%
%% Coupling :
%% Atmos - Gets density of atmosphere
%% cross - Calculates cross product
%% mag - Calculates magnitude of a vector
%%
%% References :
%% None.
%%
%%%%%%%%%%%%%%%%%%%%%%%%%%%%%%%%%%%%%%%%%%%%%%%%%%%%%%%%%%%%%%%%%%%%%%%%%%%
%% Global Constants
global MU OmegaEarth a b mone mtwo bcthree w r

%%%%%%%%%%%%%%%%% Calculate the drag terms %%%%%%%%%%%%%%%%%%%
[adrag1, Vhat1, adrag2, Vhat2, adrag3, Vhat3] = Drag (Y, X, Rot);
% adrag1=0;
% adrag2=0;
```

```
% adrag3=0;

%% calculate radius to com
rcom=mag(X(1:3));
%%calculate angular rate of orbit (rad/sec)
w=sqrt(MU/mag(X(1:3))^3);

ax2body = 2*w*Y(5) + 3*Y(2)*Y(1)/(rcom*1000)*w^2; ay2body =
-2*w*Y(4) + 3*Y(2)*w^2 + 9/2*Y(2)^2/(rcom*1000)*w^2 +
3/2*Y(1)^2/(rcom*1000)*w^2; at2body =
(-mone*(3*w^2*b^2*cos(Y(3))*sin(Y(3))+3/2*w^2*b^3*sin(Y(3))/(rcom*1000))
-
mtwo*(3*w^2*a^2*cos(Y(3))*sin(Y(3))-3/2*w^2*a^3*sin(Y(3))/(rcom*1000)))...
/(mone*b^2 + mtwo*a^2); axdrag = adrag3*Vhat3(1); aydrag =
adrag3*Vhat3(2); atdrag = (-mone*(adrag1*Vhat1(1)*b*cos(Y(3)) -
adrag1*Vhat1(2)*b*sin(Y(3))) - mtwo*(adrag2*Vhat2(1)*-a*cos(Y(3))
+ adrag2*Vhat2(2)*a*sin(Y(3))))/(mone*b^2 + mtwo*a^2);

%%%%%%%%%%%%%%%%%%% Velocity Terms in m/s in body frame %%%%%%%%%%%%%%
YDot=[Y(4); ...
    Y(5); ...
    Y(6); ...
    %%%%%%%%%%%%%%%%% Acceleration Terms in m/s^2 in body frame %%%%%%%
    % 2*w*Y(5) + adrag*Vhat(1); ...
    % -2*w*Y(4) + 3*Y(2)*w^2 + adrag*Vhat(2); ...
    % (-mone*(3*w^2*b^2*cos(Y(3))*sin(Y(3))+3/2*w^2*b^3*sin(Y(3))/...
    (rcom*1000)) - mtwo*(3*w^2*a^2*cos(Y(3))*sin(Y(3))-3/2*w^2*a^3...
    *sin(Y(3))/(rcom*1000)))/(mone*b^2 + mtwo*a^2)];

    % The following contains the equations of motion with greater order
    % of accuracy:
```

```
ax2body + axdrag; ...
ay2body + aydrag; ...
at2body + atdrag];
```

```
function [adrag1, Vhat1, adrag2, Vhat2, adrag3, Vhat3] = Drag (Y, X, Rot)

%%%%%%%%%%%%%%%%%%%%%%%%%%%%%%%%%%%%%%%%%%%%%%%%%%%%%%%%%%%%%%%%%%%%%%%%%%%%
%%
%% function Drag
%%
%% This function calculates drag for each mass.
%%
%% Author : 2Lt Ernest Maramba AFIT/ENY 937-369-6956 27 Oct 2004
%%
%% Algorithm: 1. Call global variables
%% 2. Calculate r and w for COM
%% 3. For m1: calculate r and v in km and km/s and in inertial frame
%% calculate atmospheric density
%% calculate magnitude of air drag deceleration in m/s^2
%% calculate unit vector for direction of drag term
%% 4. Repeat step 3 for m2 and m3
%%
%% Inputs :
%% X - State Vector for R and V km, km/sec
%% Y - State Vector for generalized coordinates
%% Rot - Rotation matrix
%%
%% Outputs :
%% YDot - Derivative of State Vector
%%
%% Locals :
%% Rrel - Position vector of mass three
%% r - Distance from center of Earth to satellite center of mass
%% w - Orbital spin rate
```

```
%% Vrel - Relative velocity
%% rho - Density
%% Fdrag - Drag force on balloon
%%
%%
%% Constants :
%% MU - Global constant
%% OmegaEarth - Spin rate of Earth
%% a - Length from center of mass to main satellite (mass two)
%% b - Length from center of mass to tip mass (mass one)
%% mone - Tip mass
%% mtwo - Main satellite mass
%% bcthree - Ballistic coefficient of tethered balloon
%% w - Angular rate of the satellite's com
%%
%% Coupling :
%% Atmos - Gets density of atmosphere
%% cross - Calculates cross product
%% mag - Calculates magnitude of a vector
%%
%% References :
%% None.
%%
%%%%%%%%%%%%%%%%%%%%%%%%%%%%%%%%%%%%%%%%%%%%%%%%%%%%%%%%%%%%%%%%%%%%%%%%%%%%
%% Global Constants
global MU OmegaEarth a b mone mtwo bcone bctwo bcthree

%% calculate radius to com
r=mag(X(1:3));
%%calculate angular rate of orbit (rad/sec)
w=sqrt(MU/mag(X(1:3))^3);
```

```
%%%%%%%%%%%%%%%% Calculate the drag term for m1 %%%%%%%%%%%%%%%%%%%
% Calculate r in km and in inertial frame by adding R of COM to
% rotated delx and dely
Tempr=[b*sin(Y(3)); b*cos(Y(3)); 0]; Tempr = Rot*Tempr/1000;
Rrel=[X(1)+Tempr(1);X(2)+Tempr(2);X(3)+Tempr(3)];

% Calculate v in km/s and in inertial frame by adding V of COM to
% rotated delxdot and delydot
Tempv=[b*cos(Y(3))*(Y(6)-w); -b*sin(Y(3))*Y(6) + w*b*sin(Y(3));
0]; Tempv = Rot*Tempv/1000;
Vrel=[X(4)+Tempv(1);X(5)+Tempv(2);X(6)+Tempv(3)]...
    -cross([0;0;OmegaEarth],Rrel);

% Calculate atmospheric density in kg/m^3
[rho] = ATMOS(Rrel)*(10^3);

% Calculate magnitude of air drag deceleration in m/s^2
adrag1=-0.5*rho*((mag(Vrel)*1000)^2)/(bcone);

% Calculate unit vector for direction of drag term
% - Rotated into body frame
Vtemp=Vrel/mag(Vrel); Vhat1=Rot*Vtemp;



%%%%%%%%%%%%%%%% Calculate the drag term for m2 %%%%%%%%%%%%%%%%%%%
% Calculate r in km and in inertial frame by adding R of COM to rotated
% delx and dely
Tempr=[-a*sin(Y(3)); -a*cos(Y(3)); 0]; Tempr = Rot*Tempr/1000;
Rrel=[X(1)+Tempr(1);X(2)+Tempr(2);X(3)+Tempr(3)];
```

```
% Calculate v in km/s and in inertial frame by adding V of COM to
% rotated delxdot and delydot
Tempv=[-a*cos(Y(3))*(Y(6)-w); a*sin(Y(3))*Y(6) - w*a*sin(Y(3));
0]; Tempv = Rot*Tempv/1000;
Vrel=[X(4)+Tempv(1);X(5)+Tempv(2);X(6)+Tempv(3)]...
    -cross([0;0;OmegaEarth],Rrel);

% Calculate atmospheric density in kg/m^3
[rho] = ATMOS(Rrel)*(10^3);

% Calculate magnitude of air drag deceleration in m/s^2
adrag2=-0.5*rho*((mag(Vrel)*1000)^2)/(bctwo);

% Calculate unit vector for direction of drag term
% - Rotated into body frame
Vtemp=Vrel/mag(Vrel); Vhat2=Rot*Vtemp;




%%%%%%%%%%%%%%% Calculate the drag term for m3 %%%%%%%%%%%%%%%%%%
% Calculate r in km and in inertial frame by adding R of COM to rotated
% delx and dely
Tempr=[Y(1); Y(2); 0]; Tempr = Rot*Tempr/1000;
Rrel=[X(1)+Tempr(1);X(2)+Tempr(2);X(3)+Tempr(3)];

% Calculate v in km/s and in inertial frame by adding V of COM to
% rotated delxdot and delydot
Tempv=[Y(4) - w*Y(2); Y(5) + w*Y(1); 0]; Tempv = Rot*Tempv/1000;
Vrel=[X(4)+Tempv(1);X(5)+Tempv(2);X(6)+Tempv(3)]...
    -cross([0;0;OmegaEarth],Rrel);
```

```
% Calculate atmospheric density in kg/m^3
[rho] = ATMOS(Rrel)*(10^3);

% Calculate magnitude of air drag deceleration in m/s^2
adrag3=-0.5*rho*((mag(Vrel)*1000)^2)/(bcthree);

% Calculate unit vector for direction of drag term
% - Rotated into body frame
Vtemp=Vrel/mag(Vrel); Vhat3=Rot*Vtemp;
```

```
function [adrag1, Vhat1, adrag2, Vhat2, adrag3, Vhat3] = Drag (Y,X, Rot)

%%%%%%%%%%%%%%%%%%%%%%%%%%%%%%%%%%%%%%%%%%%%%%%%%%%%%%%%%%%%%%%%%%%%%%%%%%%%
%%
%% function Drag
%%
%% This function calculates drag for each mass.
%%
%% Author : 2Lt Ernest Maramba AFIT/ENY 937-369-6956 27 Oct 2004
%%
%% Algorithm: 1. Call global variables
%% 2. Calculate r and w for COM
%% 3. For m1: calculate r and v in km and km/s and in inertial frame
%% calculate atmospheric density
%% calculate magnitude of air drag deceleration in m/s^2
%% calculate unit vector for direction of drag term
%% 4. Repeat step 3 for m2 and m3
%%
%% Inputs :
%% X - State Vector for R and V km, km/sec
%% Y - State Vector for generalized coordinates
%% Rot - Rotation matrix
%%
%% Outputs :
%% YDot - Derivative of State Vector
%%
%% Locals :
%% Rrel - Position vector of mass three
%% r - Distance from center of Earth to satellite center of mass
%% w - Orbital spin rate
```

```
%% Vrel - Relative velocity
%% rho - Density
%% Fdrag - Drag force on balloon
%%
%%
%% Constants :
%% MU - Global constant
%% OmegaEarth - Spin rate of Earth
%% a - Length from center of mass to main satellite (mass two)
%% b - Length from center of mass to tip mass (mass one)
%% mone - Tip mass
%% mtwo - Main satellite mass
%% bcthree - Ballistic coefficient of tethered balloon
%% w - Angular rate of the satellite's com
%%
%% Coupling :
%% Atmos - Gets density of atmosphere
%% cross - Calculates cross product
%% mag - Calculates magnitude of a vector
%%
%% References :
%% None.
%%
%%%%%%%%%%%%%%%%%%%%%%%%%%%%%%%%%%%%%%%%%%%%%%%%%%%%%%%%%%%%%%%%%%%%%%%%%%%%
%% Global Constants
global MU OmegaEarth a b mone mtwo bcone bctwo bcthree


%% calculate radius to com
r=mag(X(1:3));
%%calculate angular rate of orbit (rad/sec)
w=sqrt(MU/mag(X(1:3))^3);
```

```
%%%%%%%%%%%%%%%% Calculate the drag term for m1 %%%%%%%%%%%%%%%%%%%
% Calculate r in km and in inertial frame by adding R of COM to
% rotated delx and dely
Tempr=[b*sin(Y(3)); b*cos(Y(3)); 0]; Tempr = Rot*Tempr/1000;
Rrel=[X(1)+Tempr(1);X(2)+Tempr(2);X(3)+Tempr(3)];

% Calculate v in km/s and in inertial frame by adding V of COM to
% rotated delxdot and delydot
Tempv=[b*cos(Y(3))*(Y(6)-w); -b*sin(Y(3))*Y(6) + w*b*sin(Y(3));
0]; Tempv = Rot*Tempv/1000;
Vrel=[X(4)+Tempv(1);X(5)+Tempv(2);X(6)+Tempv(3)]...
    -cross([0;0;OmegaEarth],Rrel);

% Calculate atmospheric density in kg/m^3
[rho] = ATMOS(Rrel)*(10^3);

% Calculate magnitude of air drag deceleration in m/s^2
adrag1=-0.5*rho*((mag(Vrel)*1000)^2)/(bcone);

% Calculate unit vector for direction of drag term
% - Rotated into body frame
Vtemp=Vrel/mag(Vrel); Vhat1=Rot*Vtemp;



%%%%%%%%%%%%%%%% Calculate the drag term for m2 %%%%%%%%%%%%%%%%%%%
% Calculate r in km and in inertial frame by adding R of COM to
% rotated delx and dely
Tempr=[-a*sin(Y(3)); -a*cos(Y(3)); 0]; Tempr = Rot*Tempr/1000;
Rrel=[X(1)+Tempr(1);X(2)+Tempr(2);X(3)+Tempr(3)];
```

```
% Calculate v in km/s and in inertial frame by adding V of COM to
% rotated delxdot and delydot
Tempv=[-a*cos(Y(3))*(Y(6)-w); a*sin(Y(3))*Y(6) - w*a*sin(Y(3));
0]; Tempv = Rot*Tempv/1000;
Vrel=[X(4)+Tempv(1);X(5)+Tempv(2);X(6)+Tempv(3)]...
    -cross([0;0;OmegaEarth],Rrel);

% Calculate atmospheric density in kg/m^3
[rho] = ATMOS(Rrel)*(10^3);

% Calculate magnitude of air drag deceleration in m/s^2
adrag2=-0.5*rho*((mag(Vrel)*1000)^2)/(bctwo);

% Calculate unit vector for direction of drag term
% - Rotated into body frame
Vtemp=Vrel/mag(Vrel); Vhat2=Rot*Vtemp;



%%%%%%%%%%%%%%% Calculate the drag term for m3 %%%%%%%%%%%%%%%%%%
% Calculate r in km and in inertial frame by adding R of COM to
% rotated delx and dely
Tempr=[Y(1); Y(2); 0]; Tempr = Rot*Tempr/1000;
Rrel=[X(1)+Tempr(1);X(2)+Tempr(2);X(3)+Tempr(3)];

% Calculate v in km/s and in inertial frame by adding V of COM to
% rotated delxdot and delydot
Tempv=[Y(4) - w*Y(2); Y(5) + w*Y(1); 0]; Tempv = Rot*Tempv/1000;
Vrel=[X(4)+Tempv(1);X(5)+Tempv(2);X(6)+Tempv(3)]...
    -cross([0;0;OmegaEarth],Rrel);
```

```
% Calculate atmospheric density in kg/m^3
[rho] = ATMOS(Rrel)*(10^3);

% Calculate magnitude of air drag deceleration in m/s^2
adrag3=-0.5*rho*((mag(Vrel)*1000)^2)/(bcthree);

% Calculate unit vector for direction of drag term
% - Rotated into body frame
Vtemp=Vrel/mag(Vrel); Vhat3=Rot*Vtemp;
```

```
function [X2] = RK4forRandV ( IDate, stepsize, DerivType, X, Y, Rot)

%%%%%%%%%%%%%%%%%%%%%%%%%%%%%%%%%%%%%%%%%%%%%%%%%%%%%%%%%%%%%%%%%%%%%%%%
%%
%% function RK4forRandV
%%
%% This function is a fourth order Runge-Kutta integrator for a
%% 6 dimension First Order differential equation. The intended
%% use is for a satellite equation of motion. The user must provide
%% an external function containing the system Equations of Motion.
%% Notice Julian date is included since some applications in PDERIV
%% may need this. The LAST position in DerivType is a flag for
%% two-body motion. Two-Body motion is used if the 10th element is
%% set to "2", otherwise the Yes and No values determine which
%% perturbations to use.
%% The integration is done for one time step only.
%%
%% Algorithm : Evaluate each term depending on the derivtype
%% Find the final answer
%% Notice the 4th k must be mult by Dt since k1-k3 did so in assignval
%% Also, the 4th k is left as xdot since it was just calculated
%%
%% Author : Capt Dave Vallado USAFA/DFAS 719-472-4109 5 Jun 1991
%% In Ada : Dr Ron Lisowski USAFA/DFAS 719-472-4110 12 Jan 1996
%% In MatLab : Dr Ron Lisowski USAFA/DFAS 719-333-4109 16 Jan 2002
%%
%% Inputs :
%% IDate - Initial Time Julian Date days since 4713 B.C.

%% Dt - Step size sec
```

```
%% DerivType - String containing YN for incl perts "YYNYNYNY2"
%% BC - Ballistic Coefficient kg/m2
%% X - State vector at initial time km, km/sec
%%
%% Outputs :
%% X - State vector at new time km, km/sec
%%
%% Locals :
%% XDot - Derivative of State Vector
%% K1,K2,K3 - Storage for values of state vector at different times
%% (The standard Runge-Kutta K constants)
%% TEMP - Storage for state vector
%% TempDate - Temporary date storage half way between dt days since
%% 4713 B.C.
%%
%% Constants :
%% None.
%%
%% Coupling :
%% Deriv function for Derivatives of E.O.M.
%% PDeriv function for Derivatives of E.O.M. with Perturbations
%%
%% References :
%% Mathews, "Numerical Methods" pg. 423-427
%% BMW pg. 414-415
%%
%%%%%%%%%%%%%%%%%%%%%%%%%%%%%%%%%%%%%%%%%%%%%%%%%%%%%%%%%%%%%%%%%%%%%%%%%%%
global BC

%% Local VARIABLES
     %%%%%%%%%%%%%%%% Evaluate 1st Taylor Series Term %%%%%%%%%%%%%
```

```
if DerivType(10:10) == '2' ,
    [XDot] = DerivforRandV( X );
else
    [XDot] = PDerivforRandV( IDate,X,DerivType,BC, Y, Rot );
end

%%%%%%%%%%%%%%%% Update Julian Date for a half Dt %%%%%%%%%%%%
TempDate = IDate + stepsize * 0.5 / 86400.0;

%%%%%%%%%%%%%%%% Evaluate 2nd Taylor Series Term %%%%%%%%%%%%%
    K1 = stepsize * XDot;
    Temp = X + 0.5 * K1;

if DerivType(10:10) == '2' ,
    [XDot] = DerivforRandV( Temp );
else
    [XDot] = PDerivforRandV( IDate,Temp,DerivType,BC, Y, Rot );
end

%%%%%%%%%%%%%%%% Evaluate 3rd Taylor Series Term %%%%%%%%%%%%%
    K2 = stepsize * XDot;
    Temp = X + 0.5 * K2;

if DerivType(10:10) == '2' ,
    [XDot] = DerivforRandV( Temp );
else
    [XDot] = PDerivforRandV( IDate,Temp,DerivType,BC, Y, Rot );
end

%%%%%%%%%%%%%%%% Evaluate 4th Taylor Series Term %%%%%%%%%%%%%%%%
    K3 = stepsize * XDot;
```

```
    Temp = X + K3;

%%%%%%%%%%%%%%% Update Julian Date for a full Dt %%%%%%%%%%%%%-
TempDate = IDate + stepsize / 86400.0;

if DerivType(10:10) == '2' ,
    [XDot] = DerivforRandV( Temp );
else
    [XDot] = PDerivforRandV( IDate,Temp,DerivType,BC, Y, Rot );
end

%%%%%%%%%- Update the State vector, perform integration %%%%%%-
X2 = X + ( K1 + 2.0 * ( K2 + K3 ) + stepsize * XDot) / 6.0;
```

```
function [XDot] = DerivforRandV ( X )

%%%%%%%%%%%%%%%%%%%%%%%%%%%%%%%%%%%%%%%%%%%%%%%%%%%%%%%%%%%%%%%%%%%%%%%%%%%%
%%
%% function DERIV
%%
%% This function calculates the derivative of the two-body state vector
%% for use with the Runge-Kutta algorithm. Note time is not needed.
%%
%% Algorithm : Find the answer
%%
%% Author : Capt Dave Vallado USAFA/DFAS 719-472-4109 28 Aug 1989
%% In Ada : Dr Ron Lisowski USAFA/DFAS 719-472-4110 5 Jan 1996
%% In MatLab : Dr Ron Lisowski USAFA/DFAS 719-333-4109 14 Nov 2001
%%
%% Inputs :
%% X - State Vector km, km/sec
%%
%% Outputs :
%% XDot - Derivative of State Vector km/sec, km/se2
%%
%% Locals :
%% RCubed - Cube of R
%% MU_R3 - Mu / R cubed
%%
%% Constants :
%% None.
%%
%% Coupling :
%% None.
```

```
%%
%% References :
%% None.
%%
%%%%%%%%%%%%%%%%%%%%%%%%%%%%%%%%%%%%%%%%%%%%%%%%%%%%%%%%%%%%%%%%%%%%%%%%%%%%
%% Global Constants
     global MU


      %%%%%%%%%%%%%%%%% Build the XDot Vector %%%%%%%%%%%%%%%%%%%
     R= sqrt(X(1)^2+X(2)^2+X(3)^2);
     RCubed= R*R*R;
     MU_R3 = -MU/RCubed;
      %%%%%%%%%%%%%%%%%%% Velocity Terms %%%%%%%%%%%%%%%%%%%%%%%
     XDot = [X(4); ...
             X(5); ...
             X(6); ...
      %%%%%%%%%%%%%%%%% Acceleration Terms %%%%%%%%%%%%%%%%%%%%%
             X(1) * MU_R3; ...
             X(2) * MU_R3; ...
             X(3) * MU_R3];
```

Bibliography

1. Baruh, Haim. *Analytical Dynamics*. Boston, Maryland: WCB McGraw-Hill, 1999.
2. Bate, Roger R. and others. *Fundamentals of Astrodynamics*. New York: Dover Publications, Incorporated, 1971.
3. Beletsky, Vladimir V. and Evgenii M. Levin. *Dynamics of Space Tethers*, *83*. Advances in the Astronautical Sciences. San Diego, California: Univelt, Incorporated, 1993.
4. da Silva Curiel, Alex. "Micro-Bus - SSTL Modular Microsatellite Platform." http://www.ee.surrey.ac.uk/SSC/CSER/UOSAT/products/microsat.html, 2004.
5. Headquarters U.S. Air Force. *Officials Unveil 2004 Budget Proposal*. U.S. Air Force Policy Letter Digest. San Antonio: Air Force News Service, February 2004. http://www.af.mil/policy/pdf/pl2003-02.pdf.
6. Hughes, Peter C. *Spacecraft Attitude Dynamics*. New York: John Wiley and Sons, Inc., 1986.
7. James G. Roche, Former Secretary of the Air Force. "Getting It Right in Space." Speech to the 19th National SPace Symposium., 9 April 2003.
8. Kumar, Renjith R. and others. "Simulation and Shuttle Hitchhiker Validation of Passive Satellite Aerostabilization," *Journal of Spacecraft and Rockets*, *32*(5):806–811 (September-October 1995).
9. Kumar, Renjith R. and others. "Parametric and Classical Resonance in Passive Satellite Aerostabilization," *Journal of Spacecraft and Rockets*, *33*(2):228–234 (March-April 1996).
10. "Dow Corning Products." http://www.dowcorning.com/applications/productfinder/, March 2005.
11. Northrop-Grumman Space Technology. *Microsat Gravity Gradient Boom*. Technical Report DS-413. Astro Aerospace, Northrop Grumman Space Technology, Carpinteria, CA, July 2004. http://www.st.northropgrumman.com/astro-aerospace/SiteFiles/docs/pdfs/DS-413-MICROSAT.pdf.
12. Philley, Thomas Lee. *Development, Fabrication, and Ground Test of an Inflatable Structure Space-Flight Experiment*. MS thesis, AFIT/GA/ENY/03-3, Graduate School of Engineering and Management, WPAFB, March 2003 (AD-A413193).
13. Psiaki, Mark L. "Nanosatellite Attitude Stabilization Using Passive Aerodynamics and Active Magnetic Torquing," *Journal of Guidance, Control, and Dynamics*, *27*(3):347–355 (May-June 2004).
14. United States Air Force: Future Concepts and Transfrmation Division. *The U.S. Air Force Transformation Flight Plan*. Technical Report. Washington: Government Printing Office, 2004.
15. "PAM's Update Page." http://sspp.gsfc.nasa.gov/hh/teams/pamsup.html, July 2004.

16. Wertz, James R. and Wiley J. Larson. *Space Mission Analysis and Design* (Third Edition). Space Technology Series, El Segundo, California: Microcosm Press, 1999.

17. Wiesel, William. *Spacecraft Dynamics* (Second Edition). McGraw-Hill Series in Aeronautical and Aerospace Engineering, New York: McGraw-Hill COmpanies, Inc., 1997.

REPORT DOCUMENTATION PAGE

Form Approved
OMB No. 074-0188

1. REPORT DATE *(DD-MM-YYYY)*	**2. REPORT TYPE**	**3. DATES COVERED** *(From – To)*
Grad date 21-03-2005	**Master's Thesis**	27-08-2004 – 21-03-2005

4. TITLE AND SUBTITLE

A Numerical Analysis for Passive Attitude Stabilization using a Tethered Balloon on a Gravity Gradient Satellite

5a. CONTRACT NUMBER

5b. GRANT NUMBER

5c. PROGRAM ELEMENT NUMBER

6. AUTHOR(S)

Maramba, Ernest, M., Second Lieutenant, USAF

5d. PROJECT NUMBER
If funded, enter ENR #

5e. TASK NUMBER

5f. WORK UNIT NUMBER

7. PERFORMING ORGANIZATION NAMES(S) AND ADDRESS(S)
Air Force Institute of Technology
Graduate School of Engineering and Management (AFIT/EN)
2950 Hobson Way
WPAFB OH 45433-7765

8. PERFORMING ORGANIZATION REPORT NUMBER

AFIT/GA/ENY/05-M07

9. SPONSORING/MONITORING AGENCY NAME(S) AND ADDRESS(ES)
AFIT/ENY
2950 Hobson Way
WPAFB OH 45433-7765 DSN: 785-6565

10. SPONSOR/MONITOR'S ACRONYM(S)

11. SPONSOR/MONITOR'S REPORT NUMBER(S)

12. DISTRIBUTION/AVAILABILITY STATEMENT
APPROVED FOR PUBLIC RELEASE; DISTRIBUTION UNLIMITED.

13. SUPPLEMENTARY NOTES

14. ABSTRACT

This research effort analyzes the fundamental dynamics governing a satellite with a gravity gradient boom and a tethered balloon. Satellites that use gravity gradient booms for passive attitude control are characterized by undamped pitch oscillations and no roll control. The tethered balloon acts as a high drag device that accounts for the most drag on the satellite system. By attaching a drag device, the system resists rolling movements while also damping oscillations. This could potentially be a cost effective method for increasing satellite stabilization. The goal of this research is to model the dynamics and determine the feasibility of a gravity gradient stabilized satellite with an attached balloon. A simulation written in Matlab analyzes the behavior of such a satellite. The research is limited to circular orbits around a spherical Earth and includes only in-plane motion for each mass. Stable ranges for certain tether characteristics are found for three different satellites.

15. SUBJECT TERMS
Attitude Control, Dynamics, Simulation

16. SECURITY CLASSIFICATION OF:			**17. LIMITATION OF ABSTRACT**	**18. NUMBER OF PAGES**	**19a. NAME OF RESPONSIBLE PERSON**
REPORT	**ABSTRACT**	**c. THIS PAGE**			Dr. William Wiesel
U	**U**	**U**	**UU**	120	**19b. TELEPHONE NUMBER** *(Include area code)* (937) 255-6565; e-mail: William.Wiesel@afit.edu

Standard Form 298 (Rev: 8-98)
Prescribed by ANSI Std. Z39-18